LEVEL II sc ①

Calibration of Shock and Vibration Measuring Transducers

A

BLANK PAGES
IN THIS
DOCUMENT
WERE NOT
FILMED

REPORT DOCUMENTATION PAGE		READ INSTRUCTIONS BEFORE COMPLETING FORM
1. REPORT NUMBER SVM-11	2. GOVT ACCESSION NO.	3. RECIPIENT'S CATALOG NUMBER
4. TITLE (and Subtitle) CALIBRATION OF SHOCK AND VIBRATION MEASURING TRANSDUCERS		5. TYPE OF REPORT & PERIOD COVERED
		6. PERFORMING ORG. REPORT NUMBER
7. AUTHOR(s) Raymond R. Bouché		8. CONTRACT OR GRANT NUMBER(s) N00014-73-C-0232 P00004
9. PERFORMING ORGANIZATION NAME AND ADDRESS Bouché Laboratories P. O. Box 400 Tujunga, CA 90142		10. PROGRAM ELEMENT, PROJECT, TASK AREA & WORK UNIT NUMBERS K01-01
11. CONTROLLING OFFICE NAME AND ADDRESS Department of the Navy Office of Naval Research Arlington, Virginia 22217		12. REPORT DATE 1979
		13. NUMBER OF PAGES 186
14. MONITORING AGENCY NAME & ADDRESS(if different from Controlling Office) Department of Defense Shock and Vibration Information Center Naval Research Laboratory Washington, D.C. 20375		15. SECURITY CLASS. (of this report) Unclassified
		15a. DECLASSIFICATION/DOWNGRADING SCHEDULE

16. DISTRIBUTION STATEMENT (of this Report)

Approved for public release; distribution unlimited.

17. DISTRIBUTION STATEMENT (of the abstract entered in Block 20, if different from Report)

NRL/SVIC

18. SUPPLEMENTARY NOTES

SVM-11

19. KEY WORDS (Continue on reverse side if necessary and identify by block number)

Accelerometers	Shock (mechanical)
Calibration	Standards
Force gages	Test equipment
Impedance heads	Transducers
Shakers	Vibration

DDC RECEIVED DEC 28 1979

A

20. ABSTRACT (Continue on reverse side if necessary and identify by block number)

Abstract: This book is an authoritative reference on the calibration procedures used in both primary and secondary calibration laboratories. Contains well-established basic calibration methods, describes transducer, force gage, and impedance head characteristics to the limited extent necessary to aid in performing accurate calibrations. The use and interpretation of calibration results and a detailed description of errors are given. Primary and secondary standards, reciprocity and comparison methods are discussed. Describes the use of calibration shakers and shock motion calibrations. All necessary basic equations are developed.

Continued

DD FORM 1473 EDITION OF 1 NOV 65 IS OBSOLETE
1 JAN 73
S/N 0102-014-6601

Abstract Continued

The Shock and Vibration Monograph Series

Calibration of Shock and Vibration Measuring Transducers

LEVEL *II* ①

SVM-11

Calibration of Shock and Vibration Measuring Transducers

Raymond R. Bouche

Bouche Laboratories
Tujunga, California

1979
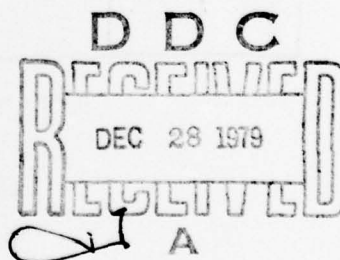
D D C

RECEIVED

DEC 28 1979

A

THE SHOCK AND VIBRATION INFORMATION CENTER
Naval Research Laboratory
Washington, D.C.

Henry C. Pusey, *Director*

Rudolph H. Volin

J. Gordan Showalter

Barbara Szymanski

Carol Healey

Edited and produced by the Technical Information Division,
Naval Research Laboratory

Library of Congress Catalog Card Number: 79-600106

Contract Number: N00014-73-C-0232

PREFACE

While working on primary vibration standards in the early 1950's, we were frequently visited by engineers from various parts of the United States and other countries. These engineers came to visit us at the National Bureau Standards with a common purpose. They simply wanted to unravel the mystery of obtaining reasonable accuracy while calibrating accelerometers and other vibration measuring instruments. A common problem was that engineers and technicians would obtain different calibration results with errors sometimes greatly exceeding 10 percent. Fortunately, with a few years of effort it was possible to reduce calibration errors by more than an order of magnitude. This was accomplished by performing the absolute reciprocity calibrations on primary vibration standards. Thereafter, it was still a problem for some laboratories to obtain good accuracy when performing calibrations. This problem had to do with certain shortcomings with calibration instruments as well as a lack of familiarity with the performance characteristics of accelerometers and how these characteristics might produce errors due to poor motion in the calibration shakers.

It helps to be familiar with the performance characteristics of accelerometers and vibration instruments. This is one of the goals of this monograph, i.e. to describe the vibration instruments in detail to provide the engineer with information to use when doing calibration work. However, this need to be familiar with accelerometer performance characteristics is minimized by using high-quality calibration shakers and high-quality standard accelerometers. Fortunately, after about 25 years of effort at the National Bureau Standards and at leading commercial calibration laboratories, these high quality shakers and high-quality, primary vibration standards are now available.

This monograph is the culmination of a very enjoyable career in performing calibrations on vibration instruments. It is hoped that it will be a widely used reference for those responsible for performing calibration of vibration instruments. Even though there has been considerable progress in most calibration laboratories, there is still a need for many concerned with shock and vibration measurements to be better informed with the performance characteristics of vibration instruments and with the use of accelerometers in making accurate measurements.

The success of writing any worthwhile manuscript depends heavily upon the assistance of others. Barney Epstein, now retired, provided a very worthwhile service in completing the final draft. His help in the final editing and illustrations is worthy of my sincere appreciation. The Shock and Vibration Information Center provided a needed service of having the manuscript reviewed by other specialists. They included John Ramboz at the National Bureau of Standards and Merv Oleson at the Naval Research Laboratory, as well as others. Their assistance

in providing detailed comments and suggestions was very helpful. As always, the staff at SVIC has done a marvelous job in the final editing process and publishing of the monograph.

R. R. BOUCHE

Tujunga, California
July 1979

CONTENTS

vii

CONTENTS (Cont.)

CONTENTS (Cont.)

CHAPTER 1
FUNDAMENTALS FOR CALIBRATION

It is important, in preparing for the calibration of shock and vibration instruments, to review the fundamental characteristics of sinusoidal motion, random vibration, and shock motion. Most shock and vibration measurements are made with accelerometers velocity pickups and displacement measuring devices are used in special applications. All of these transducers can be calibrated by sinusoidal motion excitation. Sinusoidal motion calibrations are easily performed at amplitudes up to 10 *g*. It is also desirable to perform shock motion calibrations to determine the amplitude linearity characteristics of accelerometers. Shock motion calibrations are performed at higher accelerations, up to about 10 000 *g*.

The terminology of calibration is found in a number of publications. For convenience the frequently used definitions are given in this chapter. International System (SI) units are used in this monograph, and equivalent English units are given throughout.

1.1 Sinusoidal Motion

Sinusoidal motion is illustrated in Fig. 1-1. This motion is periodic, and each cycle is an exact reproduction of all others [1]. The motion consists of steady-state vibration at a single frequency. During calibration the frequency may be changed manually or automatically over the range of interest. The frequency of vibration is given by

$$f = \frac{\omega}{2\pi} = \frac{1}{T} \tag{1-1}$$

where

f = frequency, Hz
ω = circular frequency rad/s
T = period of vibration.

The nature of sinusoidal vibration is that the variation with time of displacement, velocity, acceleration, and jerk has exactly the waveform illustrated in Fig. 1-2. The amplitudes of these quantities are given by the following equations:

$$x = \frac{D}{2} \sin (2\pi ft) \tag{1-2}$$

1
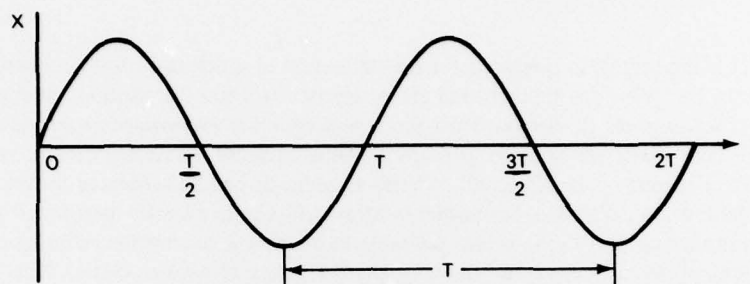
Fig. 1-1. Curve representing sinusoidal motion as a function of time
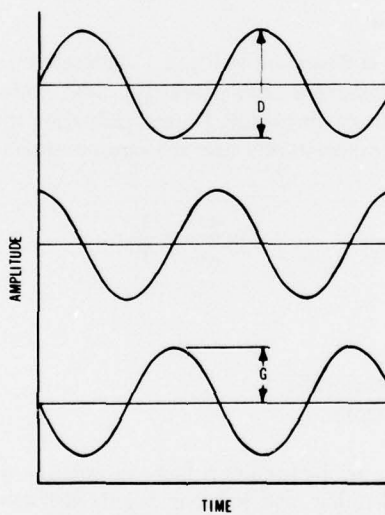
Fig. 1-2. Phase relationships between displacement velocity and acceleration of a body subjected to sinusoidal motion

$$v = \frac{dx}{dt} = 2\pi f \frac{D}{2} \cos(2\pi ft) \qquad (1\text{-}3)$$

$$a = \frac{d^2x}{dt^2} - (2\pi f)^2 \frac{D}{2} \sin(2\pi ft) \qquad (1\text{-}4)$$

$$K = \frac{d^3x}{dt^3} = -(2\pi f)^3 \frac{D}{2} \cos(2\pi ft) \qquad (1\text{-}5)$$

where

x = the instantaneous values of the displacement motion at any time t, in meters (in.)

D = the double displacement amplitude, in meters (in.)

v = the instantaneous value of the velocity motion at any time t, in meters per second (in./s)

a = the instantaneous acceleration motion at any time t, in meters per second squared (in./s^2)

K = the instantaneous jerk motion at any time t, in meters per second cubed (in./s^3)

f = frequency, in hertz

t = time, in seconds.

It is customary to refer to displacement measurements with the peak-to-peak value, as in Figs. 1-2 and 1-3. This is because displacement measuring vibration instruments normally indicate this value. These instruments include vibrating wedges, microscopes, and dial indicators. On the other hand, it is customary to express acceleration by the peak value. Accordingly, accelerometers are calibrated in terms of peak electrical output divided by peak acceleration. Similarly, velocity pickups are calibrated in terms of peak electrical output divided by peak velocity.

Indicating instruments such as voltmeters may be calibrated in rms units. An rms indicating meter provides the rms value of acceleration or velocity when used with accelerometers or velocity pickups. The rms value of sinusoidal vibration is 0.707 times the peak value. It is best to use consistent units; i.e., peak output with peak vibration amplitude. Sometimes the rms value of the electrical output and peak value of vibration amplitude are used. For example, the sensitivity of an accelerometer may be expressed as rms millivolts divided by the peak value of acceleration expressed in g units. However, the use of these mixed units should be discouraged; it is preferable to express acceleration sensitivity in units of mV/g.
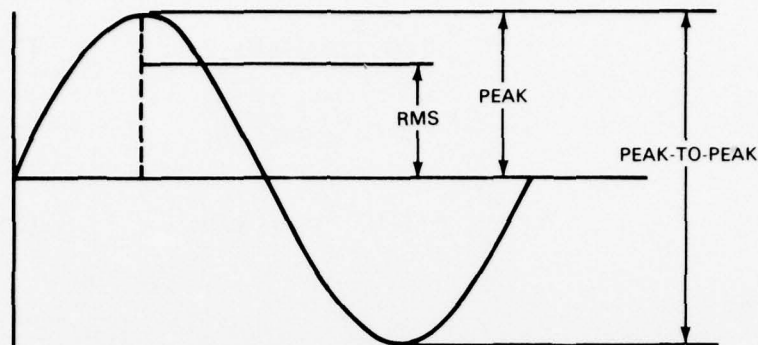
Fig. 1-3. Relative magnitudes of rms, peak, and peak-to-peak measurements of a sine wave

Note that

$$\frac{mV}{g} = \frac{mV\ pk}{g\ pk} = \frac{mV\ rms}{g\ rms} = \frac{1.41\ mV\ rms}{g\ pk}\ .$$

Equations (1-2)–(1-5) describe the relationships among displacement, velocity, acceleration, and jerk motion for all sinusoidal vibrations. The minus signs indicate simply that the acceleration motion and jerk motion are 180 degrees out of phase with displacement motion and velocity motion, respectively. Jerk motion is of interest in only a limited number of cases, such as the discomfort felt in a decelerating vehicle. Also, transducers for measuring jerk and calibrations in jerk units are not in common use.

Vibration measurements are most frequently made with accelerometers and are usually expressed as the peak value of acceleration. In low-frequency applications, for which most measurements are made below 50 Hz, the vibration is sometimes expressed as double displacement amplitude. The quantitative relationship between the peak acceleration and peak-to-peak displacement is determined from Eq. (1-4) by using unity for the sine term.

$$G = 2.014\ Df^2 \text{ for } D \text{ in meters}$$

$$G = 0.0511\ Df^2 \text{ for } D \text{ in inches}$$

(1-6)

where

G = peak acceleration in gravity units (1 g = 9.807 m/s^2 or 386 in./s^2).
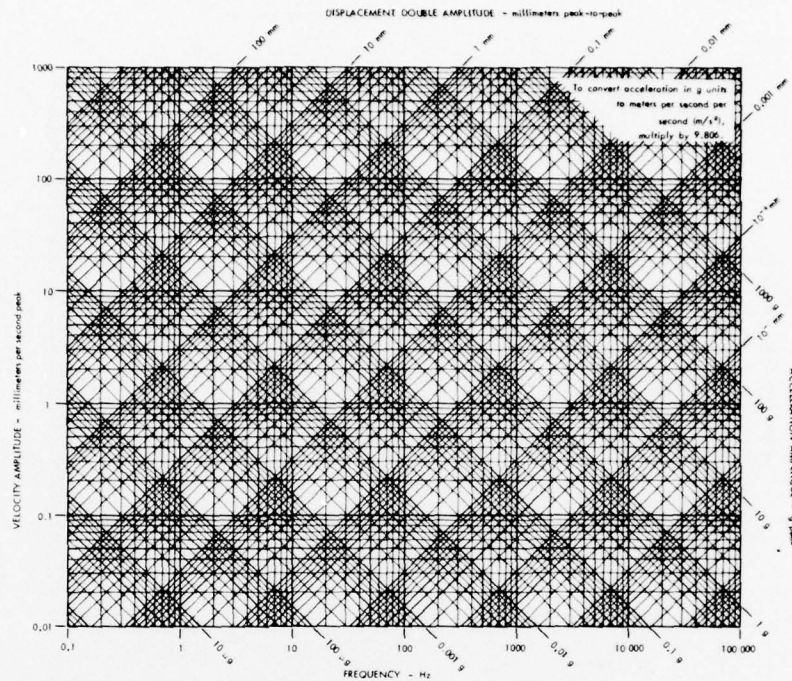
Fig. 1-4a. Linear vibration nomograph in metric units (Endevco)

It is common practice to determine double displacement amplitude from ac-
celeration measurements and vice versa. Calculators are commonly used to com-
pute Eq. (1-6). Also, the relationship among displacement, acceleration, and
velocity can be determined from the nomograms in Fig. 1-4. Figures 1-4a and
1-4b apply to rectilinear motions, and Fig. 1-4c to rotational motion.

1.2 Complex Waveforms

Harmonic Distortion

The ideal motion for calibrating vibration measuring instruments is sinusoi-
dal, with no acceleration waveform distortion. Under certain conditions har-
monic distortion is present. This distortion typically is at odd integer multiples
of the excitation frequency, usually the result of a small magnitude of odd har-
monic distortion in the shaker driving signal exciting the resonance frequency of
the transducer or shaker. For example, Fig. 1-5 illustrates the presence of a third
harmonic distortion [2]. The complex waveform is produced by the vibration
taking place in a shaker or other body being excited simultaneously at the funda-
mental and third harmonic frequency. If the complex motion contains more
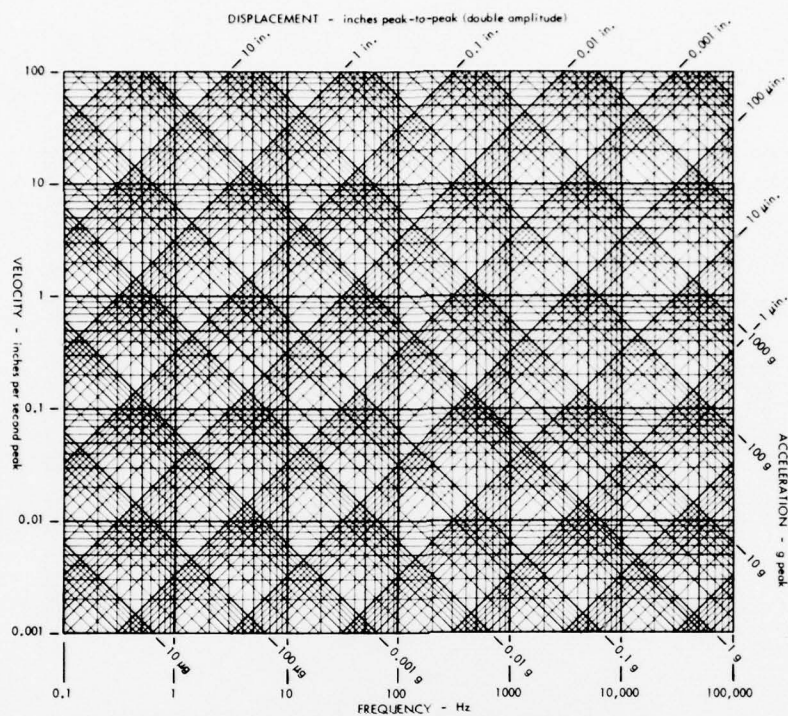
Fig. 1-4b. Linear vibration nomograph in units of inches (Endevco)

than two frequencies, these frequencies could be determined by Fourier analysis for periodic vibration. When instruments for sinusoidal calibrations are carefully selected, it is unusual for more than two frequencies to be present at one time. Usually only the third, fifth, seventh, or ninth harmonic of the excitation frequency is present. With good-quality shakers this harmonic distortion should be present only at frequencies above the operating frequency range of the vibration instrument being calibrated.

Random Vibration

Random vibration enters into calibration only in the decision of whether it can be measured accurately by the vibration instruments being used. For example, can an accelerometer calibrated with sinusoidal motion be used to measure random vibrations? The answer is provided by a brief review of the characteristics of random vibration.

Random vibration is present when the instantaneous magnitude can be specified only by the probability that the amplitude will be within a specified
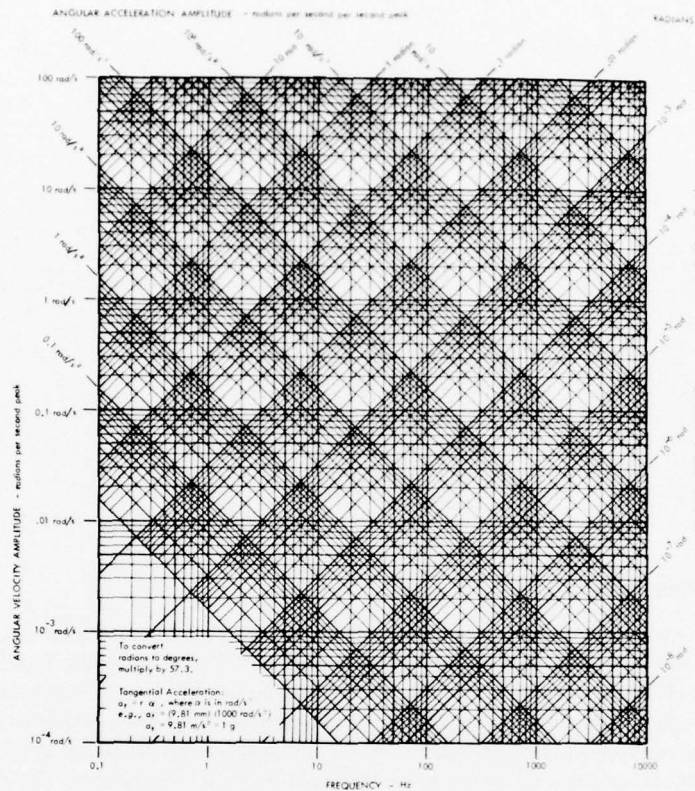
Fig. 1-4c. Angular vibration nomograph in units of rads (Endevco)

range during a specified time interval. In general, random vibrations are aperiodic and cannot be evaluated by Fourier analysis. The frequency components in random vibrations may be obtained by passing the vibration signal through narrow band-pass filters. If reasonable care is taken in selecting the vibration measuring instruments, the amplitudes and frequencies in the random vibration should correspond to the operating range of the instruments. For example, a properly selected accelerometer will be linear and have constant sensitivity throughout the amplitude and frequency range of interest. Also, it should have proportional phase response. Sinusoidal calibrations are used to verify these characteristics. Thus, sinusoidal motion calibrations are sufficient for demonstrating that properly selected vibration measuring instruments are suitable for accurate measurements of random vibrations.
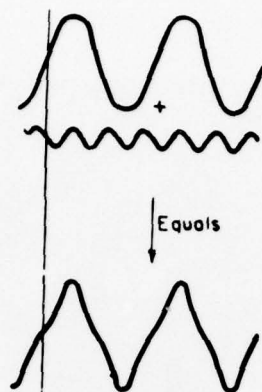
Fig. 1-5. Complex motion re-
sulting from the addition of a
third harmonic to the funda-
mental frequency

1.3 Shock Motion

The most accurate shock motion calibrations are performed on machines that
produce pulses of near half-sinusoidal waveform. Pulse durations should be
selected to correspond with those experienced in service. It is relatively simple
to produce short-duration shock motion pulses in the range from $100\,\mu s$ to 1 ms.
Present-day shock motion calibrators do not produce longer pulses up to 100
ms, which correspond to those encountered in some applications. Therefore,
sinusoidal motion calibrations are used to verify the performance of vibration
measuring instruments at low frequencies corresponding to those of the longer
shock motion pulses.

Fourier analysis is used to determine the frequency components of shock
pulses [3]. Figure 1-6 shows the frequency components contained in a half-
sinusoidal pulse, where $\omega_0 = \pi/\tau$ and τ = pulse duration. This spectrum diagram
indicates that a large number of sinusoids are present in the pulse, with signifi-
cant amplitudes up to $\omega/\omega_0 = 4$, or a frequency of up to twice the reciprocal of
the pulse duration. Accordingly, accelerometers should be selected to have an
operating frequency range corresponding to frequencies of at least twice the
reciprocal of the shortest pulse duration of intended use. The requirements are
similar for other pulse shapes encountered in shock motion applications.

Shock Spectrum

Shock testing is frequently specified by the shock spectrum [4]. The shock
spectrum is of interest in making a fragility assessment, and design work is con-
cerned with the maximum inertial loading resulting from a specified shock

motion. It is desirable to determine the maximum displacement or acceleration amplitudes produced in mechanical systems during shock excitation. The shock spectrum provides the means for computing these amplitudes for any simple single-degree-of-freedom system (Fig. 1-7) [5].

The primary shock spectrum (Fig. 1-8) indicates that a single-degree-of-freedom system having a natural frequency of about twice the reciprocal pulse duration produces an acceleration amplitude of approximately 1.7 times the peak acceleration in a half-sinusoidal pulse [6]. This acceleration is reached during the pulse. After the pulse is ended, the residual spectrum (Fig. 1-8) indicates that the acceleration amplitude reached is only slightly more than half the peak acceleration of the pulse.

The shock spectra of the various pulse shapes are of interest. It is unnecessary to consider spectra when performing shock motion calibrations. Instead, care is taken that the shock motion calibrations satisfy the requirements determined by the Fourier spectrum of the various pulse shapes of interest.
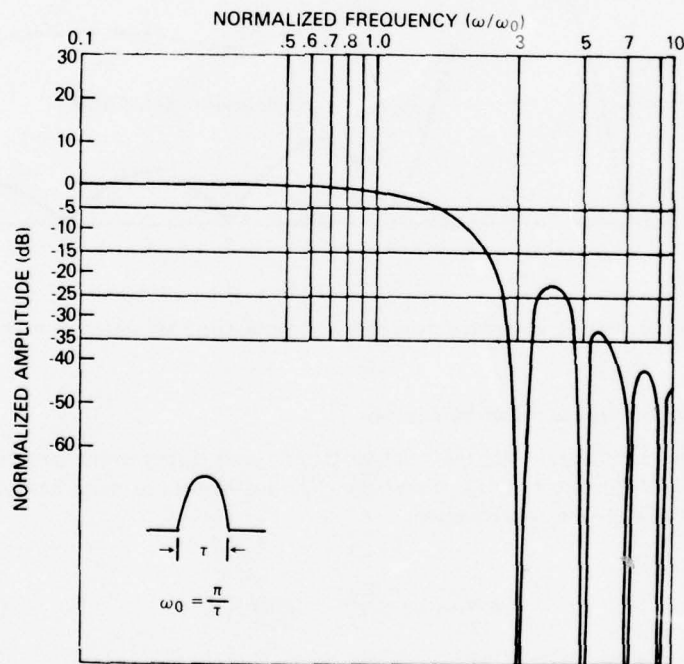
Fig. 1-6. Fourier spectra of a half-sine pulse
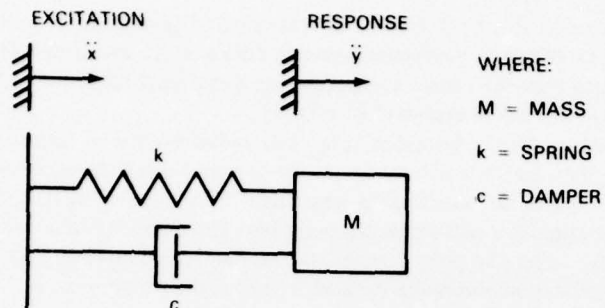
Fig. 1-7. A simple single-degree-of-freedom system
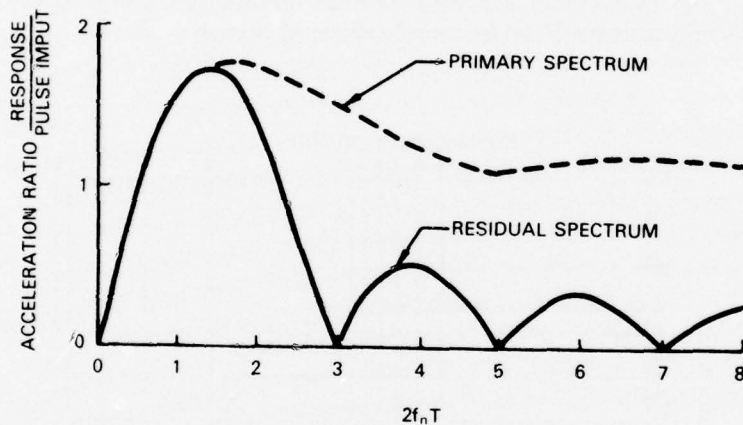
Fig. 1-8. Primary and residual shock response spectrum for a half-sine shock pulse

Velocity and Displacement Amplitudes

Some familiarity with the velocity changes and displacement amplitudes associated with shock pulses is desirable. The half-sinusoidal pulse has a peak acceleration given by the equation

$$a = A_0 \sin \frac{\pi t}{\tau} ; \quad 0 \leqslant t \leqslant \tau. \tag{1-7}$$

integrating yields

$$v = \int_0^\tau a\, dt \tag{1-8}$$

$$= \frac{A_0 \tau}{\pi} \left(1 - \cos \frac{\pi t}{\tau}\right) \tag{1-9}$$

and

$$x = \int_0^\tau v\, dt \tag{1-10}$$

$$= \left(\frac{A_0 \tau}{\pi} \quad t - \frac{\tau}{\pi} \sin \frac{\pi t}{\tau}\right) \tag{1-11}$$

where

τ = pulse duration, in seconds.

These equations apply only during the pulse, at any moment from zero to τ. It is of special interest to determine the velocity change and displacement produced at the end of the pulse. At time $t = \tau$,

$$v_0 = \frac{2A_0 \tau}{\pi} \tag{1-12}$$

and

$$d_0 = \frac{A_0 \tau^2}{\pi} \tag{1-13}$$

where

A_0 = peak acceleration, in meters per second squared (in./s^2)

v_0 = velocity change, in meters per second (in./s)

d_0 = displacement amplitude, in meters (in.).

Instantaneous velocity and displacement for a typical half-sinusoidal acceleration pulse of 1-ms duration are shown in Fig. 1-9.
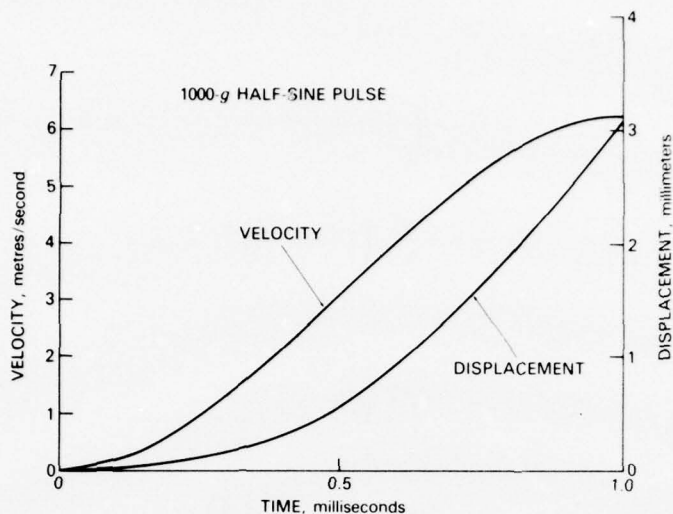
Fig. 1-9. Instantaneous velocity and displacement amplitudes for a 1-ms half-sine shock pulse

1.4 Units

It is desirable to use the International System (SI) of units in the calibration laboratory. The units most often used in calibrating vibration measuring instruments include meters, seconds, and meters per second squared. It is recommended that multiple and submultiple prefixes be used in steps of 1000 rather than using powers of 10. For example, it is better to express small displacements in units of millimeter than meters times 10^{-3}.

For convenience during the transition to the metric system, equivalent English units are generally given in parentheses after the SI units.

The most useful SI unit for length or displacement is the millimeter. The double displacement amplitude present during calibration of shock and vibration measuring instruments is of the order of 1 mm (0.03937 in.) to about 25.4 mm (1 in.). These are peak-to-peak values, since it is customary to express the double displacement amplitude during the calibration and use of these instruments.

Velocity is expressed as a single amplitude, in units of meters per second (m/s).

Acceleration is expressed as a single amplitude and has units of meters per second squared (m/s^2). However, it is customary to express acceleration as a multiple or submultiple of g, the acceleration of gravity. The standard value of gravity 1 g is equal to 9.806 65 m/s^2. Finally, the conversion from m/s^2 to g units is approximately a factor of 10. An acceleration of 98 m/s^2 is approximately 10 g.

The SI unit for time is the second (s).

The SI unit for mass is the kilogram (kg). The unit of force is the newton (N). It is good practice to observe this distinction.

The relationship of force, mass, and acceleration is given by Newton's first law of motion; expressed algebraically as

$$F = Ma \qquad (1\text{-}14)$$

where

F = force, in newtons (lbf · in./s^2)

M = mass, in kilograms (lbm)

a = acceleration, in meters per second squared (in./s^2 or g).

The unit of frequency is the hertz (Hz).

The SI unit for plane angle is the radian (rad). However, it is permissible to use the arc degree when the radian is not a convenient unit.

The accepted unit for temperature is the degree Celsius (°C). The Celsius scale has been called the Centigrade scale. The SI unit of temperature is the kelvin (K), which is not usually used in engineering work. The kelvin temperature is equal to 273.15 plus the Celsius temperature. For example, a Celsius temperature of 20°C is 293.15K.

Terminology

It is helpful to review the terms most often used in shock and vibration, particularly those concerning calibration. References 7 and 8 should be consulted for additional terms and definitions.

Acceleration. Acceleration is a vector quantity that specifies the time rate of change of velocity.

Acceleration admittance. Acceleration admittance is the complex ratio of acceleration to force using sinusoidal excitation and includes the phase angle between these quantities. It is sometimes referred to as "inertance."

Acceleration impedance (Z_a). Acceleration impedance is the complex ratio of force to acceleration during sinusoidal excitation and includes the phase angle between these quantities. It is sometimes referred to as "dynamic mass" or "apparent weight."

Charge converter. A charge converter is an electronic circuit that provides an instantaneous output voltage proportional to the instantaneous electric charge at the input.

Critical damping (c_c). Critical damping is the minimum viscous damping that will allow a displaced system to return to its initial position without oscillation.

Cycle. A cycle is the complete sequence of values of a periodic quantity that occurs during a period.

Damped natural frequency (f_d). The damped natural frequency is the frequency of free vibration of a damped linear system. The free vibration of a damped system may be considered periodic in the limited sense that the time interval between zero crossings in the same direction is constant, even though successive amplitudes decrease progressively. The frequency of the vibration is the reciprocal of this time interval. (Also see natural frequency, undamped natural frequency)

Damping ratio (ζ). The damping ratio for a transducer with viscous damping is the ratio of actual damping coefficient c to critical damping coefficient c_c.

Decibel (dB). The decibel is a unit that denotes the magnitude of a quantity with respect to an arbitrarily established reference value, in terms of the logarithm (to the base 10) of the ratio of the quantities.

Displacement. Displacement is a vector quantity that specifies the change of position of a body or particle and is usually measured from the mean position or position of rest. Practical measurements, however, express displacement magnitude in peak-to-peak values.

Displacement admittance. Displacement admittance is the complex ratio of displacement to force during sinusoidal excitation and includes the phase angle between these quantities. It is sometimes referred to as "dynamic compliance."

Displacement impedance (Z_d). Displacement impedance is the complex ratio of force to displacement during sinusoidal excitation and includes the phase angle between these quantities. It is sometimes referred to as "dynamic stiffness."

Distortion. Distortion is an undesired change in waveform. Noise and certain desired changes in waveform, such as those resulting from modulation or detection, are not usually classed as distortion.

Duration of shock pulse (τ). The duration of a shock pulse is the time required for the acceleration of the pulse to rise from some stated fraction of the maximum amplitude and then decay to a stated fraction of this value.

Error (uncertainty). An error is the algebraic difference between the indicated value and the true value of the measurand.

Excitation. Excitation is an external force or motion applied to a transducer, causing an output.

Filter. A filter is a device for separating waves on the basis of their frequency. It introduces relatively small insertion loss to waves in one or more frequency bands and relatively large insertion loss to waves of other frequencies.

Free vibration. Free vibration of a system is vibration of a system that occurs in the absence of forced vibration.

Frequency (f). The frequency of a function periodic in time is the reciprocal of the period. The unit is the hertz (Hz), in which represents cycles per second.

Gravitational unit (g). The quantity g is the acceleration produced by the force of gravity, which varies with the latitude and elevation of the point of observation. By international agreement, the exact value 9.806 65 m/s^2 (386.088 in./s^2) has been chosen as the standard acceleration due to gravity.

Harmonic. A harmonic is a sinusoidal quantity having a frequency that is an integral multiple of the frequency of a periodic quantity to which it is related.

Linearity. Linearity expresses the closeness of a calibration curve to a specified straight line. A linear transducer has a constant sensitivity over a specified range of amplitude and frequency.

Measurand. A measurand is the physical quantity, property, or condition to be measured.

Natural frequency. The natural frequency is the frequency of free vibration of a system. For a multiple-degree-of-freedom system, the natural frequencies are the frequencies of the normal modes of vibration.

Noise. Noise is any undesired signal. By extension, it is any unwanted disturbance in a useful frequency band, such as undesired electric waves in a transmission channel or device.

Peak-to-peak value. The peak-to-peak value of a vibrating quantity is the algebraic difference between the extremes of the quantity.

Period (T). The period of a periodic quantity is the smallest increment of the time variable for which the function repeats itself.

Piezoelectric transducer. A piezoelectric transducer is a transducer that depends for its operation on the deformation of certain asymmetric crystals, which generates an electric charge.

Piezoelectricity. Piezoelectricity is the property exhibited by some asymmetrical crystals that, when subjected to strain in a suitable direction, develop electric polarization proportional to the strain. Inverse piezoelectricity is the effect by which mechanical strain is produced in certain asymmetrical crystalline materials when they are subjected to an external electric field; the strain is proportional to the electric field.

Piezoresistive transducer. A piezoresistive transducer depends for its operation on the change of resistivity of a semiconductor or other crystal as a function of applied stress.

Phase angle. The phase angle of a sinusoidal vibration is the fractional part of a period through which the vibration has advanced or lagged from another such vibration.

Pulse rise time. The pulse rise time is the interval of time required for the leading edge of a pulse to rise from some specified small fraction to some specified larger fraction of the maximum value.

Quality factor (Q). The quantity Q is a measure of the sharpness of resonance or frequency selectivity of a resonant vibratory system having a single degree of freedom, either mechanical or electrical. In a mechanical system, this quantity is equal to half the reciprocal of the damping ratio. It is commonly used

only with reference to a lightly damped system, and is then approximately equal to the following:

1. Transmissibility at resonance
2. π/logarithmic decrement
3. $2\pi W/\Delta W$, where W is the stored energy and ΔW the energy dissipation per cycle
4. $f_r/\Delta f$, where f_r is the resonance frequency and Δf is the bandwidth between the half-power points.

Random vibration. Random vibration is vibration whose instantaneous magnitude is not specified for any given instant of time. The instantaneous magnitudes of a random vibration are specified only by probability distribution functions giving the probable fraction of the total time that the magnitude (or some sequence of magnitudes) lies within a specified range. Random vibration contains no periodic or quasi-periodic constituents. If random vibration has instantaneous magnitudes that occur according to the Gaussian distribution, it is called Gaussian random vibration.

Resonance frequency. The resonance frequency is the frequency at which the sensitivity of a transducer is a maximum. The resonance frequency is defined only for linear transducers with a damping ratio less than $1/\sqrt{2}$. Additional resonances corresponding to modes in which the principal displacements occur locally in the spring, housing, or attachment fittings are sometimes excited, particularly by shock motions.

Sensitivity (S). Sensitivity is the ratio of the change in transducer output to a change in the value of the measurand.

Shaker (vibration generator). A shaker is a device for subjecting a transducer or other objects to controlled and reproducible mechanical vibration.

Shock. Mechanical shock is an aperiodic excitation (e.g., a motion of the foundation or an applied force) of a mechanical system that is characterized by suddenness and severity and usually causes significant relative displacements in the system.

Shock calibrator. A shock calibrator is a device for subjecting a transducer to controlled and reproducible mechanical shock.

Shock pulse. A shock pulse is a substantial disturbance characterized by a rise of acceleration from a constant value and decay of acceleration to the constant value in a short period of time. Shock pulses are normally displayed graphically as curves of acceleration vs time.

Shock spectrum. A plot of the maximum response experienced by a single-degree-of-freedom system, as a function of its own natural frequency, in response to an applied shock. The response may be expressed in terms of acceleration, velocity, or displacement.

Sinusoidal motion. A motion such that the displacement is a sinusoidal function of time. It is sometimes called simple harmonic motion.

Standard deviation. Standard deviation is the square root of the variance; i.e., the square root of the mean of the squares of the deviations from the mean value of a vibrating quantity.

Structural impedance. Structural impedance is the complex ratio of force to motion during sinusoidal excitation, including the phase angle between these quantities. Appropriate units are used, depending on whether the impedance is expressed for displacement, velocity, or acceleration motion.

Subharmonic response. Subharmonic response is the periodic response of a mechanical system exhibiting resonance at a frequency that is a submultiple of the frequency of the periodic excitation.

Superharmonic response. Superharmonic response is a term sometimes used to denote a particular type of harmonic response that dominates the total response of the system. It frequently occurs when the excitation frequency is a submultiple of the frequency of the fundamental resonance.

Transducer (pickup). A transducer is a device that converts shock or vibratory motion into an optical, mechanical, or (most commonly) electrical signal proportional to a parameter of the experienced motion.

Undamped natural frequency (f_n). Regardless of the damping present, the undamped natural frequency of a transducer is the frequency of sinusoidal excitation at which the motion of the mass element lags behind the motion of the base or case of the transducer by a phase angle of 90 degrees. (see also Natural Frequency, Damped Natural Frequency, and Resonance Frequency).

Transverse sensitivity. Transverse sensitivity is the sensitivity of a transducer to motion in a plane perpendicular to the sensitive axis. It is usually expressed in percent, as the ratio of the maximum transverse sensitivity to the sensitivity of the transducer.

Velocity. Velocity is a vector quantity that specifies the time rate of change of displacement.

Velocity admittance. Velocity admittance is the complex ratio of velocity to force during sinusoidal excitation and includes the phase angle between these quantities. It is frequently called mobility.

Velocity impedance (Z). Velocity impedance is the complex ratio of force to velocity during sinusoidal excitation and includes the phase angle between these quantities. Velocity impedance is frequently referred to as mechanical impedance.

Vibration. Vibration is an oscillation wherein the quantity is a parameter that defines the motion of a mechanical system.

CHAPTER 2
THEORY OF SEISMIC TRANSDUCERS

Accelerometers and velocity pickups are used for measuring mechanical shock and vibration. This mechanical motion is changed into an electrical output by a transducing element. Most accelerometers are built with one of the following electrical transducing elements. Piezoelectric elements, piezoresistive strain gages, wire strain gages, differential transformers, variable-capacitance elements, variable-reluctance elements, or variable resistive potentiometric elements. Velocity pickups are built with electrodynamic inductive-coil transducers. All of these operate on the principle of the seismic transducer.

2.1 Basic Equations.

The basic elements of seismic transducers are illustrated in Fig. 2-1. Virtually all accelerometers and velocity pickups are described by this single-degree-of-freedom seismic transducer. Some transducers frequently used have a relatively low resonance frequency; the elements of such transducers are easily identified. For example, the magnet in a velocity pickup may be a mass element (m), and the wire strain gage in an accelerometer may be the spring element (k). These relatively low-resonance transducers are built with springless masses and mass-less springs.

Most accelerometers are slightly more complicated. For example, piezoelectric accelerometers have relatively high resonance frequencies. Usually the mass element consists of a dense metal component plus part of the piezoelectric ceramic elements. The spring element may consist of the piezoelectric ceramic elements plus part of the base of the accelerometer. This means that it is difficult to compute the mass and stiffness of the elements from the physical properties of its materials.

Even though the basic elements of a seismic transducer may be difficult to describe precisely, it is important to review the theoretical response of such transducers. If the resonance frequencies have been determined, for example by calibration, the theoretical equations can accurately define the frequency response and resonance characteristics of accelerometers and velocity pickups. One of the purposes of calibrating is to determine how well the accelerometer responds as a single-degree-of-freedom mechanical system.

Each of the elements possesses an infinitesimal amount of mechanical damping (c). The damping is so small in peizoelectric ceramics and strain gages, for example, that most accelerometers have nearly zero damping. Some accelerometers are filled with oil to induce significant amounts of damping and some use gas or electrical damping.

19
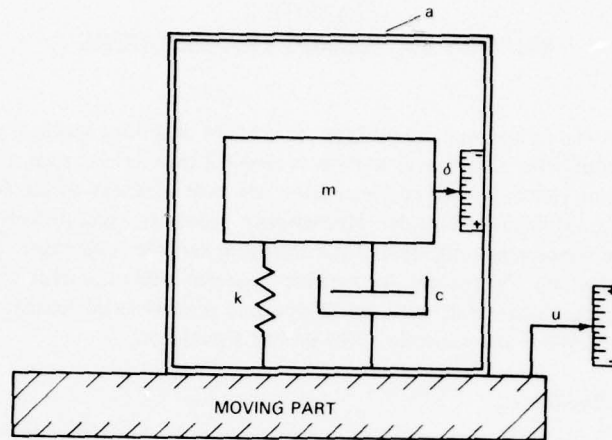
Fig. 2-1. Basic elements of a single-degree-of-freedom seismic transducer consisting of a mass element (m) supported by a spring (k) with damping (c)

The equations of the seismic transducer are used to determine the magnitude and phase relationship of the mass element's motion relative to that of the moving part to which the transducer is attached. These equations apply for sinusoidal motion. They are also useful for shock motions, since the components of a pulse can be represented by a series of sinusoids.

The motion of the mass element is sinusoidal with the same frequency as that of the case of the accelerometer or velocity pickup. The mass element's motion relative to the base of an undamped accelerometer is constant, with no time lag (i.e., zero phase angle) throughout its operating frequency range. A damped accelerometer has a constant mass element motion, but the time lag of this motion relative to that of the accelerometer base varies with frequency. The characteristics of undamped and damped velocity pickups are similar to those of accelerometers, except that the operating frequency range of an accelerometer is below its resonance frequency and the operating range of a velocity pickup is above its resonance frequency. The same equations describe both types of transducers.

The amplitude of the motion of the mass element relative to its base is given by

$$\delta = \frac{u(\omega/\omega_n)^2}{\sqrt{(1 - \omega^2/\omega_n^2)^2 + 4\,(\zeta^2\omega/\omega_n)^2}} \tag{2-1}$$

where

δ = displacement amplitude of the transducer's mass element relative to that of its case

u = displacement amplitude of the transducer case

ω = circular frequency of the transducer case or moving part: $\omega = 2\pi f$, where f is in hertz

ω_n = undamped natural circular frequency of transducer: $\omega_n = 2\pi f_n$

c = transducer damping constant

c_c = critical damping constant for the transducer.

ζ = c/c_c = damping ratio.

The undamped natural circular frequency for the transducer is given by

$$\omega_n = (k/m)^{1/2} = 2\pi f_n \text{ rad/s} \tag{2-2}$$

where

k = effective stiffness of the transducer, in newtons per meter (lbf/in.)

m = mass of the transducer, in kilograms (lbm)

g = acceleration of gravity (9.807 m/s^2; 386 in./s^2).

The critical damping constant for the transducer is given by

$$c_c = 2(km)^{1/2}. \tag{2-3}$$

The critical damping constant marks the boundary between sinusoidal and non-sinusoidal response. This means that after a sudden displacement of the mass element, its motion will not be sinusoidal if c is greater than c_c. Accelerometers and velocity pickups are designed to have a value of $c = 0$ or $c = 0.7 c_c$. One of the reasons for calibrating is to detect significant variations from these values.

The phase angle of a transducer represents the time lag of the mass element behind the case or moving element. The phase angle is given by

$$\theta = \tan^{-1} \frac{2\zeta(\omega/\omega_n)}{1 - (\omega/\omega_n)^2}. \tag{2-4}$$

It is interesting that this equation applies to both accelerometers and velocity pickups. The operating range of an undamped accelerometer is normally selected at frequencies of $\omega \leqslant 0.2\, \omega_n$, since the increase in sensitivity due to the resonance effect is theoretically only 4.1% at $0.2\, \omega_n$. Also, undamped accelerometers possess very small amounts of inherent damping, with values of about $c \leqslant 0.01 c_c$. Substituting these values into Eq. (2-4) indicates that the phase angle of the

undamped accelerometer is 0 degrees throughout its operating frequency range. Velocity pickups are used at frequencies of $\omega \gg \omega_n$. Using large values of ω in Eq. (2-4) indicates that the phase angle of a velocity pickup is 180 degrees (π rad).

2.2 Frequency Characteristics

The ideal frequency response characteristics of accelerometers and velocity pickups are determined by using the basic equation over the frequency range of interest. Accelerometers are designed for use at frequencies far below the resonance frequency of the single-degree-of-freedom seismic system. On the other hand, velocity pickups in common use are described by the responses the seismic systems at frequencies far above resonance. The responses of the ideal accelerometer and ideal velocity pickup are determined by examining the basic equations in these frequency ranges. Afterwards, calibration determines how well accelerometers and velocity pickups follow the ideal response.

Accelerometer Equations

The transducing element in an accelerometer produces an electrical output proportional to the displacement of the mass element relative to the motion of its base or of the moving part to which the accelerometer is attached. Usually the motions of the accelerometer base and moving part are identical. The sensitivity of an accelerometer is defined as the ratio of its electrical output to the acceleration motion at the point or surface at which it is attached to the moving part. The ideal response of the accelerometer is determined by solving Eq. (2-1) for the terms that describe this ratio;

$$\frac{\delta}{u\omega^2} = \frac{1/\omega_n^2}{\sqrt{(1 - \omega^2/\omega_n^2)^2 + 4\zeta^2(\omega/\omega_n)^2}}. \tag{2-5}$$

The term δ is the motion of the mass element relative to the accelerometer base, and the produce $u\omega^2$ is the acceleration at the base of the accelerometer. Accordingly, the left side of Eq. (2-5) represents the sensitivity of an accelerometer, and the right side describes how this sensitivity varies with frequency. Resonance frequency ω_n has a unique value for each accelerometer. The frequency response of the accelerometer is normalized by selecting a value of unity for the resonance frequency and a value of unity for the sensitivity at very low frequencies. The normalized acceleration sensitivity has a value of unity at frequencies far below the resonance frequency. The sensitivity is infinitely large for the undamped accelerometer when the excitation frequency equals the resonance frequency. These values are plotted in Fig. 2-2. Also, values of acceleration sensitivity are plotted for accelerometers having damping values of $\zeta = 0.7$ and $\zeta = 0.4$.
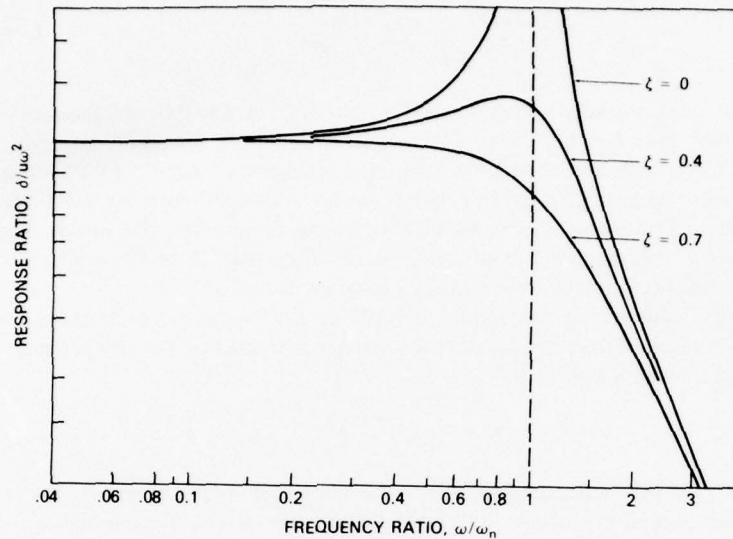
Fig. 2-2. Normalized response of an accelerometer

The response, shown in Fig. 2-2 indicates that the acceleration sensitivity is constant within practical limits at all frequencies up to 1/5 of the resonance frequency for accelerometers having damping values near to or less than 1/100 of critical damping. The ideal undamped accelerometer has a sensitivity increase of only 4.1% at the frequency equal to one-fifth of the resonance frequency. Manufacturers and users generally specify the operating frequency and range of an undamped accelerometer up to $\omega \leqslant 0.2\omega_n$ with a tolerance of ±5%. It is simple to design an accelerometer having near-zero damping; most have this ideal response over a variety of operating conditions (such as acceleration amplitudes and operating temperatures).

Accelerometers designed to have significant internal damping will have an extended range of flat frequency response. The response in Fig. 2-2 indicates that the sensitivity remains constant at frequencies up to about two-thirds of the resonance frequency if care is taken to maintain a damping value of $\zeta = 0.7$. A great deal of care is required of the accelerometer designer and user to maintain this value of damping under all amplitude and temperature conditions.

It is important to be aware of the sensitivity value at the resonance frequency. This is determined by evaluating Eq. (2-5) for its maximum value. When the damping ratio is equal to or less than 0.7, the maximum value of acceleration sensitivity is

$$\frac{\delta}{u\omega^2}\Bigg|_{max} = \frac{1}{2\zeta\sqrt{1-\zeta^2}}. \tag{2-6}$$

An undamped accelerometer having a value of ζ equal to 0.01 will increase its sensitivity by a factor of 50 or 34 dB at its resonance frequency. A damped accelerometer with a value of $\zeta = 0.7$ will have a sensitivity increase of 0.02% at its resonance frequency. It is desirable to select undamped accelerometers with resonance frequencies far above their operating frequencies; this avoids large outputs at the resonance frequency. Low-pass filters may be used in applications where significant resonance frequency excitation occurs.

The frequency of maximum response is the resonance frequency. The mathematical relationship between the resonance frequency and the undamped natural frequency is given by

$$f_r = f_n\sqrt{1-2\zeta^2} \tag{2-7}$$

where f_r is the resonance frequency. The resonance frequency equals the undamped natural frequency for undamped accelerometers. The resonance frequency is somewhat lower than the natural frequency for accelerometers having significant damping values.

The phase angle response of accelerometers is plotted in Fig. 2-3. this plot is obtained by inserting frequency values in Eq. (2-4), mostly below the resonance frequency. The response in Fig. 2-3 indicates that the phase angle is 0 degrees for the undamped accelerometer throughout its operating frequency range, which is below the resonance frequency. The phase angle of a damped accelerometer having a value of $\zeta = 0.7$ varies almost linearly with frequency throughout its operating frequency range. However, the phase angle variation with frequency is somewhat nonlinear for smaller values of damping, and it is desirable to maintain values of damping greater than 0.4 of critical damping. The damping value of 0.7 of critical damping is preferred because it provides linear phase response.

It is necessary to use either undamped accelerometers or damped accelerometers exhibiting linear phase angle response, to avoid waveform distortion in measuring complex vibrations or shock motions. Accelerometers having nonlinear phase angle response produce a nonuniform time shift of frequency components that represent the complex vibration or shock motion. This shifting produces waveform distortion. Accurate measurements of complex vibrations and shock motions are made with undamped accelerometers or damped accelerometers having damping values approaching 0.7 of critical damping.

Velocity Pickup Equations

Velocity pickups in common use are built with electrodynamic coils. The coil in a velocity pickup produces an electrical output proportional to velocity $\delta\omega$
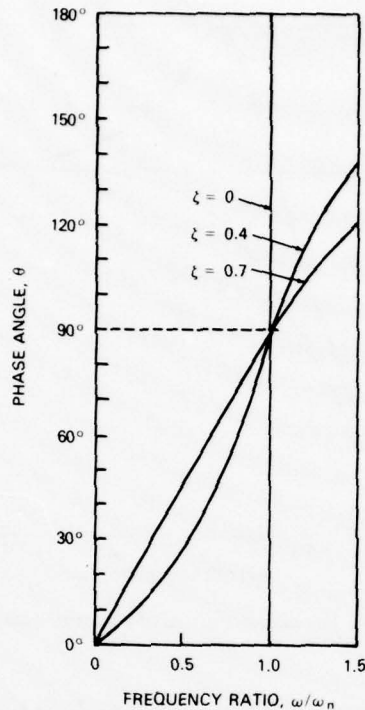
Fig. 2-3. Phase angle response of an accelerometer

relative to the case of the transducer. The ideal response of these velocity pickups is determined by solving Eq. (2-1) for the ratio $\delta\omega/u\omega$, as follows:

$$\frac{\delta\omega}{u\omega} = \frac{(\omega/\omega_n)^2}{\sqrt{(1 - \omega^2/\omega_n^2)^2 + 4\zeta^2(\omega/\omega_n)^2}} . \tag{2-8}$$

Equation (2-8), written in this form, describes the ideal response of a velocity pickup because the transducing element produces an electrical output proportional to $\delta\omega$. The left side of this equation has constant values for excitation frequency ω that are large compared to ω_n. In other words, the velocity pickup sensitivity (the ratio of its electrical output to the velocity $u\omega$ of the pickup base or moving part) is constant throughout the operating frequency range. This constant sensitivity occurs at frequencies above the resonance frequency. Note that ω could be canceled on the left side of Eq. (2-8). If this were done, the
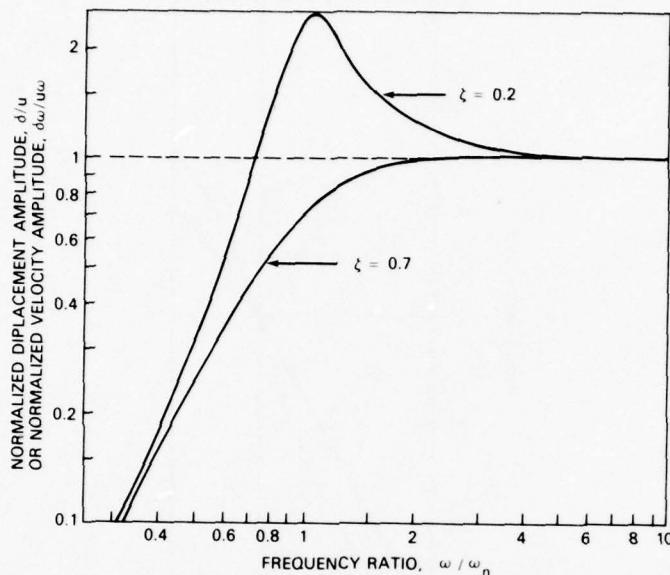
Fig. 2-4. Normalized response of a velocity transducer

ratio δ/u would represent a displacement pickup. Such a pickup would be built with a transducing element that produces output proportional to δ. The sensitivity of the displacement pickup would be constant at frequencies above resonance. Displacement pickups of this type are not in common use, however.

The values of the normalized velocity sensitivity are plotted in Fig. 2-4 for damping ratios $\zeta = 0.2$ and $\zeta = 0.7$. Usually velocity pickups are built with significant amounts of damping so that vibration measurements can be made at reasonably low frequencies close to the resonance frequency. Without significant damping, resonance frequency excitation would occur and cause waveform distortion or "bottoming" of the mass element to the case of the pickup. The sensitivity of a velocity pickup is constant at frequencies above three times the resonance frequency.

The maximum sensitivity of a velocity pickup is given by

$$\frac{\delta\omega}{u\omega}\bigg|_{max} = \frac{1}{2\zeta\sqrt{1-\zeta^2}}. \tag{2-9}$$
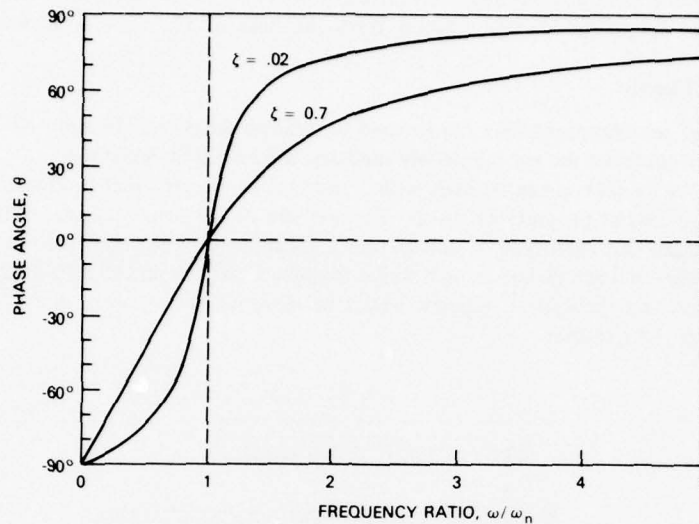
Fig. 2-5. Phase angle response of a velocity transducer

This computation from Eq. (2-8) indicates that the sensitivity increase by a factor of 2.5 at the resonance frequency when the velocity pickup has a damping value of $\zeta = 0.2$.

The equation for the resonance frequency is given by

$$f_r = \frac{f_n}{\sqrt{1 - 2\zeta^2}}. \tag{2-10}$$

This equation applied for damping values of less than 0.7 of critical damping. Velocity pickups with these values of damping have a resonance curve showing a normalized velocity sensitivity of more than unity and therefore have a resonance frequency. The resonance frequency is slightly higher than the natural frequency.

The phase angle response of the velocity pickup is illustrated in Fig. 2-5. It shows that when the transducer is operated in its normal operating range above f_n, the electrical output or mass element motion lags the motion of the driven case by close to 180 degrees. In other words, the mass element motion reaches the maximum value in the negative direction when the velocity pickup case reaches a maximum value in the positive direction. This characteristic has little significance in using or calibrating a velocity pickup except when it is desirable to identify the direction of motion of an object that is vibrating. It is good to

identify the electrical terminals to indicate positive electrical signal for positive velocity, defined as motion upward from the base of the velocity pickups.

Special Pickups

Other seismic transducers can be used to measure shock and vibration. These special transducers are not commonly used and will be briefly described.

A velocity pickup can be built with a transducing element that produces an electrical output proportional to the displacement of the mass element relative to its base. One such type of pickup uses a variable-reluctance transducing element. This velocity pickup is used in the frequency range at and near its natural frequency. Its theoretical response would be determined by solving Eq. (2-1) for ratio $\delta/u\omega$, so that

$$\frac{\delta}{u\omega} = \frac{\omega/\omega_n^2}{\sqrt{(1 - \omega^2/\omega_n^2)^2 + 4\zeta^2(\omega/\omega_n)^2}}. \qquad (2\text{-}11)$$
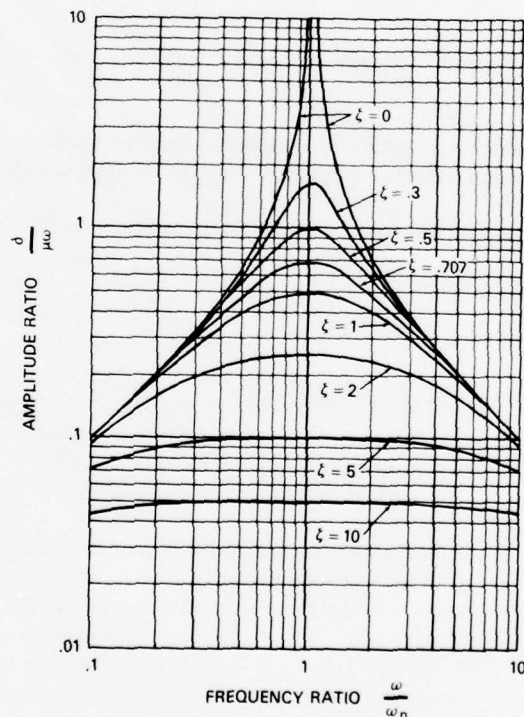
Fig. 2-6. Normalized response of a velocity transducer

Figure 2-6 gives the normalized sensitivity of a velocity pickup built with this type of transducer element. This velocity pickup may be used over a limited frequency range, up to at least twice its natural frequency if large values of damping are used.

A jerk pickup may be built with a transducing element that produces an electrical output proportional to the velocity of the mass element relative to its base. The theoretical response of such a pickup, used at frequencies far below the resonance frequency, is given by the right side of Eq. (2-5) and is illustrated by Fig. 2-2. Both the numerator and denominator of the left side of Eq. (2-5) are multiplied by ω to describe a jerk pickup. A transducer of this type could use an electrodynamic coil as a transducing element. This jerk pickup would have constant sensitivity at frequencies up to at least one-fifth of its resonance frequency.

2.3 Shock Motion Response

Several factors must be considered in making shock motion measurements and calibrations, including the resonance frequency and frequency response of the transducer at both high and low frequencies. The shock motion pulse shape and duration determine the frequency requirements. The natural period of an accelerometer must be much smaller than the pulse duration. Its low-frequency time constant must be large compared to the pulse duration. These characteristics are determined by examining the theoretical response. The theoretical response is described for the half-sine pulse most frequently used in shock calibrations. This response is similar to that of other shock motion pulses that occur in practice, such as triangular shaped pulses.

Resonance Frequency Response

The resonance frequency of an accelerometer is excited to some small amplitude during shock motion calibrations. It is preferable when calibrating and using accelerometers to have a relatively long pulse duration compared to the natural period of the accelerometer. The response, for a pulse duration selected to demonstrate resonance frequency excitation, is given in Fig. 2-7. For a pulse duration of three times the accelerometer's natural period the peak of the resonance frequency response is 17% higher than the peak value of the pulse. The actual calibration error is quite small, however, if care is taken to fair a line through the resonance frequency response. Resonance frequency excitation is insignificant if the accelerometer selected has a natural period of less than about one-fifth the pulse duration or if it has internal damping of about 0.7 of critical damping.
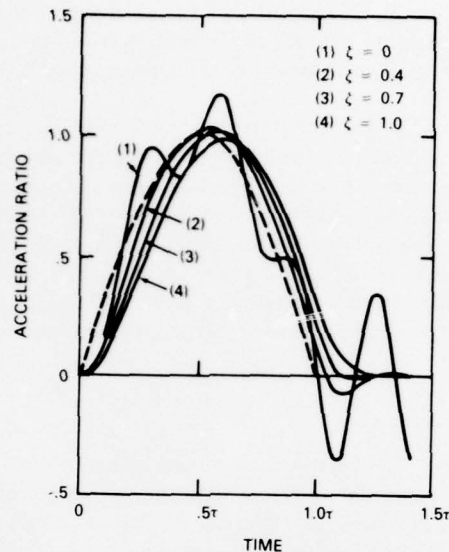
Fig. 2-7. Response of an accelerometer subjected
to half-sine shock pulse with a duration of three
times the natural period [11]

High-Frequency Response

For accurate shock motion measurements it is necessary to consider the Fourier components of the shock motion pulse. Care must be taken with damped accelerometers to ensure that the sensitivity is constant at frequencies corresponding to the frequency content of the pulse. In undamped accelerometers sensitivity is constant, because the accelerometers are selected to have a very high resonance frequency.

Fourier spectra for a half-sine pulse are given by Fig. 1-6. The frequency component at twice the reciprocal of the pulse duration is 23 dB smaller than the components at very low frequencies. Accordingly, when using damped accelerometers, it is necessary to select one that has constant sensitivity at frequencies up to at least the reciprocal of the pulse duration. It is important to perform frequency response and resonance frequency calibrations on accelerometers and velocity pickups, to demonstrate that the sensitivity is constant at high frequencies corresponding to the main frequency components of the shock motion pulse.
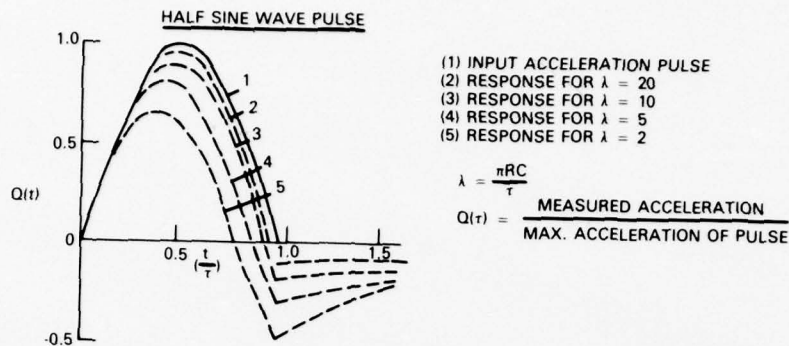
Fig. 2-8. Response of acceleration systems with various RC time constants to a half-sine shock pulse

Low-Frequency Response

Accelerometers, amplifiers, and signal conditioners must be carefully selected to ensure adequate low-frequency response. If accelerometer sensitivity is not constant at sufficiently low frequencies, the shock motion pulse will not be accurately measured and undershoot will occur after the pulse is terminated. This is illustrated in Fig. 2-8. This response indicates the need to select amplifiers used with piezoelectric accelerometers depending on the low-frequency requirements in the test application. These amplifiers roll off at frequencies below about 2 Hz. Large errors are avoided only if the reciprocal of the frequency at which amplifier output is down 3 dB is large compared to the pulse duration. These errors will be 3% when this reciprocal is at least twice the pulse duration.

Similar rules must be applied to velocity pickups used for shock motion measurements. The resonance frequency must be low enough that the sensitivity is constant at sufficiently low frequencies. In piezoresistive and wire strain-gage accelerometers, sensitivity is constant to zero frequency and low-frequency distortion does not occur.

CHAPTER 3
TRANSDUCERS AND AUXILIARY INSTRUMENTS

Transducers for measuring vibration and shock motion are built using electromechanical elements such as piezoelectric ceramics, piezoresistive and wire strain gages, variable capacitors, inductive elements, mechanical recording devices, and optical systems. It is useful to understand the characteristics of these elements as well as to evaluate the effects of various environments on these characteristics. Some of the transducers can measure low-frequency vibrations, including static accelerations. Others measure vibrations over a very wide frequency range, at both low and extremely high frequencies. These and other performance characteristics provide a basic description of the operating characteristics of accelerometers, velocity pickups, and displacement measuring instruments.

Several environmental factors may affect shock and vibration measurements. A description of the effects of temperature, transverse and rotational motions, mounting effects, strain, and high-intensity acoustic noise on the transducers provides further insight into their operating characteristics. These effects may affect measurement accuracy. Accordingly, some quantitative information is necessary to ensure that errors caused by the environment are reasonably small. In the calibration laboratory environmental effects are carefully minimized by selecting good-quality calibration shakers and shock calibrators to eliminate unneccessary calibration errors.

In our missile and space development programs it became apparent that miniature accelerometers were needed for accurate vibration and shock motion measurements in many applications. The piezoelectric accelerometer is a highly developed instrument and satisfies many of the requirements for accurate measurements. Piezoresistive and wire strain gage accelerometers accurately measure long-duration shock motions and vibrations down to zero frequency. Piezoresistive accelerometers have the advantage of high sensitivity, which indirectly extends their operating ranges to relatively high frequencies.

The principal use of inductive transducing elements is in velocity pickups.

All accelerometers and velocity pickups, regardless of the sensing element employed, operate according to the theory of seismic transducers.

3.1 Piezoelectric Accelerometers

Piezoelectric materials generate an electrical charge when subjected to a deformation or mechanical stress. The Greek word *piezein* means to squeeze or press. This effect was discovered about a century ago by Jacques and Pieree Curie,

33

who found that materials such as quartz, Rochelle salt, and tourmaline exhibit piezoelectricity. Some modern-day accelerometers are built with quartz. Their principal advantage is freedom from most temperature effects over quite wide temperature ranges.

Most accelerometers are built with piezoelectric ceramics, such as lead zirconate titanate and a variety of other ceramics. Accelerometers built with ceramics are very sensitive and are less prone than other types to exhibit errors in severe environments. Most accelerometers are usable in almost any temperature environment encountered in practice. Special ceramics are used in accelerometers for use at extremely high temperatures in excess of 600°C (112°F).

Basics of Piezoelectric Materials

To visualize piezoelectricity, consider a crystal as illustrated in Fig. 3-1 [13]. Each unit cell has a dipole resulting from a difference between the location of positive and negative charges in a unit cell. A crystal composed of identical unit cells will produce electrical charges as the crystal is squeezed or stretched in a direction parallel to the dipole. These charges appear on the surfaces of the crystal, and electrodes are attached to conduct the charges. A positive charge appears when the crystal is squeezed or compressed. A negative charge appears when the crystal is extended or, if the crystal is preloaded, as a result of a reduction in compressive stress.
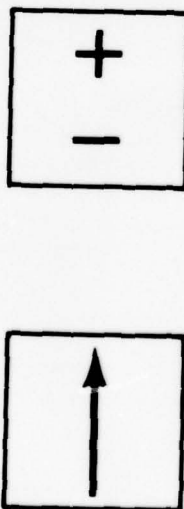
Fig. 3-1. Unit cells in piezoelectric crystal material

Ferroelectric materials are used to make piezoelectric ceramics. The ceramic is composed of a multitude of crystals, polarized by a strong d.c. field. This alines most of the dipoles parallel to the direction of the field. Care is taken in fabrication of the ceramics, including appropriate aging processess to ensure extreme stability of the piezoelectric properties. The piezoelectric properties should remain virtually unchanged with time as long as excessive environments are avoided. If changes in characteristics occur, they are usually catastrophic and are caused by exposure to environments far exceeding rated specifications. The piezoelectric constants of the material determine the amount of electrical charge generated by particular types of mechanical stress. Piezoelectric accelerometers are designed to use compressive, shear, or bending stresses. Tensor notation is used to identify the stress applicable to each piezoelectric constant.

Piezoelectric accelerometers built with polarized ceramics make use of the d_{33} piezoelectric constant. This peizoelectric constant and the compressive stress on the ceramic element are illustrated in Fig. 3-2a. The ceramic is polarized, and the z-direction electrodes are placed on top and bottom surfaces described in Fig. 3-1a. Subsequently when a compressive stress τ_{zz} is applied, a positive electrical charge is generated and measured by appropriate electronic instruments connected to the top and bottom surfaces of the ceramic element. The term τ_{zz} describes the mechanical stress consisting of a force applied in the z direction. This force acts on a cross-sectional area described by z equal to a constant. In the compression-type accelerometer the force is produced as a result of inertial loading of the mass element placed on top of the ceramic in addition to the inertial loading of the mass of the ceramic element on itself.

Compressive-type accelerometers built with quartz crystals use the d_{11} piezoelectric constant. This piezoelectric constant is applicable because X-cut quartz is used. The operating principles are the same as those described for ceramics using the d_{33} constant. However, these two types of accelerometer are quite different in performance because of differences in the piezoelectric constants.

Compression accelerometers may also be built by applying a τ_{xx} stress to a ceramic polarized in the z direction. Figure 3-2b illustrates a ceramic element using the d_{31} piezoelectric constant, which is used by applying a compressive stress consisting of force applied in the x direction on a cross-sectional area described by x equal to a constant. This ceramic element is polarized in the z direction, and the electrodes are attached to the top and bottom surfaces described by z equal to a constant, in order to measure the electrical charge generated as a result of the τ_{xx} stress.

Shear-type accelerometers use the d_{15} piezoelectric constant. This constant is illustrated in Fig. 3-2. The ceramic element may be in the shape of a hollow cylinder or a flat plate. It is polarized by applying a strong d.c. electrical field in the z direction. Subsequently, electrodes are applied to the surfaces described by x equal to a constant. The d_{15} piezoelectric constant is used when this ceramic element is subjected to shear stress τ_{zx}. This shear stress is produced by applied
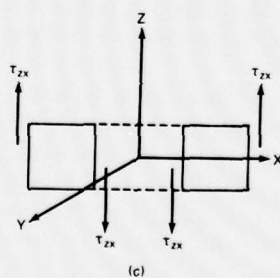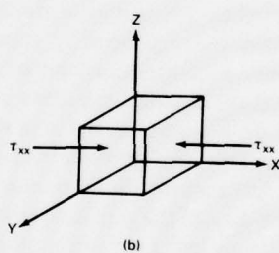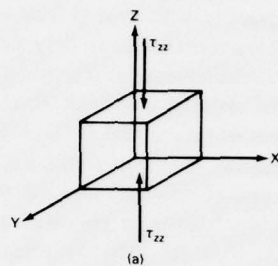
Fig. 3-2. Designation of stresses on piezoelectric ceramics

Table 3-1. Typical Values of Piezoelectric Constants

Material	d_{33} (pC/N)	d_{15} (pC/N)	Curie Temperature $(°C)$
Lead Zirconate Titanate	260	460	370
Endevco P-10	18	22	480
Endevco P-15	6	68	1200
Quartz	2*	—	570
Barium Titanate	148	225	120

*d_{11} piezoelectric constant.

Source: Ref. 14.

force in the z direction, as indicated by the arrows in Fig. 3-2c, across surfaces of x equal to constants. The electrical charges generated are measured with suitable instruments by making electrical connections to the surfaces described by x equal to constants.

Most piezoelectric accelerometers are designed to use one of the above piezoelectric constants of some materials [14] are listed in Table 3-1. (Curie temperature is the temperature at which the ceramic becomes depolarized.) The piezoelectric constants of lead zirconate titanate are much higher than corresponding constants for barium titanate and quartz. It also happens that the piezoelectric constant of lead zirconate titanate remains almost constant over a rather broad temperature range. Most accelerometers are built with lead zirconate titanate or other proprietary ceramics exhibiting good piezoelectric properties. Some are built with quartz, particularly those intended for use in special applications.

Temperature variations produce two effects in piezoelectric materials. Very large changes in temperature cause changes in the piezoelectric constant, which in turn causes a change in the sensitivity of the accelerometer. These changes are instantaneous and are known for each operating temperature. Upon return to room temperature, the piezoelectric constant returns to its original value. The second effect of temperature is known as pyroelectricity. An electrical charge is generated when the crystal material is subjected to a temperature transient. This charge superimposes itself on the charge generated due to piezoelectricity. Fortunately, temperature changes are very gradual in almost all applications, so that pyroelectric effects can be virtually eliminated by proper selection of signal conditioners having suitable roll-off characteristics at very low frequencies.

Accelerometer Construction

Most accelerometers are built with piezoelectric materials fabricated as hollow cylinders, thin circular disks, or flat plates. Compression and shear ac-
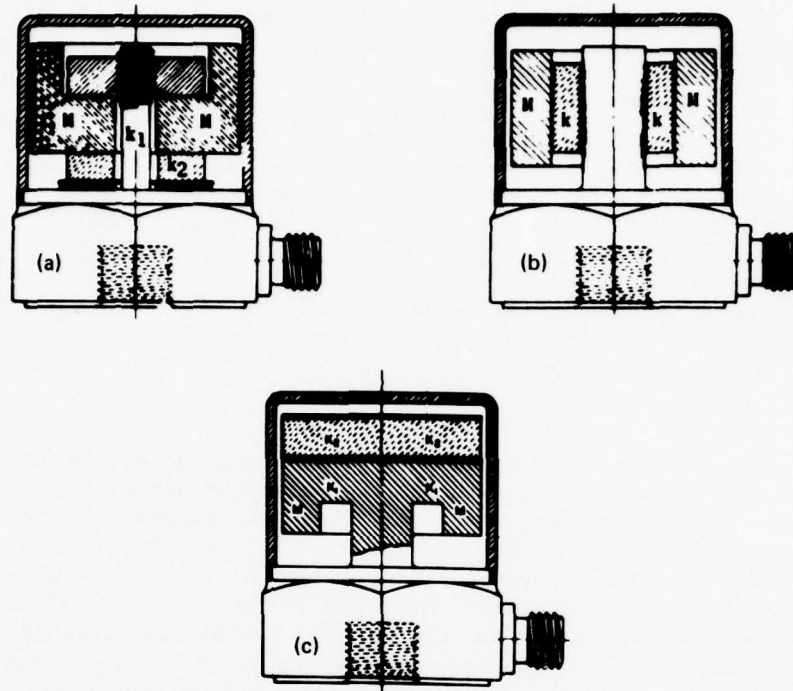
Fig. 3-3. Cross sections of typical piezoelectric accelerometers: (a) compression, (b) shear, (c) bender (Endevco)

celerometers are in very common use. Also, some accelerometers are built using the ceramic element in bending, which produces tensile and compressive stresses on the top and bottom surfaces of thin ceramic elements.

The compressive- and shear-type accelerometers shown in Figs. 3-3a and 3-3b measure shock and vibration in the direction of their axis of symmetry, which is perpendicular to the bottom of the accelerometer. When the accelerometer is moved upward the mass tends downward, toward the bottom of the accelerometer. Downward motion of the accelerometer case tends to move the mass upward. In shear-type accelerometers, this upward and downward motion applies a shear stress to the piezoelectric ceramic (k), which is cemented inside the mass element (M). Both the mass element and the piezoelectric ceramic are cylindrical. The ceramic is also attached with cement to the central post, which forms a part of the base of the accelerometer. The mass element does not touch the outer case. In this shear accelerometer design, the only stresses applied to the crystal are the dynamic stresses produced when the case is move as described above.

The compression accelerometer has a compressive static preload applied to

piezoelectric ceramic k_2. The preload is applied by tightening the nut connected to the top of post k_1. The static tension preload in the post equals the static compression preload in the ceramic. The static preloads are selected so that they greatly exceed the highest dynamic stress produced when the accelerometer case is subjected to a shock or vibration motion. Upward motion of the case produces an inertial force in the mass element, which increases the compression stress on the ceramic. Conversely, downward motion decreases the compressive stress on the ceramic.

The accelerometer illustrated in Fig. 3-3c produces bending stresses in ceramic element k_2. Essentially, the piezoelectric ceramic acts as a strain gage attached to the circular metallic structure. When the accelerometer is moved upward, mass element M tends to move downward and radial tensile stresses are produced in the ceramic. Downward motion of the accelerometer case tends to move the mass upward and produce compressive radial stresses in the ceramic. An electrical charge is generated in the ceramic by these radial stresses.

All piezoelectric accelerometers are self-generating and require no electrical excitation. The electrical charge generated on the ceramic is given by the following equations:

$$Q = d\sigma A \text{ coulombs} \qquad (3\text{-}1)$$

where

    d = piezoelectric constant of the crystal
    A = stressed area on the crystal
    σ = stress on the crystal,

and

$$Q = C_1 \delta \text{ C} \qquad (3\text{-}2)$$

where

    C_1 = constant determined by the above equation and by the specific accelerometer design
    δ = deflection of mass element relative to the accelerometer base.

The piezoelectric constant d used depends on the accelerometer type. Shear accelerometers use d_{15}, and compression accelerometers use d_{33} or d_{11}. The numerical values of these piezoelectric constants are determined by the piezoelectric material.

The acceleration sensitivity of many accelerometers can be accurately computed from the mass properties of the ceramic and mass element. The product σA equals the inertial force of the mass acting on the piezoelectric material. The inertial force is the product of effective mass M times the acceleration applied to

the accelerometer. The acceleration sensitivity is expressed as the charge output divided by the acceleration (measured in g units), and the following equation applies:

$$S = \frac{Q}{g} = dM .$$ (3-3)

For example, the d_{33} constant for a particular lead zirconate titanate ceramic is 260 pC/N (1157 pC/lbf). An accelerometer having an effective mass of 10 g and using a single piezoelectric element in compression would have an acceleration sensitivity of 26 pC/g, where g is the acceleration of gravity, 9.8 m/s^2 (386 in./s^2).

Signal Conditioners

The piezoelectric material is a capacitor whose capacitance is determined by the dielectric constant. The electrical impedance of a piezoelectric accelerometer becomes extremely large at low frequencies. Accordingly, suitable circuitry must be used on the input of the signal conditioner, to allow flat frequency response at the lowest frequency of interest. The charge amplifier is designed to provide constant gain throughout the operating frequency range. Voltage amplifiers with high input impedances are still used in some laboratories. Also, special signal conditioners such as source followers and impedance converters are used in special applications.

Charge Amplifiers. Charge amplifiers are used to measure the output of piezoelectric accelerometers throughout their operating frequency ranges. A schematic of a charge amplifier is shown in Fig. 3-4.

The output of the charge amplifier is given by the following equation:

$$E_o = \frac{-S_q A}{(C_p + C_L) + (1 + A)C_f + 1/j\omega R_s}$$ (3-4)

where

E_o = charge amplifier output per unit g
S_q = acceleration charge sensitivity of the accelerometer
A = amplifier gain
C_p = capacitance of the piezoelectric material
C_1 = capacitance of the connectors and cable
C_f = feedback capacitance used in the charge amplifier
j = imaginary vector
ω = circular frequency
R_s = shunt resistance of the accelerometer and cable.

Typical values for accelerometers and charge amplifiers include 1000 for the amplifier gain, 1000 pF for the accelerometer and cable capacitance, 1000 pF for the feedback capacitor, and 10 $M\Omega$ for the shunt resistance. Substituting these values in Eq. (3-4) shows that the output voltage is nearly equal to the charge divided by the feedback capacitance. Accordingly, Eq. (3-4) is simplified as follows:

$$E_o = -\frac{S}{C_f} V/g. \tag{3-5}$$

This ratio remains nearly constant even when extremely long cables are used between the accelerometer and the charge amplifier.

The time constant applicable to the schematic in Fig. 3-4 is given by

$$T = 1/2\pi f_c = R_s[C_p + C_L + (1 + A)C_f] \tag{3-6}$$

where f_c = the frequency at which the response is down 3 dB and the other terms are as listed above. Equation (3-6) indicates that the time constant is extremely large and the amplifier response would normally be flat to frequencies much less than 1 Hz. However, it is desirable to eliminate quasi-d.c. outputs, which can be produced in the accelerometer by pyroelectric effects. For most shock and vibration applications, flat frequency response is required only at

EQUIVALENT
TRANSDUCER
CIRCUIT   CHARGE CONVERTER
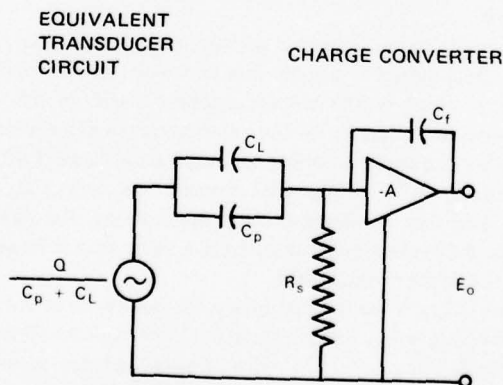
Fig. 3-4. Simplified schematic of a typical piezo-electric transducer connected to a charge converter (amplifier)

frequencies down to about 2 Hz. In some applications it is desirable to limit the flat response to frequencies somewhat above 5 Hz. One of the advantages of the charge amplifier is that any desired low-frequency response can be achieved in the amplifier design. For example, a feedback resistor R_f put in parallel with the feedback capacitor has a time constant of $R_f C_f$. For applications involving shock motions, this time constant should be long in comparison with the duration of the shock motion pulse.

Voltage Amplifiers. In the past only voltage amplifiers and cathode followers were available for use with piezoelectric accelerometers. With these instruments, it is necessary to use the voltage sensitivity of the accelerometer,

$$E_s = \frac{S_q}{C_p + C_L + C_a} \tag{3-7}$$

where

E_s = voltage sensitivity of the accelerometer
C_a = input capacitance of the voltage measuring instrument.

One of the precautions necessary in using voltage measuring instruments with a piezoelectric accelerometer is that it is difficult to achieve adequate low-frequency response for certain applications.

The low-frequency response of the cathode follower is determined simply by the product of the frequency (in hertz) times the input resistance of the cathode follower (in ohms) times the total capacitance of the accelerometer, cable, etc. (in farads). The frequency response is flat only when this fRc product is equal to or greater than one. At frequencies at which this product is less than one, the response decreases. For example, the response is down 3 dB when fRC equals about 0.16.

It is also necessary to consider this product when using other voltage amplifiers. However, the product is usually less than one only at frequencies below the low-frequency cutoff of the voltage amplifier itself. In this case, the low-frequency response characteristic of the amplifier is the determining factor. It is important that the frequency at which the response is down 3 dB, as a result of either the voltage amplifier or the fRC characteristic, occur at a low enough frequency. For example, in shock motion applications, the reciprocal of the frequency of the 3-dB-down point must have a value that is large compared to the duration of the shock motion pulse.

It is important to know the low-frequency characteristics of voltage amplifiers and cathode followers when making sinusoidal and random vibration measurements at frequencies below 50 Hz. When low-capacitance accelerometers are used, the response of cathode followers falls off rapidly at low frequencies. In addition to the flat-frequency requirement, it is necessary for the phase shift of the amplifier to vary linearly with frequency. This phase-shift requirement is not met in voltage amplifiers that have poor low-frequency response. Accordingly,

such amplifiers distort the accelerometer output in random vibration and shock motion measurements.

In addition to the low-frequency response problem with voltage amplifiers and cathode followers, it is necessary to determine the change in sensitivity brought about by changing cables. The output decreases as the capacitance in parallel with the accelerometer is increased. When cables are changed, it is necessary to compute the new sensitivity from Eq. (3-7) or to recalibrate the accelerometer.

Impedance Converters. Specialized integrated circuit elements are built into the cases of accelerometers to provide low impedance at the electrical output terminals. A monolithic integrated circuit amplifier (Fig. 3-5) is shown connected in an impedance converter for use with piezoelectric transducers [16]. The integrated circuit amplifier, and the source resistor and attenuating capacitor in parallel with the piezoelectric crystal element, are built into the accelerometer case as shown in Fig. 3-6 [16]. A coaxial cable connects the piezoelectric accelerometer to the source resistor and power supply. Connecting the source resistor to the power supply permits the use of a two-wire system, such as the coaxial cables normally used with accelerometers. The circuit operation is similar to a conventional voltage-type piezoelectric system. The charge generated on the piezoelectric elements forms a voltage at the amplifier input gate on the parallel combination of crystals, electrodes, and transistors. The amplifier converts this signal to a voltage change at its output, of equal amplitude and with the same polarity. The amplitude range of the accelerometer is usually determined by the attenuating capacitor in parallel with piezoelectric element.

Although specialized signal conditioners of this type are useful in certain applications, two limitations must be considered. First, the dynamic range is decreased because of the difficulty of changing amplifier gain to make convenient
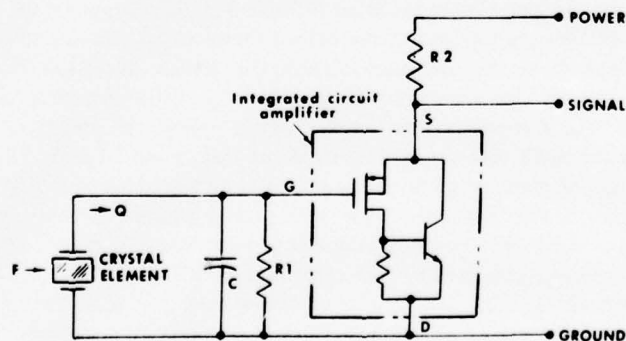
Fig. 3-5. Schematic of a typical piezoelectric transducer with an internal integrated circuit amplifier
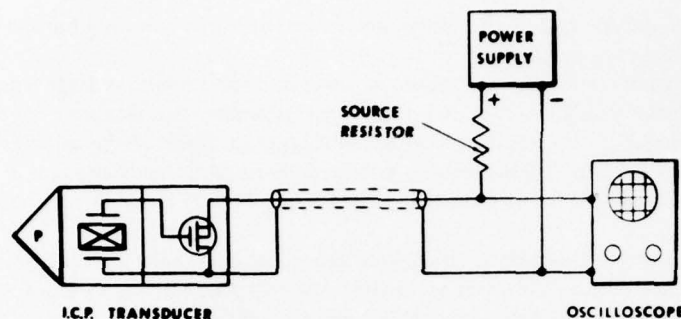
Fig. 3-6. Typical instrument connections for a piezoelectric transducer with internal electronics [16]

acceleration range changes. Second, the high-frequency response is restricted by the limited current capability of the integrated circuit amplifier.

Performance Characteristics

Performance characteristics of some piezoelectric accelerometers remain unchanged whether a charge or voltage amplifier is used. These characteristics include frequency response, resonance frequency, and amplitude linearity for accelerometers manufactured with quartz and certain proprietary ceramic materials. Accelerometers made with lead zirconate titanate ceramic have slightly different frequency response and resonance frequency characteristics when charge and voltage amplifiers are used. Except for quartz, the temperature response of most accelerometers is somewhat different when charge and voltage amplifiers are used.

Acceleration Sensitivity. The typical acceleration sensitivities for various piezoelectric accelerometers are listed in Table 3-2. For simplicity, the acceleration sensitivities are rounded to the nearest factor of 10. The acceleration sensitivity depends on the particular accelerometer design. Accelerometers can be built to have various sensitivities simply by using different ceramic and mass elements. For example, shear accelerometers using lead zirconate titanate ceramics are made with sensitivities of about 1 pC/g and 10 pC/g. Usually the shear accelerometers are made with one or two ceramic elements. Compression accelerometers are frequently made with several ceramic elements connected electrically in parallel. Therefore, the charge sensitivity is determined from the sum of the charge generated by each ceramic element.

Accelerometers built with lead zirconate titanate ceramics have the highest acceleration sensitivity. Accordingly, they have many applications, including measurement of relatively low accelerations.

Quartz accelerometers have the lowest available acceleration sensitivity.

Accelerometers made with Endevco Piezite ® 10* ceramic have acceleration sensitivities between those obtained the other two crystal materials, as shown by Table 3-2.

Frequency Response. Typical frequency response characteristics of various accelerometers are shown in Fig. 3-7.

The charge sensitivity of an accelerometer using P-6[†] and P-8[†] ceramic materials decreases about 1% for each octave increase in frequency. This is typical of lead zirconate titanate accelerometers. It happens that the capacitance of these accelerometers has the same frequency characteristic. Therefore, if the voltage sensitivity of the accelerometer is desired, the charge sensitivity at the frequency of the capacitance measurement is divided by the sum of the accelerometer capacitance, cable capacitance, and other capacitances that are connected across the accelerometer. Use of charge amplifiers eliminates the need for this computation. Accelerometers built with P-10[†] ceramic material and quartz do not have this frequency characteristic; both the charge and voltage sensitivities are constant at all frequencies up to about one-fifth the resonance frequency. As with all accelerometers, the increase in sensitivity at high frequencies is due to the resonance frequency.

It should be pointed out that the frequency response of all accelerometers is flat in a manner similar to the P-10 curve in Fig. 3-7 when voltage amplifiers with extremely small capacitances are connected between the accelerometer and the amplifier. With small external capacitances, the accelerometer experiences a

Table 3-2. Sensitivity of Piezoelectric Accelerometers

Crystal Material	Design Mode	Capacitance (pF)	Acceleration Sensitivity	
			Charge (pC/g)	Voltage (mV/g)
Lead-Zirconate-Titanate	Shear	1000	1-10	1-10
	Compression	1000-10 000	10-100	10-100
Quartz	Compression	100	1	10
Endevco P-10	Shear	100	0.1	1
	Compression	1000	1-10	1-10

Source: Ref. 15.

*"Piezite" is a registered trademark of Endevco, San Juan Capistrano, Calif.
[†] P-6, P-8, and P-10 are proprietary materials made by Endevco, San Juan Capistrano, Calif.
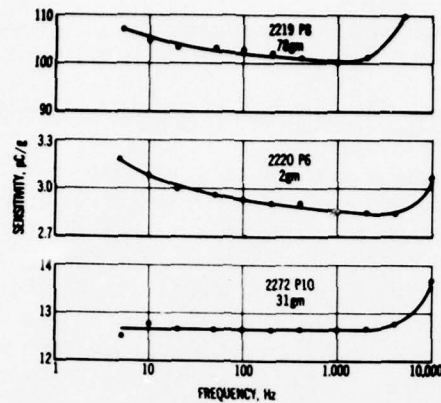
Fig. 3-7. Charge frequency response characteristics for three piezoelectric accelerometers of various designs and crystal materials

virtual open-circuit condition. However, if the external capacitance, including the cable capacitance, is near or larger than three times the accelerometer capacitance, the accelerometer experiences a virtual short-circuit condition. Therefore, with large external capacitance the response of all accelerometers is identical whether voltage or charge amplifiers are used, and the curves in Fig. 3-7 apply. If the external capacitance has a value between one and three times the accelerometer capacitance, the response of lead zirconate titanate accelerometers using voltage amplifiers will be somewhere between the two lower curves in Fig. 3-7. In other words, sensitivity decreases a fraction of 1% per octave increase in frequency; the fraction is determined by the amount of external capacitance.

Charge amplifiers are used for most shock and vibration measurements, and the curves in Fig. 3-7 apply. Corrections for the lack of flat frequency response are usually not made.

It is good practice to consider the accuracy desired and select the accelerometer type and resonance frequency to make corrections of the data unnecessary.

Resonance Frequency. The resonance frequency of an accelerometer varies slightly, depending on the rigidity with which the accelerometer is mounted. Typical variations in resonance frequency are shown in Fig. 3-8. The most rigid mounting and highest resonance frequency are achieved by using metal studs with lubricated surfaces or by cementing the accelerometer in place. For example, the resonance frequency is 34 400 Hz in Fig. 3-8a and 34 300 Hz in Fig. 3-8d. With completely dry surfaces, using a metal stud can decrease the resonance frequency to 31 040 Hz, as in Fig. 3-8b; using an insulated stud can further reduce it to 20 150 Hz, as in Fig. 3-8c. These variations in resonance frequency are typical of many piezoelectric accelerometers when various mounting techniques are used.
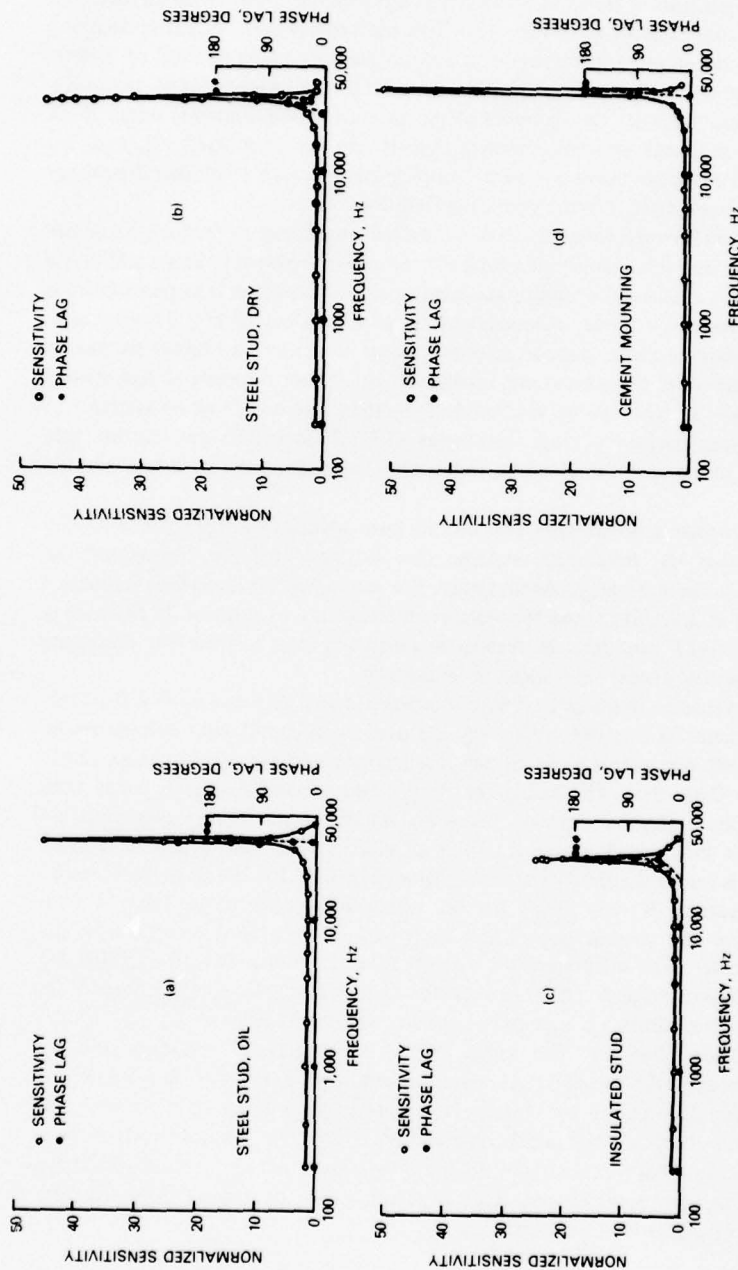
Fig. 3-8. Resonance frequency measurements on a piezoelectric accelerometer, determined with different mounting conditions: (a) steel stud using a thin film of light oil, (b) steel stud with mounting surface degreased, (c) insulated mounting stud, and (d) attached with Eastman 910 cement without any stud [17]

The magnification factor at resonance is significantly lower when an insulated mounting stud is used, as in Fig. 3-8c. This indicates that the effective damping of the accelerometers increased. The approximate damping is 0.02 of critical damping when the insulated stud is used, and 0.01 for other types of mounting. For practical purposes the damping of piezoelectric accelerometers under these mounting methods is small enough that it can be considered nil, and the theoretical response curve for zero damping can be used to predict frequency response characteristics in the operating frequency range.

Some accelerometer designs have additional resonances at frequencies above the normal operating range but below the resonance frequency. These additional resonances, called local or minor resonances, exhibit themselves as perturbations when resonance frequency measurements similar to those of Fig. 3-8 are made. These deviations from normal response occur over only a narrow frequency band at the local resonance and usually do not affect response at frequencies significantly below or above this band. They therefore do not affect response in the operating frequency range. Examples of local resonances include the plate and shell resonances found when thin-walled cases are used to house accelerometers.

Accelerometers are usually selected to have sufficiently high resonance frequencies that the frequency response can be considered flat throughout the operating frequency range. Accordingly, the accelerometer resonance frequency should be at least five times the maximum frequency of interest. If this rule is followed, slight variations in resonance frequency due to different mounting methods and any local resonance can be ignored.

The resonance frequency of accelerometers made with quartz and P-10 materials remains unchanged when they are used open circuit with voltage amplifiers or with the virtual short-circuit condition due to the use of charge amplifiers (see Table 3-3). The resonance frequencies of accelerometers made with lead zirconate titanate ceramic decreases slightly when charge amplifiers are used. This indicates that the modulus of elasticity of lead zirconate titanate ceramics is less in the short-circuit condition. The fact that the decrease in resonance frequency is only 0.6% for one shear accelerometer in Table 3-3 indicates that the ceramic contributes only part of the effective stiffness of the accelerometer. The differences in magnification factors indicated in Table 3-3 are considered insignificant. It is expected that damping in accelerometers does not depend on whether charge or voltage amplifiers are used.

Amplitude Linearity. The sensitivity of piezoelectric accelerometers increases linearly with increasing acceleration, as shown in Fig. 3-9. The amount of the increase depends on the piezoelectric material used in the accelerometer and also on the design of the accelerometer. Accelerometers designed to have relatively low dynamic stress applied to the crystal have relatively small sensitivity increases at high accelerations. This is accomplished by the use of small mass elements in such accelerometers.

Table 3-3. Typical Resonance Frequency Characteristics of
Piezoelectric Accelerometers Using Voltage and Charge Amplifiers

Accelerometer Type	Crystal Material	Resonance Frequency			Magnification Factor	
		Open-Circuit Voltage (kHz)	Short-Circuit Charge (kHz)	Change (%)	Open-Circuit Voltage	Short-Circuit Charge
Compression	Lead-Zirconate-Titanate	30.84	29.65	-3.9	57	33
Compression	Lead-Zirconate-Titante	15.40	14.92	-3.1	70	62
Shear	Lead-Zirconate-Titanate	34.2	33.0	-3.5	38	66
Shear	Lead-Zirconate-Titanate	32.2	32.0	-0.6	35	35
Compression	Quartz	32.2	32.2	0.0	23	24
Compression	Endevco P-10	29.6	29.6	0.0	45	47

Source: Ref. 15.

Similarly, when large mass elements are used, the dynamic stresses are relatively large and the increase in sensitivity at high accelerations is significant for some accelerometers. For example, a lead zirconate titante accelerometer having a charge sensitivity of 10 pC/g increases its sensitivity 1% for each 250-g increase in acceleration, whereas a similar accelerometer with a smaller mass element and a sensitivity of 1 pC/g increases its sensitivity only 1% per 2500 g. Sensitivity increases of accelerometers made with P-10 are significantly less, as indicated by Fig. 3-9. Amplitude linearity errors are insignificant in shock and vibration applications, provided accelerometers are selected to have low sensitivity when measuring relatively high accelerations.

Temperature Response. The sensitivity of a piezoelectric accelerometer changes with temperature. These changes can be attributed solely to variations in the piezoelectric constant of the crystal material, provided that care has been taken in the design of the accelerometer. Typical sensitivity variations due to temperature are shown in Fig. 3-10. The variations are quite small for accelerometers made with P-10 ceramic or quartz. The operating temperature range is highest for accelerometers made with P-10 ceramics.
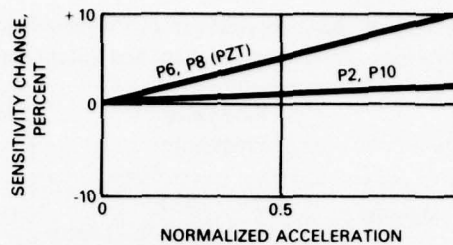
Fig. 3-9. Typical increases in sensitivity of piezo-
electric accelerometers with increase of accelera-
tion [15]
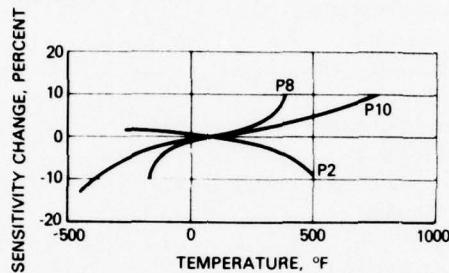
Fig. 3-10. Typical temperature response charac-
teristics: changes in charge sensitivity of piezo-
electric accelerometers using different crystal
materials [15]

Modulus-of-elasticity and damping changes in accelerometer materials are
relatively small throughout the operating temperature range. For this reason, the
resonance frequency of an accelerometer changes only very slightly over the
operating temperature range. Since accelerometers are used only at frequencies
up to one-fifth the resonance frequency, their frequency response is constant
at all temperatures.

Usually it is unnecessary to correct data for changes in sensitivity at various
temperatures. It is good practice to select accelerometers that have small enough
sensitivity changes over the desired temperature range that such correction is
unnecessary. Possible exceptions to this rule are measurements below about
-184°C (-300°F) and above about 260°C (500°F) where the changes exceed 5%.

The capacitances of most piezoelectric accelerometers change with tempera-
ture. The capacitance change of a good-quality accelerometer is about twice the
charge sensitivity change as a function of temperature. The voltage sensitivity
equals the charge sensitivity divided by the capacitance. Therefore, when voltage
amplifiers are used the sensitivity varies significantly as external capacitance

changes. This is one reason why charges amplifiers are preferred for use with piezoelectric accelerometers.

Environmental Effects

Environmental effects concern the extremes to which an accelerometer can be exposed without permanent changes in performance characteristics. Also, certain environments can cause error signals in the accelerometer output when shock and vibration measurements are made. One reason for identifying the characteristics discussed below as environmental effects is that it is usually not practical to correct data for errors produced by the environment. However, if accelerometers are properly used, environmental errors should be insignificant. Measurement errors are avoided by recognizing the environmental effects and taking certain precautions in the use of accelerometers.

Transverse Sensitivity. The sensitivity axis of the crystal in an accelerometer deviates slightly from being perfectly perpendicular to the mounting surface. This results from practical limitations in fabricating ceramic materials and machining of the various accelerometer parts. In addition, static preload stresses are applied to the crystal in some accelerometer designs, and these tend to change the poled axis of the crystal slightly. These effects combine in the accelerometer so that it produces some output as a result of excitation in a direction parallel to the mounting surface on the accelerometer. This transverse sensitivity is illustrated schematically in Fig. 3-11.
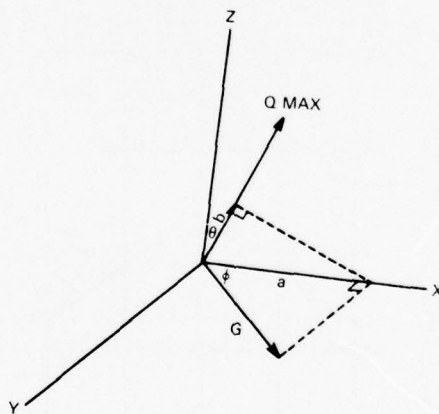
Fig. 3-11. How transverse and axial accelerations combine to produce an output along the sensing direction of an accelerometer [15]

The poled axis of the crystal is represented by a vector in the xz plane. The mounting surface of the accelerometer lies in the xy plane. A transverse acceleration G applied in the xy plane has a component $G \cos\phi$ along the x-axis. This x-axis component has a component $G \cos\phi \sin\theta$ along the poled axis of the crystal. An acceleration G applied perpendicular to the mounting surface has a component $G \cos\theta$ along the poled axis of the crystal. The transverse sensitivity of the accelerometer is the ratio of the two components along the poled axis, such that

$$\% \text{ transverse sensitivity } = 100 \tan\theta \cos\phi. \qquad (3\text{-}8)$$

The factor of 100 is introduced to express the transverse sensitivity as a percent of the axial acceleration sensitivity. For each fabricated accelerometer $\tan\theta$ is a fixed value, assuming that no environmental effects change the poled axis of the crystal. Angle ϕ is determined by the direction of the applied motion in the plane of the mounting surface. Therefore, the transverse sensitivity varies as the accelerometer is rotated about the z-axis. The cosine variation in transverse sensitivity is illustrated in Fig. 3-12 for various values of ϕ.

Several experimenters make this plot on polar graph paper. Usually the transverse sensitivity is small enough that only the maximum value in Fig. 3-12 need be considered. In other words, the accelerometer is selected so that the maximum transverse sensitivity is small enough to produce negligible errors in most shock and vibration measurement applications. The transverse sensitivity
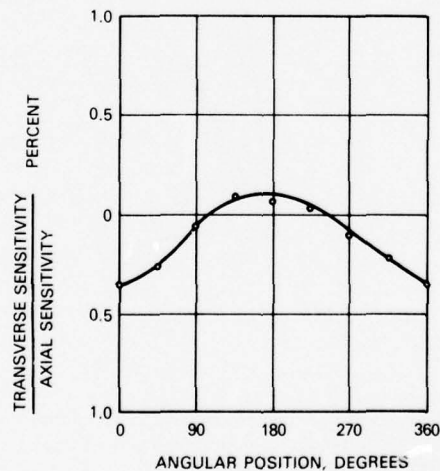
Fig. 3-12. Variation in transverse sensitivity of a piezoelectric accelerometer as it is rotated about its sensitive axis [18]

value provided by the manufacturer is the maximum value of transverse sensitivity.

In good-quality piezoelectric accelerometers, the transverse sensitivity is constant throughout the operating frequency range because care is taken in design to ensure that all local resonances are above the operating frequency range. Sometimes measurements give a false indication of variations in transverse sensitivity at certain frequencies in the operating range. These variations in output are caused by transverse motion in the shaker used for the measurements or by other environmental effects applied to the accelerometer while the transverse sensitivity is being measured. It is important to distinguish one environmental effect from another. For example, errors due to environmental effects, such as certain local resonances, would be present in the output even though no transverse motion were applied to the accelerometer. Responsible accelerometer manufacturers use extreme care in design and conduct extensive tests to ensure that all local resonances are above the operating frequency range. The manufacturer should make sure that all environmental effects are minimized in the accelerometer design.

Transient Temperature Effects. Piezoelectric accelerometers produce outputs while the temperatures of their crystals are being changed. This is called pyroelectricity. In almost all testing applications, the temperature changes in accelerometers occur gradually over a period of several seconds or minutes. As a result, pyroelectric outputs are generally not detected because most amplifiers have inadequate low-frequency response to measure the slowly varying pyroelectric outputs. The pyroelectric outputs contain only extremely low frequency components, usually less than 1 Hz. However, these outputs must be considered if the amplifier passes the low frequencies or if the outputs are large enough to overload the amplifier input and make it inoperative while the output is present. The pyroelectric characteristics of piezoelectric crystals are known, and the output for any particular accelerometer-amplifier combination can be experimentally determined under specified temperature conditions.

There are three types of pyroelectric outputs. A primary pyroelectric output is the charge produced as a result of a uniform temperature change throughout the crystal. A secondary pyroelectric output is the piezoelectric charge produced as a result of a dimensional change in the crystal, caused by a uniform temperature change. A tertiary pyroelectric output is a piezoelectric output caused by a temperature gradient across the crystal. Pure primary pyroelectric outputs occur when crystals are constrained to prevent dimensional changes. Pure secondary and tertiary pyroelectric outputs occur when crystals are unconstrained. Primary pyroelectric outputs are present only on the crystal surfaces perpendicular to the direction of polarization, whereas secondary and tertiary outputs appear on the electrode surfaces of the crystal regardless of polarization. Shear-type accelerometers are designed so that the electrode surfaces are not in the direction of polarization. Consequently, shear accelerometers do not produce primary pyroelectric outputs and generally are less affected by temperature changes than compressive accelerometers, which do produce primary pyroelectric outputs.

All ceramic crystals produce secondary pyroelectric outputs. However, quartz produces only tertiary pyroelectric outputs. Therefore, accelerometers using quartz are preferred when amplifiers designed for use at frequencies near or below 0.1 Hz are used. These amplifiers are required for shock motion testing involving extremely long pulses (e.g., pulses of 100-ms duration). In most shock and vibration testing applications, amplifiers that cut off at frequencies near or above 2 Hz are used, and no errors due to pyroelectric outputs arise.

Radiation Effects. Nuclear reactions involve the splitting of atoms to produce a bombardment of particles. Heat, associated with the release of gamma rays and neutrons, is produced when these particles collide with surrounding atoms. Large doses of this nuclear energy can affect the properties of materials. At moderate levels, gamma radiation produces a temperature environment *to that present in other accelerometer applications.*

The fission process can be produced with Uranium-235 when a free neutron strikes the heavy U-235 nucleus, breaking it into two fragments and releasing two or three new neutrons. The kinetic energy of the flying fission fragments are converted to heat when they collide with surrounding atoms. The released neutrons cause a chain reaction by initiating new fissions in other atoms. Some 30 billion fissions occur each second to release each watt of energy. The job of the nuclear reactor is to control the fission reaction and to remove the heat and convert it to electrical energy, use it in propulsion systems, etc.

Fusion is another means of releasing energy in a nuclear reaction. However, a fusion reaction requires temperatures in the millions of degrees. This can be achieved in a fission reaction, which is then used to initiate fusion. Atoms of deuterium and tritium, which are heavy isotopes of hydrogen, combine to form helium atoms. Fusion is used to produce thermonuclear explosives, which are considerably more powerful than pure fission explosives.

During the fission process high-speed neutrons are released; they are difficult to stop. Neutral particles are also released in the form of gamma rays, which carry heat and have other characteristics similar to those of X-rays. The neutrons and gamma radiation are absorbed by the materials in transducers. In addition to the normal thermal effects on the properties of the materials, sufficiently large doses of radiation can cause permanent changes in material. The neutron density is the number of neutrons per cubic centimeter. The neutron flux is the density multiplied by the average velocity of the particles; it is expressed in units of neutrons per square centimeter per second. The time-integrated flux is determined by multiplying the flux by the period of exposure and has units of neutrons per square centimeter, written as n/cm^2. The roentgen unit, denoted by the symbol R, can be used to measure gamma radiation. In energy units 84 ergs $(8.4 \times 10^{-8} J)$ are absorbed per gram of air for each roentgen. One R is also equivalent to 87 ergs per gram absorbed in carbon $(87 \text{ erg}/g \ (C))$. Another unit used is the rad, which equals $100 \text{ erg}/g(C) \ (1 \times 10^{-5} J/g(C))$.

Extremely large doses of radiation are required to deteriorate the materials in accelerometers. Accordingly, in most nuclear applications accelerometers are

affected merely by the heat produced or by the measurement errors produced by the radiation field. Little, if any, permanent damage is produced directly by the radiation in accelerometers built with radiation-hardened components.

Very large doses of radiation cause depolarization of piezoelectric materials. For example, X-rays have been used to adjust frequency characteristics (Radiation effects decrease the resonance frequencies of crystals.) Quartz crystals are less excited by radiation than lead zirconate titanate ceramics. The threshold of radiation damage approached a neutron fluence of 10^{20} n/cm^2. However, no information is available concerning the testing of piezoelectric accelerometers at such high levels of radiation. Piezoelectric accelerometers have no lattice changes at neutron fluences as high as 10^{18} n/cm^2. However, it is necessary under such conditions to avoid the use of organic materials such as Teflon, ® which can be damaged by nuclear radiation and cause malfunction due to breakdown of insulation resistance. The most radiation-resistant accelerometers are of the piezoelectric type. However, in the more severe environments, it is necessary to use accelerometers built with high-temperature ceramics according to manufacturers' recommendations.

Mounting Conditions. An accelerometer tends to alter slightly the motion of the structure or component to which it is attached. This produces a slight error in measuring the motion that would exist if the accelerometer were not present. This error is usually insignificant and need be considered only when making measurements on light and flexible structures. Very light accelerometers should be selected for these applications. The specific requirement is that the dynamic mass of the accelerometer must be less than the dynamic mass of the structure at the point of attachment. The magnitude of the dynamic mass of an accelerometer is simply equal to its total weight, because accelerometers act as rigid bodies throughout their normal operating frequency range. The dynamic mass of the structure will be large enough if the accelerometer is attached at a point where the cross-sectional dimensions of the structure are large compared to the dimensions of the accelerometer. Applications where the structure's dynamic mass may be relatively small include thin plates and beams, panels, and circuit boards, particularly at frequencies at which resonance takes place. Accurate measurements can be made even on these structures, since piezoelectric accelerometers weighing a fraction of a gram are available.

In some extreme applications, the case of an accelerometer can be distorted significantly when high strains are present in the mounting surface of the accelerometer or structure. These strains may be produced by mechanical loads or by nonuniform heating. Their effect on the performance of accelerometers is determined on beams that are vibrated so that the radius of curvature is 1000 in. (25.4 m) and the bending strain is 250 microstrain. These test conditions are given in published standards. The strain sensitivity of most shear-type accelerometers is extremely small, and in most test applications mounting strains can be ignored. The strain sensitivity of compressive accelerometers is sometimes significant. Accelerometers with high-performance characteristics (e.g., extremely

high resonance frequency and extremely high acceleration rating) are usually more susceptible than others to output errors due to strain. In test applications where the static or dynamic surface strain in the structure is near or above 250 microstrain, it may be desirable to use insulated studs or rigid fixtures as strain filters. This need be considered only when high-performance accelerometers are used in testing applications where it is also necessary to measure low accelerations and when excessive strains are expected. A better solution for these applications is to select accelerometers that have high vibration sensitivity and therefore low strain sensitivity.

Acoustic Sensitivity. Although modern accelerometers produce negligible error signals when exposed to high-intensity acoustic sound fields, it is interesting to explore the mechanics of gas or fluid pressures applied to an accelerometer case. The same types of forces are applied to an accelerometer in acoustic fields as when dynamic fluid pressures are present.

When pressure is applied to an accelerometer case, the case deflects and produces a pressure on the crystal due to compression or expansion of the gas in the accelerometer. An approximate calculation on a typical compressive accelerometer indicates that the stiffness of the accelerometer is sufficient to attenuate the pressure about 55 dB and produce an error signal of about 0.003 g/psi of external pressure.

The pressure outside the accelerometer produces radial strains in the accelerometer base. Many compression accelerometers have the crystal mounted on the inner surface of the base, and in these the crystal experiences the same radial strain. As a result the ceramic material produces an output from the d_{31} piezoelectric constant. For compression accelerometers typical error signals due to radial strain are about 0.03 g/psi

For shear accelerometers error signals due to internal gas pressure and radial strain are much less and can be considered nil.

A third effect, present in all accelerometers, is produced because the external pressure changes the height of the accelerometer base. For dynamic pressures this change in height applies a motion to the accelerometer crystals. The equivalent acceleration at the top surface of the base increases with increasing frequency. For a typical accelerometer the error produced by this effect is about 0.04 g/psi at 10 000 Hz and much less at lower frequencies.

All these errors are negligible when the accelerometer is subjected to extremely intense acoustic fields. False indications of acoustic sensitivity have been previously reported because of the difficulty of separating the above-mentioned outputs from the accelerations applied to the mounting surface of the accelerometer by the acoustic field. In other words, the accelerometer truly measures the acceleration applied to the accelerometer, even though this acceleration is produced by the acoustic field acting on the structure to which the accelerometer is attached.

3.2 Wire Resistive and Piezoresistive Accelerometers

Wire resistive strain gages have been widely used in a number of applications. Such a strain gage consists of a fine wire that changes its resistance when its length is changed, as strain is applied to a structure to which it is attached. Similarly, wire strain gage accelerometers have been used for shock and vibration measurements at moderate accelerations over limited frequency ranges. These accelerometers are built by using a fine wire strain gage element to support a mass element from the case of the accelerometer. Such accelerometers have relatively low acceleration sensitivities because the gage factors of the materials used for the wires are limited to a value of about two.

Recently, strain gages have been developed from piezoresistive materials that have a much higher gage factor. Piezoresistive strain gage elements are now used in a variety of accelerometers used for shock and vibration measurements. Because of the high gage factors, the piezoresistive accelerometers have higher sensitivities and higher operating frequency ranges than wire strain gage accelerometers.

Piezoresistive Accelerometers

The gage factor of a strain sensing material is the ratio of its change in resistance to initial resistance divided by its change in length to its initial length. For a piezoresistive material this ratio is given by

$$K = \frac{\dfrac{\Delta R}{R}}{\dfrac{\Delta L}{L}} = (1 + 2\mu + E\pi_1) \tag{3-9}$$

where

K = gage factor of resistance element
ΔR = change in resistance
R = initial resistance
ΔL = change in length of resistance element
L = initial length of resistance element
μ = Poisson's ratio for the sensing material
E = modulus of elasticity for the sensing material
π_1 = piezoresistive coefficient for the sensing material.

The sum of the first two terms, $1 + 2\mu$, is almost 2, which also happens to be the gage factor ordinarily achieved in wire strain gages, because for them π_1 is near zero. For piezoresistive materials, the third term, $E\pi_1$, can have values well above 100, which is about 50 times the gage factor for wire strain gages. This

advantage makes possible accelerometers with high resonance frequencies and sensitivities.

The piezoresitive strain gage element is built into an accelerometer in such a way that the change in length of the gage is proportional to the motion of the mass element in the accelerometer relative to its case. Accordingly, the above equation for the change in resistance can be simplified as follows:

$$\Delta R = C_2 \delta \tag{3-10}$$

where

    C_2 = constant determined by the specific accelerometer design
    δ = deflection of the mass element relative to the accelerometer base.

Equation (3-10) indicates that a piezoresistive accelerometer will have frequency response characteristics like the theoretical response of the seismic accelerometer. Many piezoresistive accelerometers have resonance frequencies near and above 30 000 Hz, like piezoelectric accelerometers. It is difficult to induce artificial damping in these high-frequency accelerometers, and the theoretical curves for zero damping apply. Accordingly, the normal operating range of these accelerometers is up to about one-fifth the resonance frequency where the sensitivity increase is less than 5%. The important difference in piezoresistive accelerometers is that their sensitivity is constant to zero frequency. Therefore, piezoresistive accelerometers are used for measuring constant accelerations as well as extremely long duration shock motions. Piezoresistive accelerometers are also built with resonance frequencies significantly below 5000 Hz. For those low-frequency accelerometers it is practical to introduce artificial damping, and the theoretical curves for 0.7 of critical damping apply.

The internal construction of a piezoresistive accelerometer is shown in Fig. 3-13 [14]. The peizoresistive strain gage elements are identified as R1, R2, R3, and R4. These elements are fastened on each side of slots machined in a cylindrical member. When upward motion is applied to the base of the accelerometer along the sensitive axis, the mass element part of the cylinder bends very slightly toward the base, causing the length and resistance of R1 and R3 to increase while the length and resistance of R2 and R4 decrease. These piezoresistive elements are connected electrically in a Wheatstone bridge in a similar way to other resistance strain gage circuits. Direct current voltage excitation is applied to the bridge input, and the bridge voltage output varies with time along with the time variation of the acceleration applied to the accelerometer. Frequently this voltage output requires no amplification; it is measured by using the same readout instruments used with other strain gage accelerometers. If desired, other instruments can be used, such as constant-current power supplies and d.c. amplifiers, which are normally used with strain gage circuits.
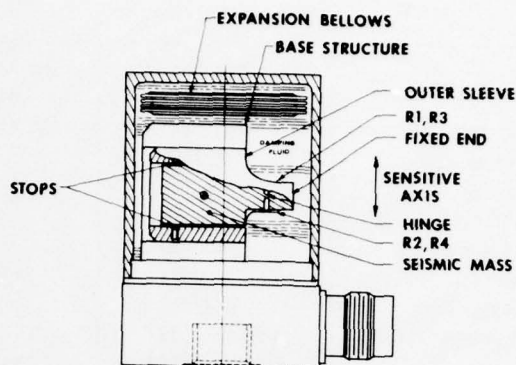
Fig. 3-13. Internal construction of a piezoresistive accelerometer

Performance Characteristics. A summary of performance characteristics of piezoresistive accelerometers is given in Table 3-4.

In addition to those for which acceleration ranges are given in Table 3-4, other piezoresistive accelerometers are available, with ranges below and above 2500 *g*. The sensitivities of these accelerometers are related to their acceleration ranges. Accelerometers designed for high shock motion measurements have low sensitivity. Accelerometers with high sensitivities, for example 50 mV/g, are intended for vibration measurement applications at relatively low accelerations, up to 25 *g*. The sensitivity given in Table 3-4 applies when the rated excitation voltage is provided at the input of the Wheatstone bridge in the accelerometer.

The results of shock and vibration calibrations on piezoresistive accelerometers are illustrated in Fig. 3-14. These data indicate that sensitivity is constant over the operating ranges of the accelerometers. Shock calibrations on piezoresistive accelerometers indicate freedom from zero shifts, which frequently occur in piezoelectric accelerometers used at high accelerations. Accordingly, piezoresistive accelerometers are preferred for cases in which it is desirable to perform electrical integration of the accelerometer output to determine the velocity change in shock motion testing applications.

The frequency response characteristics of piezoresistive accelerometers with damping near zero are similar to those of piezoelectric accelerometers. Oil damping is provided in the accelerometer having a resonance frequency of 2700 Hz. The damping is in the range of 0.4 to 0.7 of critical damping at room temperature. With this damping, sensitivity is nearly constant from 0 to 750 Hz over the full operating temperature range. The piezoresistive accelerometer using oil

Table 3-4. Typical Performance Characteristics of
Piezoresistive Accelerometers

Characteristics	High-Acceleration Model	Low-Acceleration Model
Acceleration Range, g	± 2500	± 25
Sensitivity, mV/g	0.1	50
Excitation V d.c.	10	24
Resonant Frequency Hz	30 000	2700
Damping Ratio	0.03	0.4–0.7
Frequency Range Hz	0–6000	0–750*
Temperature Range °C (°F)	–54 to 121 (–65 to +250)	–7 to 93 (20 to +200)
Resistance, Ω	500	1500
Transvere Sensitivity %	< 3	< 3

*Recommended frequency range over full operating temperature range.
Source: Ref. 15.
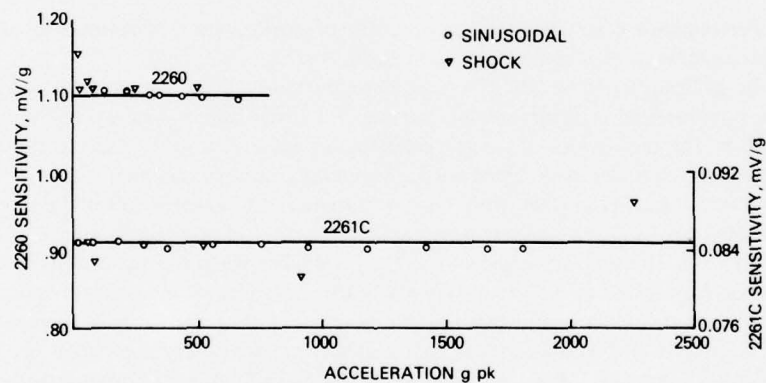
Fig. 3-14. Calibrations indicating typical linearity characteristics of piezoresistive accelerometers

damping is intended for use in the temperature range from -7°C to 93°C (20°-200°F).

At high temperatures the viscosity of the oil decreases, resulting in low damping. The viscosity increases at lower temperature, which causes high damping. Accordingly, the frequency response characteristics change as a function of temperature, as illustrated in Fig. 3-15a.
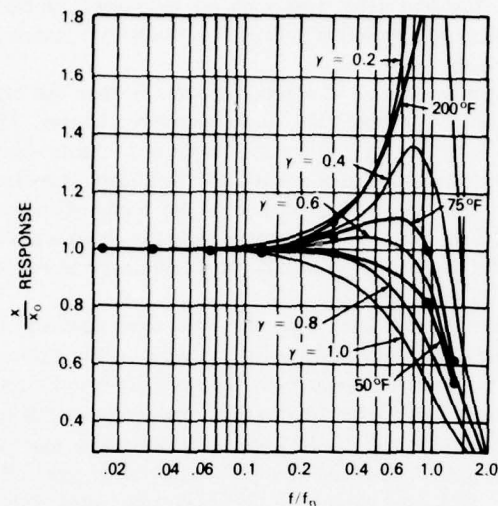
Fig. 3-15a. Typical frequency response of a piezoresistive accelerometer with oil damping
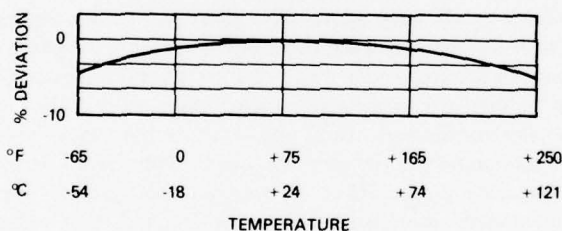
Fig. 3-15b. Typical temperature response of a piezoresistive accelerometer [15]

At 93°C (200°F) the damping is near 0.2 of critical damping, and at 10°C (50°F) the damping is about 0.7. For accelerometers using oil damping it is desirable to perform frequency response calibrations throughout the operating temperature range if the accelerometer is normally used at temperature extremes. In addition to the frequency response changes near the resonance frequency at various temperatures, the sensitivity varies as a function of temperature, as shown in Fig. 3-15b, in a manner similar to that of undamped piezoresistive and peizoelectric accelerometers. This change in the sensitivity is caused by changes in the gage factor and is determined by the temperature characteristics of the modulus of elasticity and the piezoresistive coefficient of the piezoresistive

sensing element. The sensitivity deviations are minimized, as indicated in Fig. 3-15b, by installing compensation resistors in the bridge circuit in the piezoresistive accelerometer.

One final effect present in the accelerometer is that the bridge becomes slightly unbalanced when subjected to temperature changes. This unbalance (zero measurand output) is due to small differences in resistance changes of the sensing elements as a function of temperature. This change in resistance produces small changes in the d.c. voltage output of the bridge. Care is taken in the design of the piezoresistive accelerometer to keep the changes in the d.c. voltage output a small fraction of the output at the maximum rated acceleration of the accelerometer.

Environmental Effects. The environmental characteristics of transverse sensitivity and the effect of the accelerometer mass on the motion of the structure are similar in piezoresistive and piezoelectric accelerometers. The typical values of near or less than 3% for the maximum transverse sensitivity are common for piezoresistive accelerometers. Just as for piezoelectric accelerometers, it is desirable to select piezoresistive accelerometers that weigh significantly less than the mass represented by the cross-sectional dimensions of the structure to which the accelerometer is attached. If this is done, the accelerometer will not significantly change the motion of the structure. Frequently, this requirement is satisfied simply by care in selecting the mounting location on the structure.

Piezoeresistive accelerometers are capable of withstanding shock and vibration accelerations significantly above their rated acceleration ranges. However, the piezoresistive materials used are quite brittle and it is necessary to limit the applied stresses. In accelerometers designed for high shock motions, the moving elements can be designed to avoid excessive stresses even at the highest shock motions normally encountered. However, some precautions are necessary with piezoresistive accelerometers designed for use at moderately low accelerations. In the high-sensitivity piezoresistive accelerometers designed for use at low accelerations the stresses are minimized by built-in stops that limit the motion of the mass element. The stops engage at deflections corresponding to applied accelerations of several times the rated acceleration range.

It is sometimes desirable to take special precautions to avoid damage to piezoresistive accelerometers used in extremely severe shock environments. For example, shock motions of ship structures subjected to underwater explosions produce a high-frequency excitation that tends to excite the resonance frequency of the accelerometer, which may cause damage. To overcome this problem, the accelerometer may be installed in a mechanical shock isolation fixture, as shown in Fig. 3-16, which is attached to the structure. The urethane disks are designed to have enough stiffness, when supporting the accelerometer and steel slug, that high frequencies are filtered out to prevent damage. Of course, the transmissibility of this shock isolation system is near unity for the frequency components that represent the shock motion being measured. This method of mounting accelerometers may be used in similar shock measurement applications.
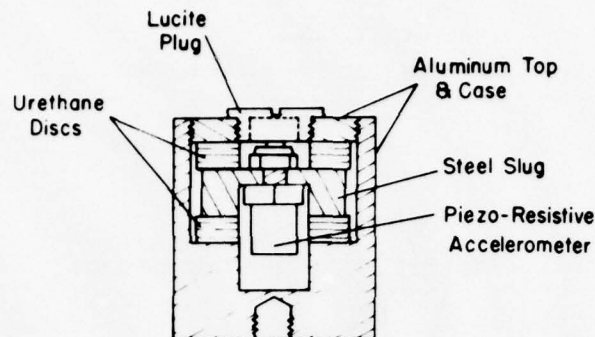
Fig. 3-16. Mechanical shock isolation fixture that reduces excitation of the resonance frequency of an accelerometer [20]

Piezoresistive accelerometers are used in some testing applications in the presence of nuclear radiation environments. Piezoresistive accelerometers cannot withstand radiation environments as well as piezoelectric accelerometers. Neutron fluence of the order of 10^{13}-10^{15} n/cm^2 and gamma radiation of 10^8 erg/g(C) tend to damage the silicon crystals used in piezoelectric accelerometers. The ability to withstand these high radiation environments depends on the particular semiconductor material and processing used. For example, radiation-hardened piezoresistive accelerometers operate satisfactorily during transient nuclear radiation environments.

The sensing elements in piezoresistive transducers have a high temperature coefficient of resistance. Shunt calibration techniques such as those used with wire strain gage transducers should be avoided. Since these elements are resistive and are energized with an external d.c. voltage or current, they generate low-level, low-frequency noise typical of resistive elements.

3.3 Capacitive Accelerometers

A capacitive accelerometer has the characteristics of a seismic transducer. One of the capacitive plates is supported by a spring of flexure mechanism from the case of the accelerometer. The change in capacitance is a function of the displacement of the capacitor plate relative to the accelerometer base. Figure 3-17 illustrates the construction of a capacitive accelerometer. The change in capacitance per unit of acceleration applied to the base is given by the following equation:

$$\frac{\Delta C}{g} = \frac{K r^2}{d^2} f_o^2 \qquad (3\text{-}11)$$
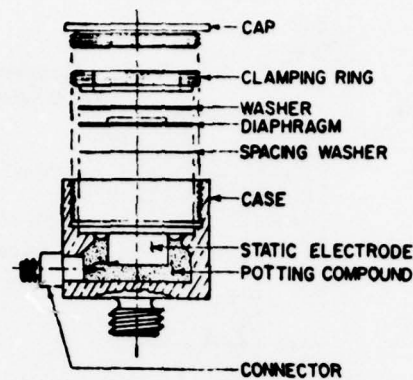
Fig. 3-17. Exploded view of a laboratory model capacitive accelerometer

where

ΔC = change in capacitance
K = constant determined by the design of the accelerometer
r = radius of the capacitive plates
d = spacing between the plates
f_o = resonance frequency of the accelerometer.

The acceleration sensitivity of the accelerometer is proportional to the change in capacitance. A capacitive accelerometer is inherently nonlinear, since the change in capacitance is inversely proportional to the spacing of the plates. The shock motion calibration documented in Table 3-5, performed on a capacitive accelerometer, is an example of this nonlinearity. The changes in sensitivity at high accelerations exceeding 10% limit the usefulness of this accelerometer. A frequency response calibration is illustrated in Fig. 3-18. It indicates significant deviations from the nominal response of a seismic accelerometer. These calibration results indicate the importance of performing sensitivity, frequency response, resonance frequency, and shock motion calibrations.

3.4 Inductive Transducers

Various inductive transducers are used for measuring vibration and shock motion. They include the proximity, movable-core, and seismic transducers listed in Table 3-6. A proximity pickup is attached to a fixture and positioned with a small gap between it and the object whose motion is being measured. It does not mechanically load the object. In the case of movable-core transducers part of the transducer must be attached to the vibrating object and the other part to a rigid fixture.

Table 3-5. Amplitude Linearity Calibration of a Capacitive Accelerometer

Applied Acceleration (g)	Acceleration Sensitivity (mV/g)
92	0.495
980	0.475
1650	0.450
2250	0.420
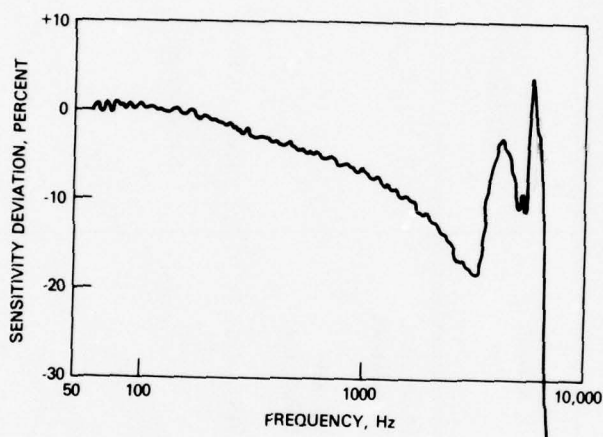
Fig. 3-18. Frequency response calibration of a capacitive accelerometer

The most popular of the seismic inductive transducers is the electrodynamic type. It is designed to have a very low natural frequency and is used as a velocity pickup. Differential-transformer and variable-reluctance seismic transducers are used as accelerometers. Some inductive transducers are in limited use. The inductive transducers must be calibrated to establish their accuracy within their operating frequency ranges. Some are quite large and require special fixtures when calibrations are performed on small shakers. The most widely used inductive transducers are the electrodynamic velocity pickup and the variable-reluctance accelerometer. The descriptions of these transducers provide information helpful when performing calibrations. More detailed information about the design and description of the other inductive transducers may be found by consulting the bibliography.

Table 3-6. Types of Shock and Vibration Pickup Using Inductive Principles

Motion Sensed	Proximity	Movable Core	Seismic		
				Used Above Natural Frequency	Used Below Natural Frequency
Displacement	Mutual Inductance	Differential Transformer		—	—
Displacement	—	Variable Reluctance		—	—
Velocity	Electrodynamic	Electrodynamic		Electrodynamic	—
Acceleration	—	—		Eddy Current	Differential Transformer
Acceleration	—	—		—	Variable Reluctance
Jerk	—	—		—	Magnetostrictive

Electrodynamic Velocity Pickups

A typical electrodynamic velocity pickup is illustrated in Fig. 3-19. A coil of wire forms part of a seismic mass, which is supported on a column by springs. When the case of the velocity pickup is vibrated the coil slides up and down the column at frequencies above the natural frequency of the single-degree-of-freedom spring-mass system. The coil remains virtually motionless as the case vibrates. Therefore, the magnetic lines of force from the magnet vibrate up and down about the coil. The output voltage of the coil is proportional to the relative velocity of the coil and magnet. The open-circuit voltage generated in the coil is

$$e = - B\ell v\,(10^{-12})\tag{3-12}$$

where

e = output voltage generated, in volts
B = flux density, in teslas
ℓ = total length of the coil wire, in centimeters (in.)
v = relative velocity of coil and magnetic, in centimeters per second (in./s).

It is common to use air or oil damping in velocity pickups to limit excessive motion of the coil, particularly when it is subjected to vibration and shock motions and at frequencies near the natural frequency. A typical calibration performed on a velocity pickup is plotted in Fig. 3-20. The sensitivity decreases sharply at frequencies below resonance, in accordance with the nominal response for seismic transducers used above the natural frequency. Sensitivity decreases at the higher frequencies above resonance are due to eddy-current losses.
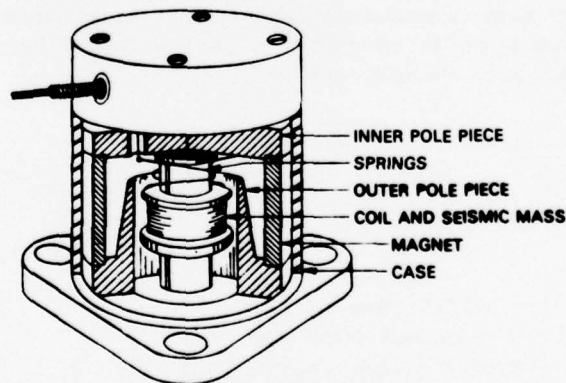
Fig. 3-19. Construction of an electrodynamic velocity pickup [22]
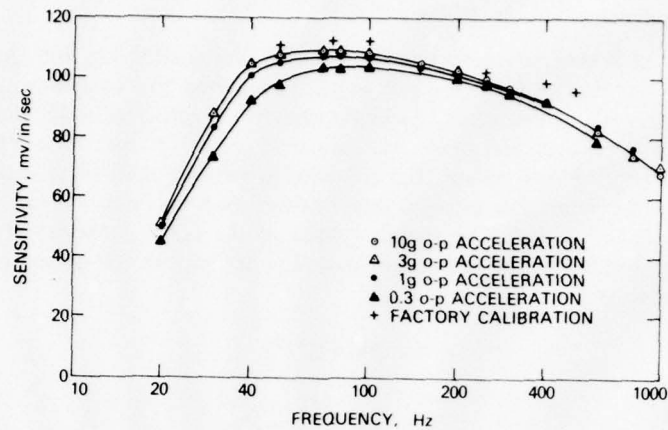
Fig. 3-20. Frequency response of a velocity pickup [22]

Variable-Reluctance Accelerometers

The construction of a variable-reluctance accelerometer is illustrated in Fig. 3-21. Almost all inductive transducers are quite large; this design uses miniature components to keep the size small. Miniature accelerometers have little effect on the shock and vibration motions of structures to which they are attached.

The mass element consists of magnetic material suspended by a flat spiral spring from the case of the accelerometer. Since the operating range of the seismic accelerometer is at frequencies below resonance, the mass element experiences small deflection motions up and down when the case is vibrated. This motion varies the gap between the magnetic mass element and the coils, which are fixed to the accelerometer case. As this occurs the inductance of one coil increases while that of the other decreases. The inductance of the coils is given approximately by the following equation:

$$L = \frac{4\pi n^2 S(10^{-9})}{\ell} \qquad (3\text{-}13)$$

where

L = coil inductance, in henries
n = total number of coil turns
S = area of the gap, in square centimeters (in.^{2})
ℓ = length or thickness of the gap, in centimeters (in.).
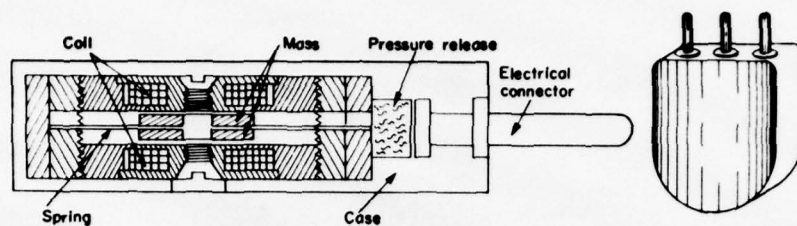
Fig. 3-21. Construction of a miniature variable-reluctance accelerometer [23]

Since the inductance is inversely proportional to the length of the gap, the acceleration sensitivity is inherently nonlinear. Amplitude linearity calibrations are made to determine the degree of nonlinearity. A typical variable-reluctance accelerometer has a resonance frequency of about 200 Hz. Oil damping is used to extend the operating frequency range to about two-thirds of the resonance frequency. Temperature response calibrations are performed to determine the variation of accelerometer sensitivity at the various temperatures encountered in service.

3.5 Servo Accelerometers

Servo accelerometers are used for measuring low-amplitude vibrations at frequencies ranging from zero to several hundred hertz. Servo accelerometers are used extensively as guidance instruments in aircraft and space vehicles. They are also useful for various applications requiring the measurement of small accelerations, such as those present in buildings subjected to machinery vibrations and earthquakes. The construction and operating principle of a servo accelerometer are illustrated in Fig. 3-22. When subjected to motion, the proof mass tends to deflect relative to the base of the accelerometer, and the pickoff changes its capacitance as a result of changes in the damping gap. As this occurs, the servo supplied current to the coil, located in the gaps of the permanent magnets. The resulting force restores the coil to its equilibrium position. The output signal is a measure of the coil current and is proportional to the applied acceleration.

Servo accelerometers have high acceleration sensitivities and wide frequency ranges. Typical values for the accelerometer illustrated in Fig. 3-22 are a sensitivity of 250 mV/g and an operating frequency range of 0 to 500 Hz.

3.6 Self-Contained Recording Instruments

Mechanical instruments used for recording shock and vibration are used for measuring vibration of transmission lines, impacts occurring in railroad vehicles, and impact studies with explosions. A simple peak-reading acceleration recorder is shown in Fig. 3-23. This particular recorder has eight separate reeds, for
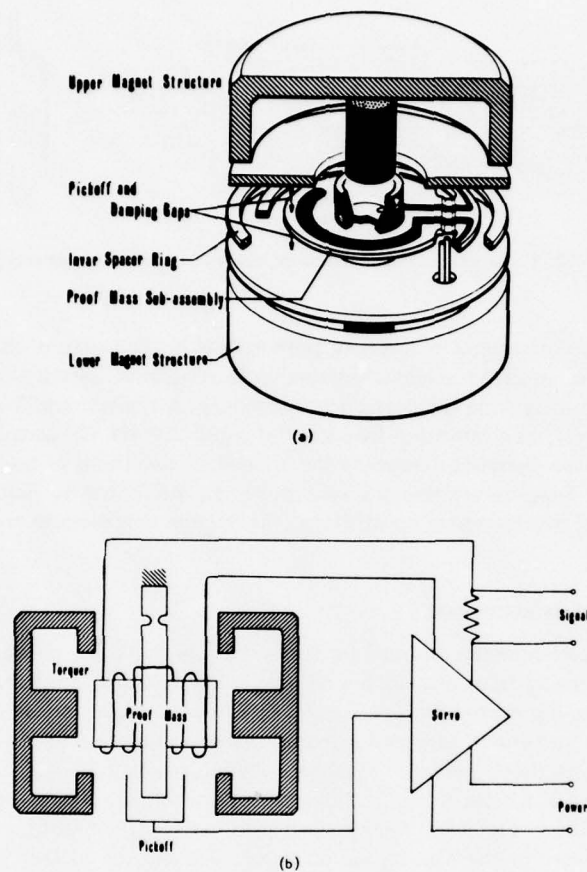
Fig. 3-22. Construction of a miniature variable-reluctance acceler-
ometer [23]

recording various accelerations up to 10 000 g. Each reed has a diamond-tipped
stylus on the free end to inscribe a permanent record on a gold-plated disk.
Calibration sheets give the resonance frequency and acceleration sensitivity of
each reed.

The Impact-O-Graph self-recording instrument is used for measuring shock
motions and impact in vehicles. This recording instrument uses a low-frequency
mass-spring system that includes a recording stylus. The stylus assembly is built
with a 10-to-1 amplifying linkage. The stylus motion is recorded on wax- or
plastic-coated tape. Three of these mechanisms are assembled in one instrument
to record accelerations in three mutually perpendicular directions. Some

Reed Plate and Record Hub   ACTUAL SIZE
(for Sensing and Recording)

TYPICAL RECORD
(10 Times Size)
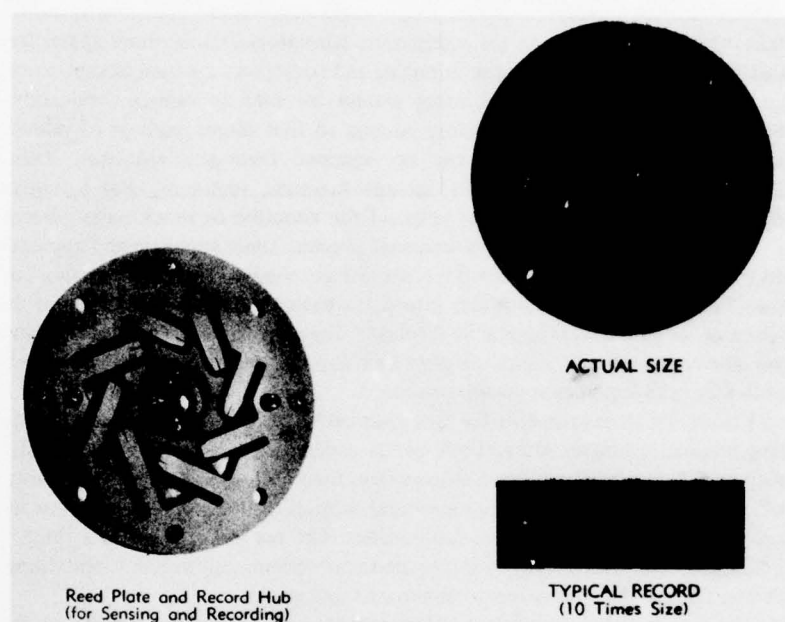
Fig. 3-23. Peak-reading mechanical shock recording accelerometer (Engdahl Enterprises)

instruments use a moving tape to record frequency and accelerometer amplitude data. Accelerometer measurements are made in ranges from 1 to 20g.

A self-recording instrument for measuring vibrations of overhead conductors is used in the electric power industry. This recorder consists of a mechanical linkage system that provides a magnification factor of five to a stylus, which is used to record the vibrations. The stylus scribes the vibrations on a tape traveling at a constant speed so that both displacement amplitude and frequency are recorded.

To obtain accurate data, it is important to perform calibrations on both vibration and shock motion self-recording instruments. Moving parts tend to wear and are sometimes damaged during use.

3.7 Auxiliary Instruments

. The simplest instruments to use in measuring vibration and shock motion are the electronic voltmeter and the oscilloscope. These instruments allow the amplitude of the vibration to be read from the output of the signal conditioner used with the transducer. The oscilloscope permits viewing the vibraton or shock motion waveform. A dual-trace oscilloscope permits measuring two

outputs simultaneously to obtain phase angle data. These instruments are the least that are required in the calibration laboratory. Other more specialized instruments are available for use in testing and sometimes are used in calibration.

A number of vibration-indicating meters are used in various applications. Some include electronic integrating circuits so that direct readings of velocity and displacement amplitudes may be obtained from accelerometers. Other basic voltmeter-type instruments include low-pass, high-pass, and band-pass filters for limiting the frequency range of the vibration or shock measurement.

Digital indicating instruments represent a recent, more sophisticated approach to making measurements. Rectifying circuits are used to change the analog outputs from the signal conditioners into d.c. signals so that the amplitude of the vibration or shock motion may be displayed digitally. Some of these instruments are also equipped with digital displays of the pulse amplitude and the width of pulses from shock motion measurements.

Use of digital instruments for vibration calibrations reduces calibration time and minimizes human error. Their use is generally encouraged. However, it is recognized that small additional errors (less than 1%) are introduced as a result of using these instruments for sinusoidal motion calibrations. These errors are acceptable in most calibration laboratories. On the other hand, the Primary Standards Laboratory may want to perform certain calibrations with voltage divider circuits and voltmeters to eliminate these errors.

The use of digital instruments is important in shock motion calibrations. For example, shock motion calibration errors of about 2% are frequently present when peak accelerations are read from an oscilloscope. These errors can be eliminated by using digital instruments to measure peak accelerations.

System calibrations are frequently performed on accelerometers and signal conditioners used as shock and vibration standards. This has the advantage of yielding the acceleration sensitivity including the gain of the amplifier. However, it is unnecessary to perform the system calibration of the accelerometer and amplifier together with the auxiliary instruments. Auxiliary instruments can be calibrated electrically to demonstrate their accuracy, so that vibration and shock motion calibration laboratories can use them with confidence.

3.8 Displacement Measurements

Displacement measurements are made with inductive proximity pickups and with a variety of optical instruments, including lasers. The inductive pickups are useful when direct measurement of displacement amplitudes is necessary and where it is practical to use the proximity pickups. These pickups are in limited use in calibration laboratories. Direct-viewing optical instruments and lasers are useful for certain types of calibrations, including absolute measurements at high frequencies.
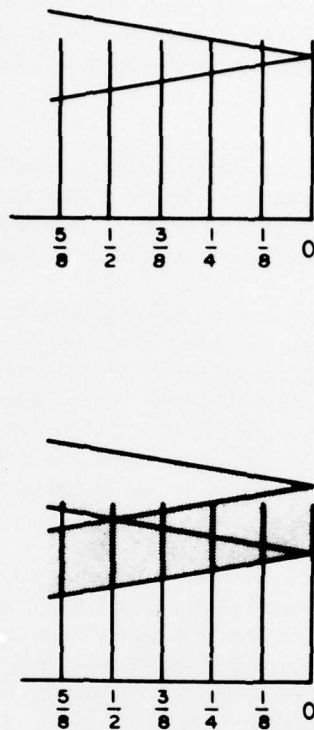
Fig. 3-24. The vibrating wedge displays peak-to-peak displacement

Direct-Viewing Optical Instruments

The simplest optical vibration measurement is made with the naked eye. The vibrating wedge (Fig. 3-24) is a useful and reasonably accurate instrument for direct-viewing measurements. It consists of accurately drawn lines that appear to intersect when the wedge is vibrated. When the wedge is subjected to sinusoidal vibration, the velocity is zero when the displacement amplitude is at its positive and negative maxima. This causes the wedge to dwell at the displacement maxima. The vibration measurement is made by observing the intersection of the lines and reading the graduated scale at the bottom of the wedge.

A microscope may be used for making direct-viewing vibration measurements. Reflective tape or other highlights on a sinusoidal vibrating shaker are used to provide an image on a graduated scale.

The vibrating wedge and measurements with microscopes are useful in the calibration laboratory when it is necessary to perform calibration at frequencies near and below 50 Hz. Otherwise more modern techniques are generally used.

Lasers and Holography

Optical holography and laser interferometry are valuable tools that are making significant advances in vibration analysis and in other applications. These techniques are useful for making ultrahigh-frequency shock and vibration calibrations and for making certain evaluations on calibration shakers or other vibrating objects.

Holography uses a laser beam to record light interference fringes on a photographic plate. Illuminating the plate, after development, produces a three-dimensional image of the original object used to make the hologram on the plate. Lasers are required because they provide a coherent light source. Spatial coherence implies uniformity of the wavefront in the plane transverse to the light beam. Lasers have almost perfect spatial coherence. Any lack of spatial coherence results in background noise in the hologram for a portion of the object, as a result of scattering of the light. Such noise is worse for opaque objects than for transparent ones.

Temporal coherence is achieved by maintaining uniform intensity along the length of the beam. Each wave has the same intensity as other waves along the length of the beam. For the perfectly monochromatic source single-free light, the temporal coherence is infinite. In other words, good-quality fringes would be produced regardless of the path lengths of the object and reference beams. However, lasers contain a number of frequencies in a narrow bandwidth, which results in limited temporal coherence. This produces irregularities in the light wave at the distance corresponding to odd-integer multiples of the length of the cavity in the laser. This limits the field of depth to less than the cavity length because fringes disappear at distances corresponding to these lengths. The coherence length is about 7 in. (180 mm) for lasers used in holography, and this is the limit for the size of the object. However, the various modes of the laser are in phase again at even multiples of the cavity length, which means that present-day lasers can be used in certain interferometry applications at path length differences up to several kilometers.

Holograms are made of vibrating objects in a form of double-or multiple-exposure interferometry. It should be possible to perform a complex motion analysis on a vibrating object when coherent lasers of controlled pulse durations are available. However, experimental work at present is limited to sinusoidal motion excitation; the hologram is thus the same as if a double exposure were made at the extremes of the displacement amplitude.

Figure 3-25 shows the test setup for studying the vibration of a sonar transducer. Photographs of the reconstructed hologram are shown in Fig. 3-26. These depict the transducer vibrating at its fundamental mode; the number of fringes gives a quantitative measure of the vibration amplitudes at various locations on
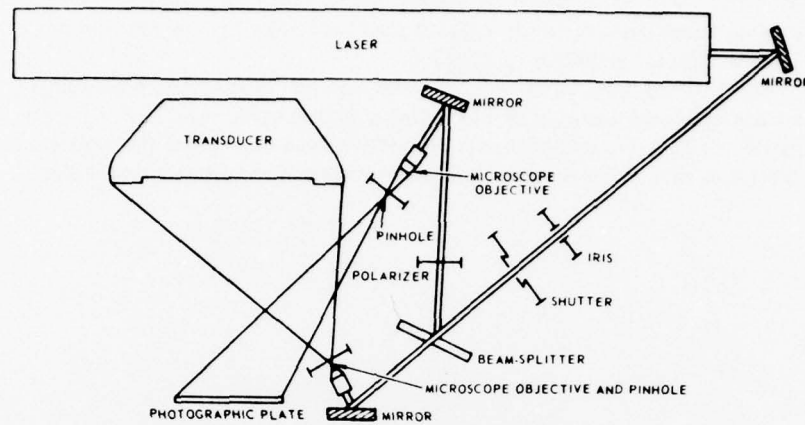
Fig. 3-25. Typical setup for using a laser beam to measure vibration of an acoustic transducer [25]
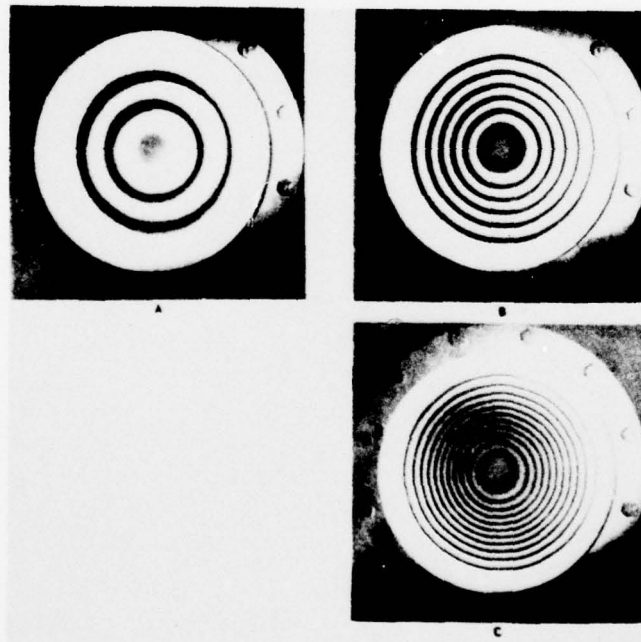
Fig. 3-26. Photographs of reconstructed holograms made with the setup shown in Fig. 3-25 [25]

the object. For higher mode resonances, the hologram is a more complicated array of fringe patterns which makes it practical to identify the resonant mode in addition to the amplitude of vibration.

Conventional interferometry does not use the holographic procedure of reconstructing an image after developing a photographic record of the fringe pattern. Usually conventional interferometry is used to examine the motion or dimension of a point, whereas holography makes a record of entire surfaces.

CHAPTER 4
CALIBRATION SHAKERS

The shaker, or vibration generator, is the heart of any calibration system. Very accurate calibrations can be performed on almost any shaker. However, this accuracy is achieved only at those frequencies for which the vibration is rectilinear and free of transverse motion and acceleration waveform distortion. When a shaker is selected for calibrations it is necessary first to perform rather elaborate evaluations to determine the frequency ranges in which this pure sinusoidal motion is produced. It is best to select shakers that are virtually free of transverse motion and accelerometer waveform distortion throughout their operating range. Good-quality calibration shakers are commercially available. One is shown in Fig. 4-1.

Most calibrations are performed with electrodynamic shakers. Electrodynamic shakers are generally capable of producing sinusoidal motion at frequencies between 10 and 50 000 Hz. Special shakers are used for calibrating at frequencies lower than 10 Hz. Some piezoelectric shakers are used at selected high frequencies to produce the sinusoidal motion required for interferometric calibrations. A special mechanical shaker is used for transverse sensitivity calibrations.

4.1 Electrodynamic Shakers

The electrodynamic shaker is the counterpart of the inductive velocity pickup. In the shaker the inductive coil is used in its reciprocal sense, to produce rather than measure vibration. The coil is wound on an armature and becomes the moving element of the shaker. The coil is positioned in the gap of a strong magnet. Motion is produced by applying a sinusoidal alternating current to the coil. The resulting alternating magnetic field produced by the coil interacts with the steady flux of the magnetic field of the magnet to produce sinusoidal vibration.

Two characteristics are important in the design and use of calibration shakers: (1) the size and weight of the armature and (2) the suspension system used to support it in the magnetic structure. The armature should be small, so that its resonance is as high as possible. The resonance of the armature should be above the operating frequency range of the shaker. The suspension system used in the shaker should be as soft as practical and substantially free of effects due to suspension resonances. The soft suspension system also provides freedom from acceleration waveform distortion at low frequencies. Air-bearing shakers permit low-frequency operation without distortion and eliminate suspension resonance

77
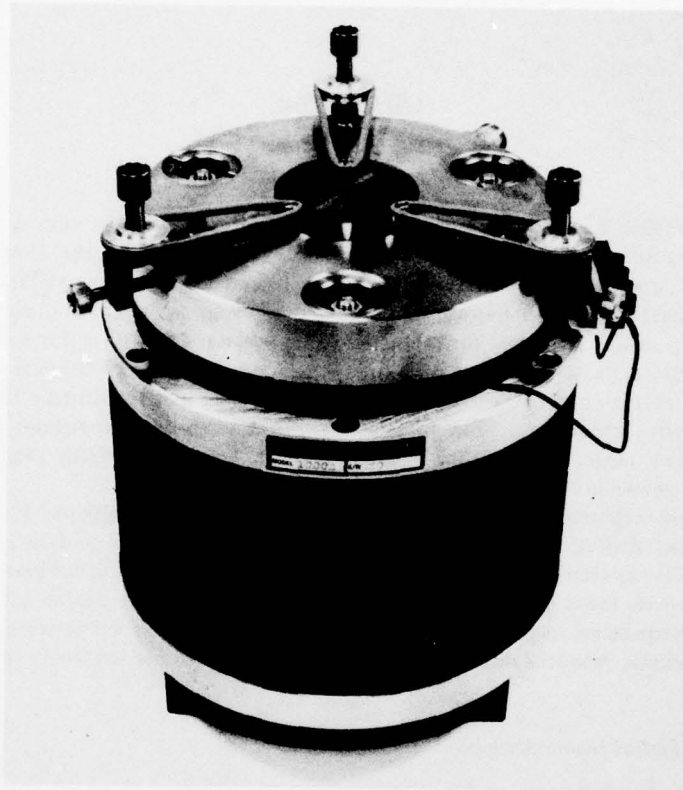
Fig. 4-1. Shaker designed for calibrating accelerometers and other vibration transducers. (Bouche Laboratories)

effects. Flexure plate supports used in other shakers have resonances that produce transverse motion in certain frequency ranges.

Armature Materials

Selection of the material for the moving element in the calibration shaker is the key to achieving a high resonance frequency. Many calibration shakers use a moving element fabricated from a single piece of material. The resonance frequency is determined by the mechanical properties of the material.

Evaluations of prototype high-frequency calibration shakers using beryllium alloy, alumina (sintered aluminum oxide), and magnesium alloy have provided useful performance data. The important properties of these materials are shown in Table 4-1. Beryllium alloy, like alumina, has a high modulus of elasticity,

Table 4-1. Characteristics of Materials Used for Shaker Armatures

Characteristic	Material		
	Beryllium Alloy	Alumina	Magnesium Alloy
Modulus of Elasticity, E, 10^9 N/m^2 (10^6 lbf/in.^{2}))	290 (42)	345 (50	45 (6.5)
Density δ, 10^{-3} kg/cm^3 (lbm/in.^{3})	1.9 (0.067)	3.9 (0.14)	1.8 (0.065)
Root Modulus/Density, $(E/\delta)^{1/2}$, cm$^{1/2}$/(10^3 in.$^{1/2}$)	40 (25)	30 (19)	16 (10)
Normalized Resonance Frequency, Hz	2.5	1.9	1
Internal Damping, Logarithmic Decrement	0.000 05	0.000 06	0.3*

*Achievable only when the material is mechanically stressed at 500 psi or above.
Source: Ref. 26.

while magnesium alloy has a low value. Alumina has the disadvantage of a density approximately twice that of beryllium and magnesium alloys. Taking the square root of the ratio of the modulus to the density shows that the resonance frequencies of shaker armatures of similar design are highest when the armatures are of beryllium alloy. Table 4-1 shows that the resonance frequency of the shaker with beryllium alloy is 2.5 times that obtained with magnesium alloy and 1.9 times that obtained with alumina.

One of the reasons for considering magnesium alloy is that under certain conditions high internal damping is obtained; whereas the internal damping is quite small for beryllium alloy and alumina. If high damping is achieved, the magnification at resonance is small and harmonic distortion in the motion caused by exciting the resonance is also small. However, this high damping is achievable only when magnesium alloy is subjected to significant mechanical stresses. In these prototype shakers there was no indication that high stresses are produced at resonance, and the magnesium alloy armature exhibited high magnification, like armatures built with beryllium alloy or alumina. Thus, there is no apparent advantage in using magnesium alloy for the moving element. The magnesium alloy armature has the disadvantage of a much lower resonance frequency, which

Table 4-2. Summary of Prototype Shaker Performance Characteristics

Characteristic	Specification			
	Shaker A	Shaker B	Shaker C	Shaker D
Moving Element, material	Beryllium Alloy	Beryllium Alloy	Alumina	Magnesium Alloy
Moving Element, mass kg (lbm)	0.18 (0.4)	0.32 (0.7)	0.45 (1)	0.45 (1)
Resonance Frequency kHz	55	35	30	10
Relative Motion at Maximum Frequency %	2	4	5	10
Sensitivity and Frequency Response Calibration Hz	5-10 000	5-10 000	5-10 000	5-5 000
Resonance Frequency Calibration Hz	5-50 000	- - -	- - -	- - -
Acceleration Distortion %	2	2	3	5

Source: Ref. 26.

causes excessive relative motion when the shaker is used to calibrate at high frequencies.

The alumina armature has almost as high a resonance frequency as the beryllium alloy armature. However, the mass of an alumina moving element is significantly higher, and more power is required to drive it. The alumina armature has the further disadvantage that the material is brittle and is more easily damaged by handling. It is apparent that beryllium alloy is the best material for the armatures of calibration shakers.

Shaker Performance

A summary of specific performance characteristics of prototype shakers built with these materials is shown in Table 4-2. The resonance frequency of the shaker was measured by putting a noninductive resistor in series with the driving coil. The current through the resistor, therefore, was identical in magnitude and

phase angle to the current in the driving coil. A high-resonance frequency accelerometer was attached to the shaker's moving element. The resonance frequency of the accelerometer was significantly higher than that of the shaker. The resonance frequency of the shaker was determined by observing when the ratio of accelerometer output to coil current was maximum and the phase angle between these signals changed from 0 degrees through 90 degrees and up to 180 degrees. Some care is required in interpreting such data if local resonances are present in the shaker's moving element or in the accelerometer used.

The resonance frequency measured on four prototype shakers is given in Table 4-2. The performance of these shakers is in agreement with the mechanical properties listed in Table 4-1. The shaker built with magnesium alloy has the lowest resonance frequency, and the beryllium alloy shaker has the highest. The slight variations between the mechanical properties of the material and the resultant shaker performance were caused by the fact that the moving elements of the different prototype shakers had somewhat different dimensions.

Relative Motion. An accelerometer standard is mounted in the calibration shaker armature to measure the motion of the armature table. The signal from the standard establishes the reference acceleration with which the test accelerometer is calibrated. Any motion between the standard and the mounting surface to which other accelerometers are attached is called relative motion. Relative motion is significant at high frequencies and varies with the mass of the test accelerometer mounted on the armature.

The relative motion between an accelerometer standard built into the shaker armature and the surface to which the other accelerometers are attached is determined by using a test accelerometer subassembly whose resonance frequency is not significantly changed when it is built with various accelerometer bases having masses up to 100 g. In other words, the distributed stiffness of the various bases, together with the stiffness of the mounting joint, are large compared with the effective stiffness of the seismic system in the accelerometer. Since the resonance frequency of the accelerometer with these bases is nearly unchanged, any variation in the ratio of the output of the standard built into the shaker would be a direct measure of the relative motion in the shaker.

The result of an evaluation of prototype shaker A is given in Fig. 4-2. For any accelerometer having the larger mass, 100 g, the motion at the base of the accelerometer was more than that for an accelerometer having a low mass, such as 20 g. Accordingly, the correction factor for heavy accelerometers is slightly less than 1.00. For shaker A, the amount of the correction for most accelerometers is less than 2% for calibrating at 10 000 Hz. The relative motion and correction factors for the other prototype shakers are given in Table 4-2. (Acceleration distortion in a shaker is usually caused by harmonic distortion in the driving power signal.) In the case of the magnesium alloy shaker, the relative motion is excessive, and corrections to calibration data at frequencies at or above 5 kHz would not be practical.
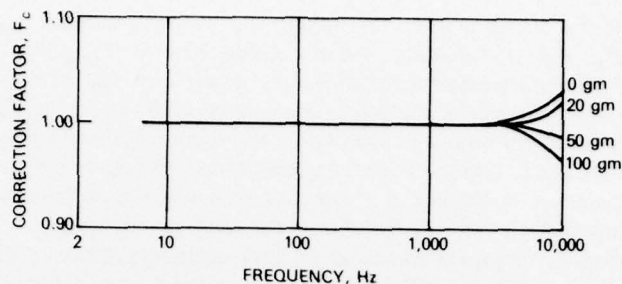
Fig. 4-2. Correction factors in measuring frequency response for a calibration shaker with various weights attached to the armature [26]

Distortion. The principal source of distortion in the acceleration motion of the shaker at high frequencies is harmonic excitation of the armature resonance frequency. The power amplifiers used with shakers produce harmonic distortion principally at odd harmonic frequencies of 3, 5, 7, 9, etc., times the excitation frequency. Accordingly, the shaker produces motion at the odd harmonics in addition to the motion produced at the fundamental or excitation frequency. It follows that shakers with lower axial resonance frequencies have more distortion for the same operating frequency range. The distortion of the various shaker designs is measured using a commercial distortion meter on the output of the accelerometer mounted on the shaker.

Transverse Motion. Transverse motion in a shaker produces calibration errors because the accelerometer standard and the accelerometer being calibrated produce a small output when subjected to vibration in a direction transverse to the axial motion of the shaker. This output is due to the transverse sensitivities of the accelerometers. Generally, the transverse sensitivity of the accelerometer standard is less than that of the accelerometer being calibrated, and most of the error is due to the latter.

The transverse sensitivity stated for an accelerometer is the maximum transverse sensitivity that occurs in a particular direction in the plane perpendicular to the accelerometer sensitive axis. When the accelerometer is vibrated in a direction that is in the transverse plane and also perpendicular to the direction of maximum transverse sensitivity, the output of the accelerometer is extremely small since the transverse sensitivity in that direction is small or zero.

If the transverse motion of the armature happens to occur in the direction of maximum transverse sensitivity of the accelerometer, the error can be computed by taking the product of the accelerometer transverse sensitivity and the armature transverse motion. For example, the maximum error would be 0.75% if the transverse motion were as large as 25% and the transverse sensitivity were 3%. However, it is very unlikely that the direction of transverse motion would exactly coincide with the direction of maximum transverse sensitivity. The

calibration error caused by transverse motion is nearly always considerably less than this value.

Another error produced by transverse motion is the output caused by the strain sensitivity of the accelerometer. When the armature experiences transverse motion, dynamic strains are produced in the accelerometer mounting surface. These strains can produce a measurable output in accelerometers with high strain sensitivities.

Significant transverse motion calibration can be avoided by using shakers with reasonably low transverse motions. The transverse motion of a shaker is often measured with a miniature triaxial accelerometer that is suitable for measurements throughout the frequency range of the shaker. The shaker is slowly swept through the frequency range, and measurements are made at each frequency exhibiting significant transverse motion, as indicated by the outputs from the X-and Y-axes of the triaxial accelerometer. The transverse motion of the shaker is computed by the ratio of the X-axis output divided by Z-axis output and the Y-axis output divided by the Z-axis output.

The maximum transverse motion is less than 25% for all the shakers listed in Table 4-2. This transverse motion occurs at several frequencies in the operating range up to 10 000 Hz. As discussed above, this performance produces very small calibration errors.

Low-Frequency Shakers

Most commercial shakers designed for calibration purposes have a low-frequency limit of 5 to 10 Hz. This makes it necessary to devise special fixtures that permit vibration calibrations at lower frequencies. The air-bearing shaker illustrated in Fig. 4-3 uses an extension table for these low-frequency calibrations. A second longitudinal air-bearing surface guides the moving element, permitting it to vibrate at amplitudes of at least 2.5 cm peak-to-peak. Elastic supports are used to apply a slight torsional moment against the second air bearing to eliminate torsional motion. The elastic supports also position the armature drive coil properly in the magnetic field. A servo accelerometer is built into the armature and serves as the calibration reference standard.

Some accelerometers and velocity pickups contain magnetic parts and are adversely affected by magnetic fields. This is especially noticeable when low-frequency calibrations are done because of the requirement to vibrate at large displacement amplitudes in order to maintain adequate signal-to-noise ratio in the outputs. At large displacement amplitudes the transducers move through a nonuniform stray magnetic field emanating from the magnetic structure of the shaker. This produces, at the operating frequency, an error signal that is either in or out of phase with the vibration output. Whether this error is present may be determined by repeating the low-frequency calibrations when the transducer is attached to an extension rod several inches in length. The transducer is vibrated several inches further away from the magnet structure at a point where
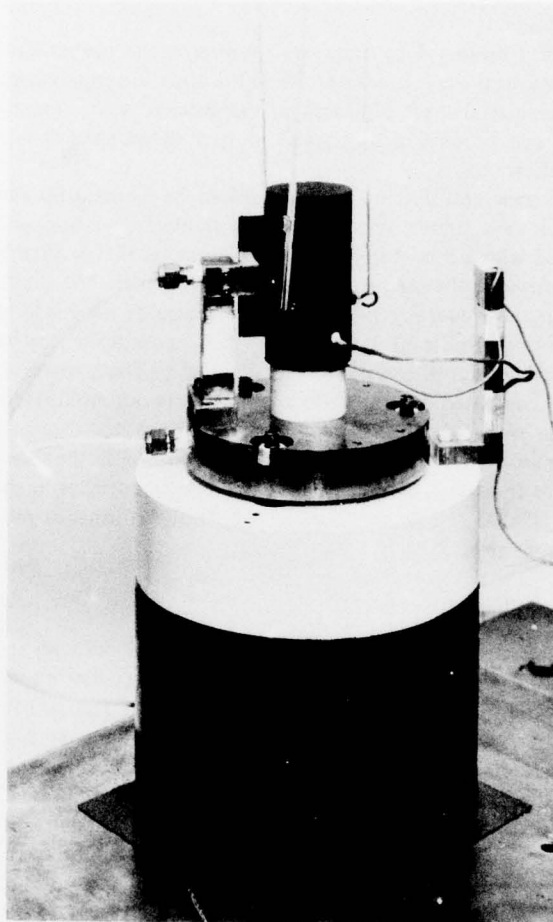
Fig. 4-3. Calibration shaker with provision for calibrating accelerometers at frequencies below 10 Hz (National Bureau of Standards)

the stray magnetic field is much lower. Care must be taken that the motion remains sinusoidal with the extension in place.

4.2 Piezoelectric Shakers

Piezoelectric shakers are built for those primary standards laboratories performing interferometric calibrations at high frequencies. Piezoelectric shakers
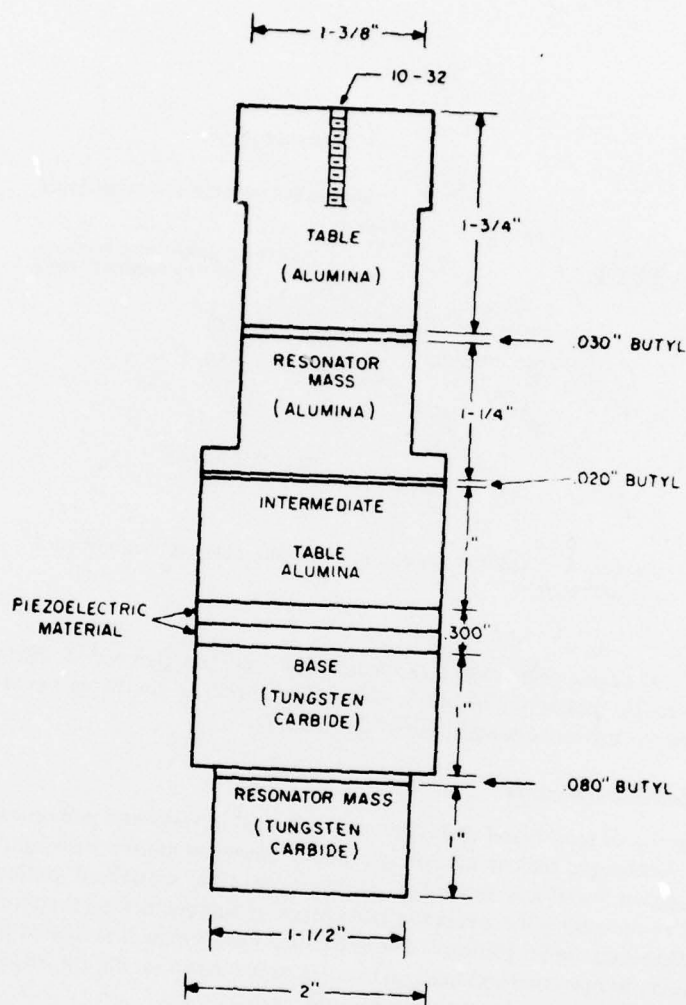
Fig. 4-4. Construction of a piezoelectric shaker [27]

consist of combinations of damped resonance cylindrical elements. They are built so that multiple resonances are present, to provide sinusoidal motion over the designed frequency range. These shakers are used mainly at selected frequencies as high as 100 kHz. However, most interferometric calibrations are performed at frequencies below about 10 kHz.

The design of a piezoelectric shaker is illustrated in Fig. 4-4. This shaker
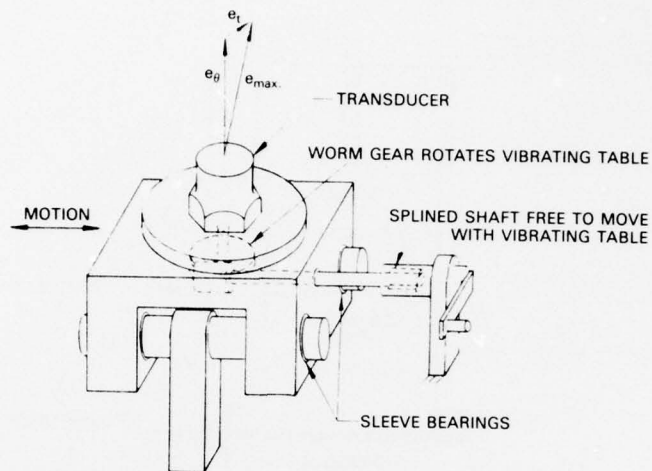
Fig. 4-5. A mechanical shaker for measuring transverse sensitivity of accelerometers

consists of alumina elements, piezoelectric disks, and tungsten carbide elements, separated by thin layers of butyl rubber. The shaker in the figure has several damped resonances between about 10 and 50 kHz.

4.3 Mechanical Shakers

The use of mechanical shakers should be limited to transverse motion calibrations. Mechanical shakers inherently produce sinusoidal motion with significant acceleration waveform distortion. However, in such specialized calibrations (such as measuring the transverse sensitivities of accelerometers) the effects of this distortion are insignificant. The reason for using mechanical shakers is their simplicity in operation and freedom from transverse motion at the low frequencies at which these calibrations are usually performed.

The shaker in Fig. 4-5 uses a scotch-yoke mechanism to produce quasi-sinusoidal motion. Virtually no transverse motion is produced because of the large displacement amplitude and because guides are used to prevent it. The transverse sensitivity calibrations are performed by first attaching the accelerometer to the shaker so that its sensitive axis is parallel to the shaker motion and its output is recorded. The accelerometer is then remounted so that its sensitive axis is perpendicular to the shaker motion. The mechanism in the shaker permits rotating the accelerometer about its sensitive axis through 360 degrees. The output of the accelerometer is observed as it is rotated. The ratio of the maximum

transverse output to the output in the sensitive direction, multiplied by 100, is the transverse sensitivity.

Chapter 5
PRIMARY SHOCK AND VIBRATION STANDARDS

A primary standard is one that is calibrated by an absolute method. The accuracy of a primary standard is determined by two factors. The first is the uncertainty of the measurements made while performing the absolute calibration on the primary standard. Second are the performance characteristics of the primary standard and their influence on the calibration results, which must be determined quantitatively.

The absolute calibration methods for shock and vibration standards are reciprocity, interferometry, direct-viewing optical, and centrifuge calibration, as well as calibration in the earth's gravitational field. The reciprocity method is used extensively in primary standards laboratories. Its most important advantages include high accuracy and broad frequency range. The principal advantages of interferometric calibration is its usefulness at very high frequencies (up to at least 10 000 Hz). Calibration in the earth's gravitational field is very useful for calibrating accelerometers having zero frequency response. The measurements made in performing these absolute calibrations are carefully evaluated so that calibration errors can be identified and recorded.

5.1 Description and Performance Characteristics

Piezoelectric accelerometers and electrodynamic velocity pickups are used as primary standards. The piezoelectric accelerometer has the advantage that it can be used as both a vibration and shock motion standard. It is designed to be used as a standard and to have nearly constant sensitivity over the frequency and amplitude ranges within which calibrations are performed. The electrodynamic velocity standard has a limited frequency range.

Piezoelectric Accelerometer Standards

A piezoelectric accelerometer standard is illustrated in Fig. 5-1. This accelerometer has an integral mounting stud that is electrically insulated from the case. The connector on the side of the accelerometer is also electrically insulated from the case, but it has a knurled grounding nut that is screwed in or out from the case to ground or insulate the accelerometer output. A seismic accelerometer is built inside the case, as close as possible to the top mounting surface. The mass element and piezoelectric crystals are designed for a very high resonance frequency. The top mounting surface has a threaded hole to accept threaded adaptors that accommodate the thread sizes used in mounting most accelerometers. It is most important to mount these accelerometers flush with the top

89
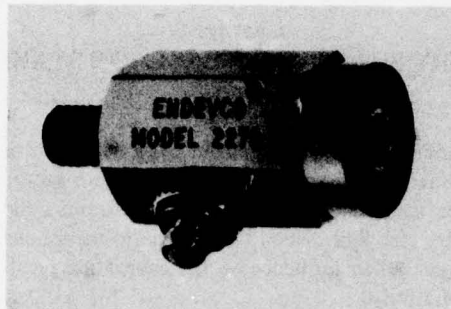
Fig. 5-1. A piezoelectric accelerometer standard (Endevco)

mounting surface of the standard; this minimizes calibration errors at high frequencies. Fixtures that separate the mounting surface of any test accelerometer from that of the accelerometer standard should be avoided.

The performance characteristics of a piezoelectric shock and vibration standard are listed in Table 5-1. These performance characteristics are established by rigorous evaluation tests.

Sensitivity. The value of 0.5% for the error and stability of the sensitivity is obtained by performing numerous reciprocity calibrations and carefully analyzing the various error sources. The mass effect on the sensitivity is 0.2% when 100 g is attached to the mounting surface. In other words, the piezoelectric accelerometer standard is deformed minutely by mechanical stresses, due to mounting torque and inertial forces created by the test accelerometer. Acutally, the errors due to this effect are much less than 0.2% because the mass of most accelerometers is less than 100 g.

Frequency Response and Relative Motion. The frequency response of the accelerometer standard is determined by performing comparison calibrations using an accelerometer previously calibrated at the National Bureau of Standards. The comparison is made by attaching this accelerometer to the mounting surface of the standard and measuring the ratio of their outputs at frequencies from 5 to 10 000 Hz. Typical results for this comparison calibration are given in Fig. 5-2. The sensitivity of this accelerometer standard is constant at frequencies up to 2000 Hz. The sensitivity gradually increases to about 2% at 10 000 Hz. This sensitivity of 1.02 mV/g is applicable for test accelerometers having a mass of 20 g, the mass of the National Bureau of Standards calibrated accelerometer used in this comparison calibration.

The sensitivities applicable at high frequencies for test accelerometers having various masses are determined by performing additional comparison calibrations. These calibrations are performed using several accelerometers, of known frequency

Table 5-1. Shock and Vibration Standard, Endevco Model 2270

Performance Characteristic	Specification
Sensitivity Error	±0.5%
Sensitivity Stability at 100 Hz	±0.5%/year
Mass Effect on Sensitivity at 100 Hz	±0.2%/100 g
Frequency Response and Relative Motion Sensitivity Change, 5-5000 Hz with up to 100 g Attached Mass	-2%*
Sensitivity Change, 5-10 000 Hz with up to 50 g Attached Mass	±4%*
Amplitude Linearity Sensitivity Change	±0.1%/1000 g
Transverse Sensitivity	3%, maximum
Temperature Response Charge Sensitivity	+0.3%/10°C
Strain Sensitivity	0.001 g/microstrain

*Estimated maximum error of correction made from curves showing that the nominal response is ±1%.
Source: Ref. 28.
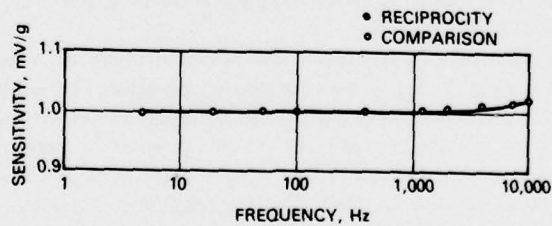
Fig. 5-2. Calibration of accelerometer standard against an accelerometer calibrated by the National Bureau of Standards [29]
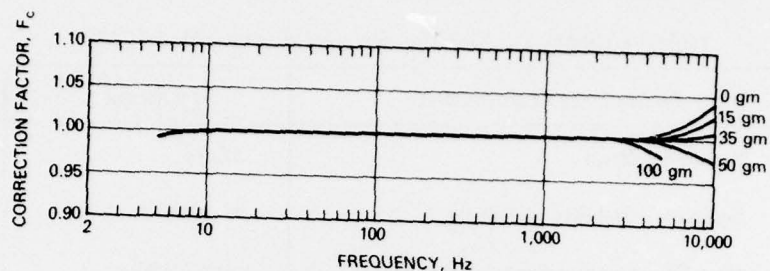
Fig. 5-3. Calibration of a standard accelerometer with accelerometers having various masses [30]

response characteristics and with masses ranging up to 100 g. The frequency responses of these accelerometers can be established from resonance frequency calibrations. However, it is preferable to have each of the accelerometers previously calibrated up to 10 000 Hz by either comparison or absolute methods traceable to the National Bureau of Standards. The results of these calibrations (Fig. 5-3) determine the change in sensitivity of the accelerometer standard at high frequencies.

The correction factor is + 2% for a test accelerometer weighing 15g and – 2% for one having a mass of 50 g. In other words, the acceleration sensitivity of a standard must be changed by this amount when comparison calibrations are performed on test accelerometers having masses corresponding to those listed in Fig. 5-3. These changes in sensitivity at high frequencies are caused by relative motion. (That is, the motion of the mounting surface is changed as a function of the mass attached to it.) It follows that the sensitivity of the accelerometer standard is the ratio of its electrical output to the acceleration motion at the mounting surface. Since this motion changes at high frequencies depending upon the attached mass, sensitivity also changes at high frequencies. It is customary to apply these correction factors when making comparison calibrations on various accelerometers. As indicated in Table 5-1, these correction factors are made with an uncertainty of ±1%.

Amplitude Linearity. It is known that the sensitivity of a piezoelectric accelerometer increases linearly with applied acceleration. For useful accuracy in shock motion standards, this sensitivity increase should not exceed a few percent at the highest acceleration of intended use. It would be even better if the sensitivity increases were as small as 1% throughout the rated acceleration range. It is difficult to prove experimentally that the sensitivity increase is only 1% at high accelerations up to 10 000 g, because shock motion calibration errors can be as large as 5%. Accordingly, to prove that the amplitude linearity deviations of a shock standard are less than 1%, it is necessary to perform calibrations on the standard at accelerations five times the maximum acceleration of intended use. For example, a shock calibration with errors up to 5% performed at

accelerations up to 50 000 g is adequate for confidence in the linearity of the standard for use at accelerations up to 10 000 g. Similarly, shock calibrations performed on standards up to 10 000 g provide confidence of adequate linearity in the standard at accelerations up to only 2000 g.

Calibrations at accelerations up to the equivalent of 50 000 g are performed by building a special accelerometer standard with an extra heavy mass element. By this means the same mechanical stress is applied to the crystals at low accelerations as would be present at high accelerations if a light mass element were used. For example, if the ratio of the heavy mass to light mass is 10, the equivalent acceleration will be 25 000 g if 2500 g is applied. If the mass element ratio 20, the equivalent acceleration would be 50 000 g, and so on. Performing comparison calibrations in this way determines the accelerometer standard sensitivity applicable at various amplitudes throughout the range of intended use.

The results of these comparison shock motion calibrations are shown in Fig. 5-4. Each point in the figure is obtained from an oscillogram from which the ratio of the output of the heavy mass element to that of the light mass element is measured. All the data points are used in a least-squares computation to determine the plotted line describing the amplitude linearity. The sensitivity increase is 5% at 50 000 g, 1% at 10 000 g, and 0.1% at 1000 g. Accordingly, correction factors of plus 0.5% are included when this standard is used to make comparison shock motion calibrations at 5 000 g, and 1% corrections are made at 10 000 g.

Transverse Sensitivity. The maximum transverse sensitivity of the accelerometer standard in Table 5-1 is ± 3%. This value is very acceptable because the transverse motion of good-quality calibration shakers is small. Errors due to the transverse sensitivity of the standard are negligible if reasonable care is used in selection and use of calibration shakers.
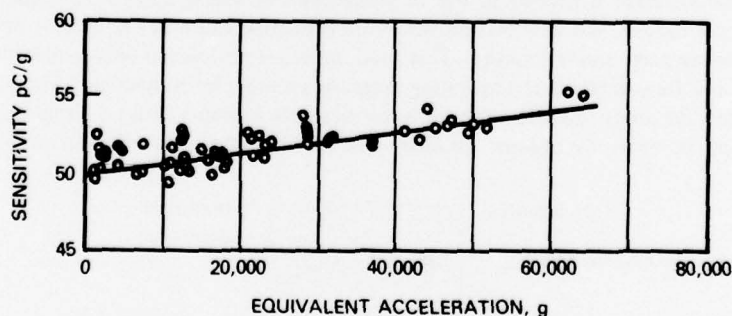
Fig. 5-4. Shock motion calibration of an accelerometer standard to establish amplitude linearity [28]

Temperature Response. Sensitivity calibrations are performed while the accelerometer standard is vibrated in a temperature chamber. These temperature response acceleration sensitivity calibrations are performed over the temperatures in the range from about 20°-30°C. However, if the standard is to be used for temperature response calibrations on other accelerometers it is important to calibrate the standard at both the high and low temperatures of intended use. The charge acceleration sensitivity of the standard in Table 5-1 increases 0.3% per 10°C. It is unnecessary to correct for the small temperature changes that occur in the calibration laboratory.

Strain Sensitivity. The strain sensitivity of the accelerometer standard is determined on a beam that applies known bending stresses to the mounting surface that is normally attached to calibration shakers. The maximum strain sensitivity of the standard in Table 5-1 is 0.001 g per microstrain. This indicates that the design of the standard provides good isolation from bending stresses. These stresses would be applied to the standard if the shaker used for calibrations had resonances that produced transverse motion within the operating frequency range.

Electrodynamic Velocity Standards

The electrodynamic standard consists of the velocity sensing coil and permanent magnet illustrated in Fig. 5-5. This standard is part of an electrodynamic shaker. The velocity sensing coil, driving coil, and mounting table are attached to a hollow shaft to form the moving parts of the shaker, which are suspended with the leaf springs. A constant magnetic field is developed around the driving coil as a result of supplying direct current to the field magnetic coil. Alternating current is supplied to the driving coil to create a sinusoidally varying magnetic field, which interacts with the constant magnetic field to produce sinusoidal vibration along the axis of symmetry of the moving parts. The electrodynamic standard is limited in use to frequencies at which there is negligible transverse motion and acceleration waveform distortion caused by resonances in the moving parts and leaf springs. This good motion is achieved at only a limited number of frequencies in the operating range. As a result, electrodynamic velocity standards are rarely used. However, it is instructive to examine their performance in detail in order to become familiar with the absolute reciprocity method.
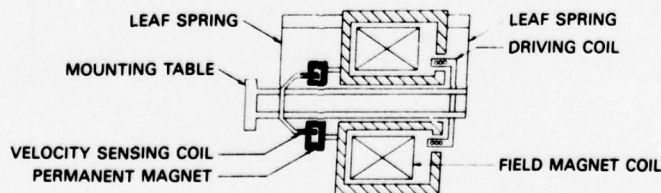
Fig. 5-5. Construction of a velocity standard

5.2 Reciprocity Calibrations

The reciprocity calibration is an absolute method for determining the sensitivity of a primary shock and vibration standard. The method requires the use of a reciprocal transducer. A reciprocal transducer is one that is capable of generating motion as a result of electrical excitation, producing an electrical output as a result of being subjected to mechanical shock or vibration. Piezoelectric accelerometers and electrodynamic velocity transducers are reciprocal transducers.

Accelerometers are designed to produce large electrical outputs when used to measure shock and vibration. Conversely, they do not produce very large motions when subjected to electrical excitation. Accordingly, it is desirable to use another transducer in the reciprocity calibration. It happens that the driving coil of the electrodynamic shaker is suitably designed to act as a reciprocal transducer. It is used both to produce vibration and to measure it during separate parts of the reciprocity calibration procedure.

Electrodynamic Standard Calibration

The equations that relate the mechanical and electrical quantities of an electrodynamic primary standard operating within its linear range are [31, 32]

$$V_t = CF_t + AL_1E_d \tag{5-1}$$

$$I_d = - AL_2F_t + BL_1E_d \tag{5-2}$$

$$E_s = HF_t + NL_1E_d \tag{5-3}$$

where V_t and F_t are, respectively, the velocity and force at the mounting table; I_d and E_d are, respectively, the current and applied voltage in the driving coil; and E_s is the voltage generated in the velocity sensing coil. The constants $L_1 = 2.249 \times 10^{-7}$ and $L_2 = 2.540 \times 10^{-8}$, are multiplying factors used when inches, pounds, seconds, amperes, and volts are used for the dimensions of the other quantities.* The constants A, B, C, H, and N depend on the construction of the standard. All the above symbols except L_1 and L_2 represent complex numbers in the manner commonly used in alternating current electrical theory.

The reciprocity relation for this combined electromechanical system is

$$\frac{F_t}{L_1 I_d}\bigg|_{V_t \approx 0} = - \frac{E_d}{L_2 V_t}\bigg|_{I_d = 0}.$$

---

*These equations were originally developed using English units of inches and pounds for length and mass, respectively. These units are retained in this theoretical discussion and in the data obtained from measurements made at that time.

This relation is determined by evaluating Eq. (5-1) when $V_t = 0$ and Eq (5-2) when $I_d = 0$ and solving the two pairs of equations simultaneously.

To develop the equations that make possible calibration of the electrodynamic vibration standard, we define calibration factor F of the standard as $F = E_s/V_t$, the ratio of the voltage in the velocity sensing coil to the velocity at the mounting table. If an object with mechanical impedance Z is attached to the table in such a way that F_t is its only reaction, then

$$F_t = -V_t Z \qquad \text{lbf}(N) . \tag{5-4}$$

Substituting Eq. (5-4) into Eqs. (5-1) and (5-3) and combining the results by eliminating E_d, we obtain

$$F = a + bZ \qquad V/\text{in.}/s \; (V/m/s) , \tag{5-5}$$

where a and b are combinations of the above-mentioned constants.

The relationship for the transfer admittance I_d/E_s between the coils is obtained by substituting Eq. (5-4) into Eq. (5-1) and then substituting the result into Eqs. (5-2) and (5-3). Thus,

$$\frac{I_d}{E_s} = \frac{B + (BC + A^2 L_2)Z}{N + (NC - AH)Z} . \tag{5-6}$$

Now consider attaching on the mounting table weights of known acceleration impedance $Z_a = j\omega m = j\omega W/g$ where m is the mass in kilograms, W is the weight in pounds, ω is the circular frequency in radians per second, j is the unit imaginary vector, and g is the acceleration of gravity (386 in./s^2; 9.80 m/s^2) From Eq. (5-6) we can form the relationship

$$\frac{W}{\left.\dfrac{I_d}{E_s}\right|_w - \left.\dfrac{I_d}{E_s}\right|_0} = J + QW, \tag{5-7}$$

where $I_d/E_s|_w$ and $I_d/E_s|_0$ are the values, respectively, of the transfer admittance at a given frequency with a weight of W pounds attached to the mounting table, and with no weight attached. J and Q are combinations of j, ω, g, and the above-mentioned constants. Note that if the transfer admittance is measured with at least two known weights attached to the table and with no weight attached, intercept J and slope Q of Eq. (5-7) can be determined.

An expression for the voltage ratio,

$$R = \frac{E_s}{E_d}\Big|_{I_d} = 0,$$

is obtained by letting $I_d = 0$ in Eq. (5-2) and substituting the result into Eq. (5-3), so that

$$R = \frac{E_s}{E_d}\Big|_{I_d = 0} = \frac{-HBL_1 + ANL_1L_2}{AL_2}. \tag{5-8}$$

Having formed these relationships, we can show by considering the relationship of all the constants that, in Eq. (5-5),

$$a = 0.01711\sqrt{j\omega J \frac{E_s}{E_d}\Big|_{I_d = 0}}$$

$$b = 6.601\, Q\sqrt{\frac{1}{j\omega J}\frac{E_s}{E_d}\Big|_{I_d = 0}}. \tag{5-9}$$

Thus we can determine the calibration factor of the electrodynamic standard at the frequencies ω desired by measuring (a) voltage ratio R and (b) transfer admittance G with a series of weights on the mounting table, and also with no weight on the table, to establish J and Q.

Voltage Ratio Measurement. Voltage ratio E_s/E_d when $I_d = 0$ is measured by driving the standard with a second vibration exciter through a mechanical connector. The magnitude of the voltage ratio is measured by using a voltage dividing circuit and a high-impedance voltmeter. The accuracy of the measurements depends only on how accurately the impedance values of the components in the circuit are known and on the repeatability of the voltmeter reading. The phase angle of the voltage ratio is measured with a phase angle meter or computed from a polygon of voltages. The polygon is constructed from voltage readings taken with a simple circuit connected across the driving coil. Determination of the phase angle depends on the accuracy of the voltmeter. The electrical impedance of the components of the circuits is such that at all frequencies the driving coil is effectively open-circuited. In making the voltage ratio measurements, care is taken to avoid frequencies at which transverse motion is present.

The results of the voltage ratio measurements (E_s/E_d when $I_d = 0$) on an electrodynamic standard are shown in Fig. 5-6. The first axial resonance occurs at approximately 1500 Hz. Above this frequency the driving coil and the velocity sensing coil move in opposite directions. There is another resonance near 4500 Hz, where another phase shift occurs. It is difficult to perform an accurate
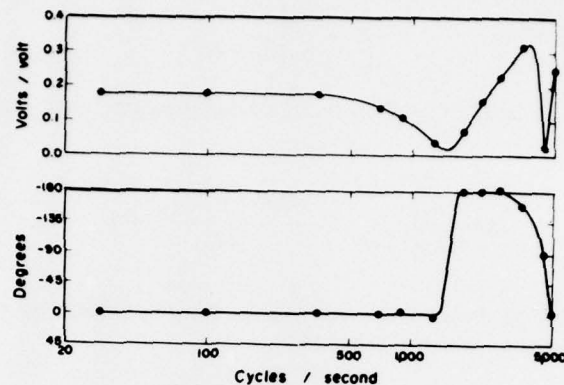
Fig. 5-6. Variation in the magnetic and phase angle of voltage ratio

calibration near resonance frequency because significant changes in the voltage ratio result from small changes in frequency and the large amplitude of the driver coil may exceed its linear range.

The effect of temperature on the voltage ratio is also particularly significant near resonance because of its effect on elastic constants and the tightness of joints. At frequencies considerably below the first axial resonance, the effect of temperature on the electromechanical characteristics of the standard are small.

Transfer Admittance Measurement. Transfer admittance measurements are made by putting a known resistor in series with the driving coil. The magnitude and phase of the transfer admittance is measured by connecting the circuits used for the voltage ratio measurements across this resistor.

The transfer admittance is measured with a sequence of weights attached to the mounting table at each frequency at which the voltage ratio is measured, but frequencies near the resonance are avoided. Care is taken to make transfer admittance and voltage ratio measurements at the same temperature. Transfer admittance values are separated into their real and imaginary parts, and the computation

$$\frac{W}{\left.\dfrac{I_d}{E_s}\right|_w - \left.\dfrac{I_d}{E_s}\right|_0} = \frac{W_n}{Y_{ew} - Y_{eo}}$$
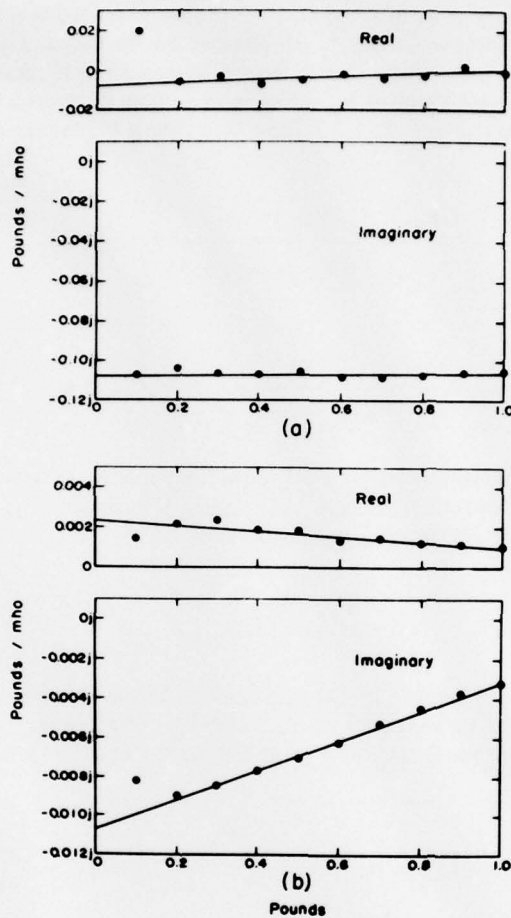
Fig. 5-7. Plot of transfer admittance as a function of mass
at (a) 900 Hz and (b) 5000 Hz

is performed. Typical results of these values at frequencies of 900 and 5000 Hz
are plotted in Fig. 5-7. The data are fitted by a weighted-least-squares procedure
to a straight line.

Weighted-Least-Squares Procedure. To determine intercept J and slope Q of
Eq. (5-7), it is necessary to measure transfer admittance Y_{en} with at least two
known weights W_n attached to the mounting table and Y_{eo} with no weight
attached. These measurements must be made at each frequency where J and Q
are desired. Plots of the real and imaginary parts of $W_n/(Y_{en} - Y_{eo})$ yield the

real and imaginary parts of J and Q. If more than two weights are used and the corresponding additional transfer admittances are measured, J and Q will be more accurately determined. Usually several weights (5 to 10, depending on the frequency) are used. Weights W_n are selected so that $W_n = n (\Delta W)$ and $\Delta W = W_n - W_{n-1}$, where $n = 1, 2, 3, \ldots$, and W_{n-1}, for $n = 1$ implies no weight. We have in general

$$\frac{W_n(Y_{enr} - Y_{eor})}{(Y_{enr} - Y_{eor})^2 + (Y_{eni} - Y_{eoi})^2} = J_r + Q_r W_n \qquad (5\text{-}10)$$

and

$$\frac{W_n(Y_{eni} - Y_{eoi})}{(Y_{enr} - Y_{eor})^2 + (Y_{eni} - Y_{eoi})^2} = - J_i - Q_i W_n \qquad (5\text{-}11)$$

where the additional subscripts r and i respectively refer to the real and imaginary parts of these quantities. Except near certain resonances, $(Y_{eni} - Y_{eoi}) \gg (Y_{enr} - Y_{eor})$. Consider the approximate value

$$\frac{W_n}{(Y_{eni} - Y_{eoi})} \qquad (5\text{-}12)$$

on the left side of Eq. (5-11). Let δ_{eni} and δ_{eoi} be the experimental errors that occur during the measurement of Y_{eni} and Y_{eoi} respectively. Then, assuming negligible experimental error in W_n, the left side of Eq. (5-11), i.e., Eq. (5-12), becomes

$$\frac{W_n}{(Y_{eni} - Y_{eoi}) + (\delta_{eni} - \delta_{eoi})} = \frac{W_n}{(Y_{eni} - Y_{eoi})} \left(1 - \frac{\delta_{eni} - \delta_{eoi}}{Y_{eni} - Y_{eoi}}\right), \qquad (5\text{-}13)$$

if other than first-order terms are neglected in the expansion of the small error quantities. Experiments show that $(Y_{eni} - Y_{eoi}) \approx n(\Delta Y_{ei})$, where ΔY_{ei} is the change in the imaginary part of the transfer admittance due to the addition of weight ΔW to the mounting table. If this approximation is applied to the error terms, Eq (5-13) becomes

$$\frac{W_n}{(Y_{eni} - Y_{eoi}) + (\delta_{eni} - \delta_{eoi})} = \frac{W_n}{(Y_{eni} - Y_{eoi})} - \left[\frac{1}{n} \frac{\Delta W}{(\Delta Y_{ei})^2} (\delta_{eni} - \delta_{eoi})\right].$$

$$(5\text{-}14)$$

The quantity in brackets is the error that results in the left side of Eq. (5-11) due to the experimental error $(\delta_{eni} - \delta_{eoi})$ of the transfer admittance measurements. Now, if $(\delta_{eni} - \delta_{eoi})$ is assumed to be nearly constant for all values of n, Eq. (5-14) shows that the error is proportional to $1/n$. For example, the error in the left side of Eq. (5-11) for $n = 10$ is $1/10$ that for $n = 1$. Likewise it can be shown that the errors for the real parts of the transfer admittances, the left side of Eq. (5-10), behave in the same manner.

Let y_{nr} represent the left side of Eq. (5-10). Then the equations for the usual least-squares procedure are

$$r_1 = y_{1r} - (Q_r W_1 + J_r)$$

$$r_2 = y_{2r} - (Q_r W_2 + J_r)$$

$$\cdots \qquad \cdots$$

$$r_n = y_{nr} - (Q_r W_n + J_r).$$

However, in our case the residuals or errors r_n are proportional to $1/n$. To properly adjust our least-squares procedure for the best fit of the data, the procedure should be modified as follows:

$$r_1 = y_{1r} - (Q_r W_1 + J_r)$$

$$2r_2 = 2y_{2r} - 2(Q_r W_2 + J_r)$$

$$\cdots \qquad \cdots$$

$$nr_n = ny_{nr} - n(Q_r W_n + J_r).$$

Squaring these equations and summing the results, we find that the sum of the squares of the residuals is least when

$$J_r \, \Sigma \, n^2 + Q_r \, \Sigma \, n^2 W_n = \Sigma \, n^2 y_{nr}$$

$$J_r \, \Sigma \, n^2 W_n + Q_r \, \Sigma \, n^2 W_n^2 = \Sigma \, n^2 W_n y_{nr}.$$

For $W_n = 0.2, 0.4, \ldots, 2.0$ lb, the real parts of J and Q are

$$J_r = 0.042\,040\,980\,7 \, \Sigma \, n^2 y_{nr} - 0.025\,100\,401\,6 \, \Sigma \, n^2 W_n y_{nr} \qquad (5\text{-}15)$$

and

$$Q_r = -0.025\,100\,401\,6 \, \Sigma \, n^2 y_{nr} + 0.015\,972\,982\,8 \, \Sigma \, n^2 W_n y_{nr}. \qquad (5\text{-}16)$$

Similarly, for the same set of weights, the imaginary parts of J and Q are

$$J_i = -0.042\,040\,890\,7\,\Sigma\,n^2 y_{ni} + 0.025\,100\,401\,6\,\Sigma\,n^2 W_n y_{ni} \qquad (5\text{-}17)$$

and

$$Q_i = 0.025\,100\,401\,6\,\Sigma\,n^e y_{ni} - 0.015\,972\,982\,8\,\Sigma\,n^2 W_n y_{ni}, \qquad (5\text{-}18)$$

where y_{ni} represents the left side of Eq. (5-11).

The ordinate intercepts J and the slopes Q are determined with the above equations. The values of J and Q are substituted, together with the voltage ratio measurements at their respective frequencies, into Eq. (5-9) and the values of a and b are computed.

Calibration Results. Substituting the values of a and b into Eq. (5-5) gives at each of the calibration frequencies an expression for the calibration factor of the electrodynamic standard as a function of the mass of any vibration pickup that is attached to the mounting table. To illustrate the effect of a transducer on calibration factor F, the factors have been computed for transducers having masses of 0, 0.5, and 1.0 lb (0.45 kg). These factors are shown in Fig. 5-8. The calibration factors are constant to within 1% at frequencies up to 900 Hz. Also, for this particular electrodynamic vibration standard, the effect of transducer mass up to 1 lb (0.45 kg) is negligible at frequencies up to 900 Hz. Above 900 Hz this effect becomes significant, being greatest at 5000 Hz. This is due to relative motion between the velocity sensing coil and the mounting table.

Piezoelectric Standard Calibration

Piezoelectric accelerometer standards have the advantage of broad frequency range. The acceleration sensitivity of such a standard is usually constant throughout the range from about 10 to almost 5000 Hz. The small variations in sensitivity at higher frequencies (up to 10 000 Hz) are determined by comparision calibrations traceable to the National Bureau of Standards. The accuracy of the primary standard is enhanced by performing the absolute reciprocity calibration at a low frequency in the range at which sensitivity is constant. The particular frequency selected will depend on the characteristics of the electrodynamic shaker selected.

It is important to recognize that there is no relative motion in the standard throughout the frequency range in which the sensitivity is constant. This is confirmed by the fact that slope Q in the plots of transfer admittance vs mass tends to zero, and Eq. (5-9) indicates that term b in Eq. (5-5) may be ignored. These particular equations apply only for veloicty standards. Making them applicable to acceleration standards requires merely dividing the right side of Eq. (5-9) by the circular frequency, $j\omega = j2\pi f$. Accordingly, the sensitivity of an accelerometer standard calibrated by the reciprocity method becomes [29]
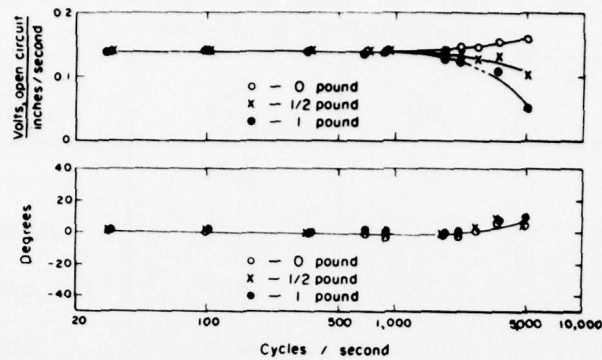
Fig. 5-8. Variation in magnitude and phase angle of the calibration factor of an electrodynamic standard, as computed for various transducer masses

$$S_s = 2635 \sqrt{JR/jf} \qquad\qquad (5\text{-}19)$$

where

S_s = sensitivity (mV/g) of the piezoelectric accelerometer standard

J = transfer admittance intercept (the intercept of a plot of weight vs transfer admittance ratio, in lbm/mho where transfer admittance ratio G is driver-coil current/piezoelectric-accelerometer voltage output, and weight refers to the 10 valves (0.1-1 lbm) used for the calibration here described)

R = voltage ration (voltage output of the piezoelectric accelerometer standard divided by the voltage output of the driver coil when the shaker is driven by a second driver coil and the first driver coil is open-circuit)

j = $\sqrt{-1}$, the 90-degree vector

f = the frequency in hertz at which the voltage ratio is measured

The transfer admittance intercept is given by

$$J = 0.042\,04 \,\Sigma\, n^2 Y_{nr} - 0.050\,2 \,\Sigma\, n^2 W_n Y_{nr}. \qquad\qquad (5\text{-}20)$$

In Eq. (5-20),

n = integers from 1 to 10 corresponding to the number of weight increment W_n (see Table 5-2)

W_n = weight, in lbm (N), increments of 0.1 lbm, from 0.1 to 1.0 lbm in this calibration see Table 5-2).

Table 5-2. Transfer Admittance Measurements on Piezoelectric
Standard PX-SP46 Serial Number 10

n	W_n (lb)	G_n (A/V)	Y_{nr} (lb-V/A)
–	0.0	24.84	–
1	.1	31.55	0.014 92
2	.2	38.17	.015 00
3	.3	44.74	.015 08
4	.4	51.55	.014 98
5	.5	58.14	.015 02
6	.6	64.72	.015 05
7	.7	71.17	.015 11
8	.8	78.03	.015 04
9	.9	84.64	.015 05
10	1.0	91.32	.015 04
–	.0	24.84	–

Source: Ref. 29.

The term Y_{nr} in Eq. (5-20) is computed as follows:

$$Y_{nr} = W_n/(G_n - G_o), \qquad (5\text{-}21)$$

where

G_n = the transfer admittance ratio, as defined for Eq. (5-19)
G_o = the transfer admittance ratio with no weight attached to the shaker.

Use of these equations is further simplified by examining the phase angle of the measurement quantities. It is helpful to operate the shaker selected for the

reciprocity calibration at a frequency far below the axial resonance of the moving element. This assumes that the moving element acts as a rigid body and that there is no relative motion between the reciprocal velocity coil in the shaker and the acceleration standard. It is also concluded, from Newton's second law of motion, that the acceleration motion of the piezoelectric standard is in phase with the force exerted by the table, and therefore, that the phase angle between the acceleration motion of the reciprocal coil and piezoelectric standard is 0 degrees.

For sinusoidal motion, the phase angle of velocity is 90 degrees relative to the acceleration. Accordingly, the phase angle of the voltage ratio is 90 degrees and cancels the 90-degree vector j in Eq. (5-19). Furthermore, it is known that the phase angle between the driver coil current and the output of the piezoelectric accelerometer standard is 0 degrees. This follows from a similar consideration of Newton's second law of motion and the fact that the force generated in the coil is proportional to the current. This physical interpretation of the piezoelectric standard and electrodynamic shaker characteristics is justified as long as care is taken to perform the reciprocity calibration at a low frequency. This analysis eliminates the necessity of measuring phase angle during the reciprocity calibration procedure and thereby eliminates errors that would be present in phase angle measurements.

Reciprocity Calibration Procedure. A shaker selected for the reciprocity calibration of piezoelectric accelerometer standards is illustrated in Fig. 5-9. The moving element of the shaker is equipped with two driving coils, one (coil no. 1) of which is used as the reciprocal transducer. Coil no. 2, near the center of the shaker, is used merely to produce sinusoidal motion, while the first coil is used as velocity transducer during the voltage ratio measurement of the calibration procedure. The axial resonance frequency of the moving element of this shaker is more than ten times the reciprocity calibration frequency. The frequency selected for performing reciprocity calibration is 100 Hz, which is far below axial resonance and assures that there is no relative motion between the reciprocal coil and the accelerometer standard.

The calibration procedure is summarized in the following steps:

1. Calibrate 10 weights in equal increments of 0.1 16 from 0.1 to 1.0 16 on a scale balance.

2. Determine transfer admittance ratio G with each weight and with no weight attached to the shaker. This requires measuring the driver coil current and piezoelectric accelerometer voltage output at each step, since these quantities form this ratio.

3. Sum the transfer admittance measurements as indicated by Eqs. (5-20) and (5-21), and calculate J.

4. Measure the voltage ratio R (the piezoelectric standard output divided by the open-circuit driver coil output when the shaker is driven by a second driver coil or shaker).
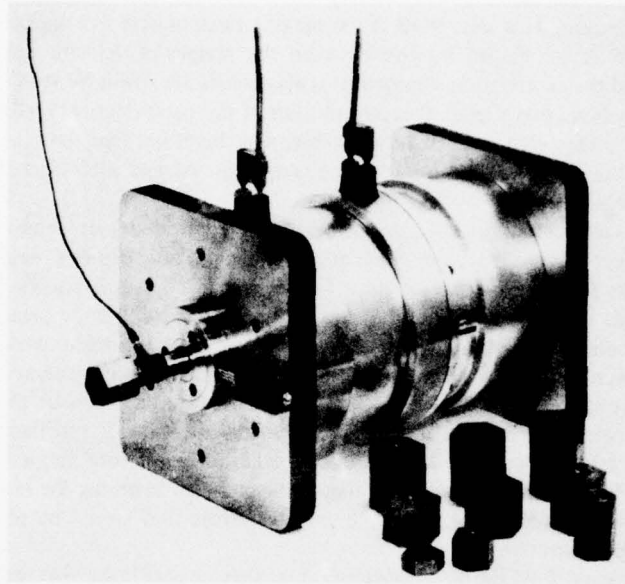
Fig. 5-9. Setup for transfer admittance measurement

5. Use an electronic counter to measure the frequency at which step 4 is performed.

6. Using the values of J, R, and f from steps 3, 4, and 5 respectively, compute from Eq. (5-19) the sensitivity of the piezoelectric accelerometer standard.

Transfer Admittance Measurement. A sample calibration that follows the above procedure will be described. First to be discussed will be the transfer admittance measurements, the block diagram for which is illustrated in Fig. 5-10. Although two driver coils are permanently built into the shaker, only the reciprocal driver (coil no. 1) is used for the transfer admittance measurements.

The shaker is free of excessive transverse motion and has a sinusoidal motion whose distortion is less than 1%. Also, the driver coil current I_d and the standard accelerometer outputs E_o have a phase angle of 0 degrees as verified by the oscilloscope. All of these shaker characteristics are present throughout an appreciable frequency range, including the calibration frequency.

Each of the ten weights is attached to the shaker for measurements of transfer admittance (G_n), which is defined as

$$G_n = 1/D_n = \left.\frac{I_d}{E_o}\right|_n \tag{5-22}$$
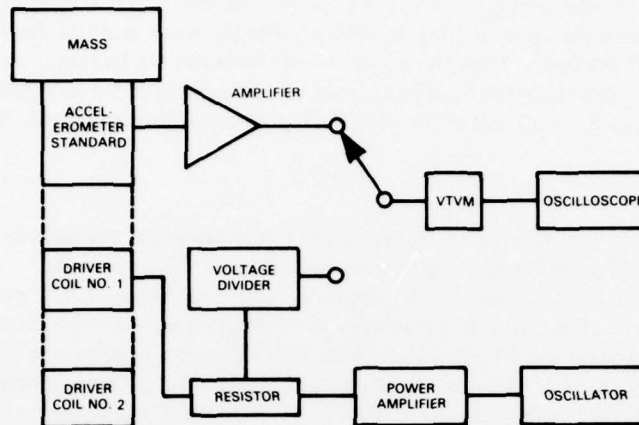
Fig. 5-10. Equipment for transfer admittance measurements
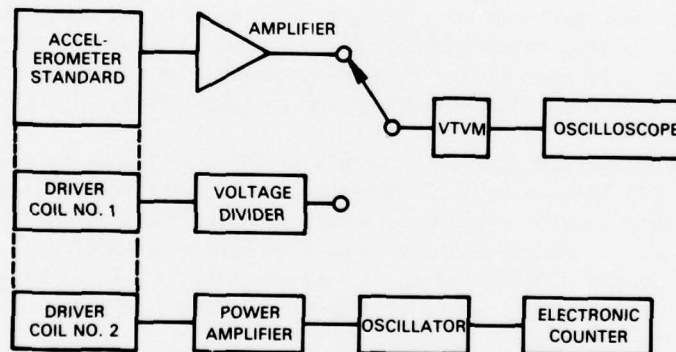
Fig. 5-11. Equipment for voltage ratio measurement [29]

where D_n is the divider setting that exactly equates divider voltage output to the output from the piezoelectric standard. The voltage divider and resistor, $1\text{-}\Omega$ precision type, should be noninductive and of a quality commonly found in standards laboratories.

Table 5-2 lists the values of G_n and the corresponding values of Y_{nr} computed for a typical reciprocity calibration. When the products of $n^2 Y_{nr}$ and $n^2 W_n Y_{nr}$ are summed and substituted in Eq. (5-20), J is computed to be 0.015 03 lb-V/A for the measurements listed in Table 5-2.

Voltage Ratio Measurement. Figure 5-11 illustrates the block diagram for this measurement. The setup is the same as for Fig. 5-10 except that the masses are

removed and the second driver coil is used to excite the shaker. The oscilloscope or a phase angle meter is used to indicate that the phase angle of the voltage ratio is 90 degrees, and the electronic counter measures the frequency at which the voltage ratio is taken. As before, an adjustment is made of the voltage divider output until it equals that of the piezoelectric standard. Voltage ratio R, then, is

$$R = D_r$$

where D_r is the setting on the voltage divider. As an example, the value of R was 0.047 9 V/V at 50 Hz on PX-SP46 piezoelectric standard serial no. 10.

Equation (5-19) is used in the computation, with the values of J, R, and f obtained above; this results in a sensitivity of 10.00 mV/g for piezoelectric accelerometer standard no. 10. Close agreement with this value is shown by a previous calibration at the National Bureau of Standards. The latter calibration, an average of 38 points from 10 to 4000 Hz, established a sensitivity of 10.02 mV/g with 0.5% standard deviation.

Reciprocity Calibration Accuracy. The calibration results described above are included in Table 3-5, which also includes results obtained on other vibration standards calibrated by the reciprocity method. All the standards were adjusted so that their sensitivities were multiples of 10 for simplicity of use. All are piezoelectric standards except for the first row, which covers the electrodynamic standard. In the last column of the table the standard deviation is expressed as a percentage of the average sensitivity of all the calibrations performed on each standard.

The piezoelectric accelerometers used in these calibrations are specially designed to have a minimum of calibration errors due to temperature, strain, and other environmental factors. For these accelerometers, the sensitivity was adjusted prior to the first calibration in Table 5-3 by inserting capacitance or adjusting the gain of the standard amplifier shown in Figs. 5-9 and 5-10. In the case of the electrodynamic standard the proper value of resistance was put in series with the coil to obtain the desired sensitivity.

An error analysis of the reciprocity calibration method is given in Table 5-4, where an estimate of the individual errors is listed for the various error sources present. In addition to 100 Hz, the reciprocity errors apply to any frequency at which the 0-degree admittance and 90-degree voltage ratio phase angles are present. The square root of the sum of the individual errors squared is determined, to yield the final estimated error.

The 0.5% sensitivity error listed in Table 5-4 agrees closely with the standard deviations for piezoelectric accelerometer standards listed in Table 5-3. A similar analysis for the electrodynamic velocity standard produces an estimated error of 0.3%, which is close to the standard deviation in Table 5-3.

In addition to performing the low-frequency reciprocity calibration for the piezoelectric accelerometer standards, it is necessary to obtain accelerometer response at higher frequencies. This is done by a comparison calibration up

Table 5-3. Summary of Reciprocity Calibration Results
on Primary Vibration Standards

Standard	Calibration History (years)	Number of Reciprocity Calibrations	Average Sensitivity*	Standard Deviation (%)
Electrodynamic[†]	3	10	99.8	0.5
P6SP31 1[†]	1	4	100.2	.4
P6SP31 2[†]	1	2	99.9	.1
P10SP46 3	6	10	10.00	.3
P10SP46 4	6	8	9.97	.4
P10SP31 5	6	8	100.8	.8
P10SP46 10[‡]	3	3	10.01	.0
P10SP46 11[†]	2	2	10.05	.0
P10SP46 12	4	3	10.04	.3
P10SP46 14[†]	2	3	9.97	.2
2270NA09[#]	4	13	1001	.2
2270NA21[§]	4	8	1000	.1
2270PA06[§]	3	4	1003	.2

*Units per pC/g or mV/g ; for the electrodynamic velocity standard the units are applicable at 50 Hz only.

[†]Calibrations have been discontinued, since these standards are no longer in use.

[‡]Standard no. 10 was also calibrates at N.B.S.; 10.02 mV/g was the average sensitivity reported up to 4 kHz with a standard deviation of 0.5%.

[§]Calibrated with a charge amplifier using the gain range of 1000 mV/g.

[#]Standard NA09 was also calibrated from 10 Hz to 10 000 Hz at N.B.S. on the gain range of 1 000 mV/g; the average of all the calibration points was 100.4 MV/g with a standard deviation of 0.9%.

Source: Ref. 29.

to 10 000 Hz with an accelerometer standard previously calibrated at the National Bureau of Standards. The errors of this comparison calibration are included in Table 5-4.

5.3 Interferometric Calibrations

Interferometry is used in some primary standards laboratories for absolute calibrations at high frequencies to supplement reciprocity calibrations. The reciprocity calibration errors increase at high frequencies at which significant relative motion is present. Accordingly, there is a choice between using reciprocity or interferometry at frequencies in the range of about 2000 to 10 000 Hz. Sometimes interferometric calibrations are performed at higher frequencies, up to about 40 000 Hz.

Table 5-4. Analysis of Calibration Errors in Determining the Sensitivity of the Endevco Model 2270 Accelerometer Standard at Various Frequencies

Reciprocity Calibration, 100 Hz		Comparison Calibration, 5-10 000 Hz	
Measurement	Error (%)	Measurement	Error (%)
	percent		percent
Mass	0.5	Optical Calibration, 5 Hz	1.0
Transfer Admittance Intercept	0.2*	NBS Calibration, 10-900 Hz	1.0
Voltage Ratio	0.2*	NBS Calibration, 900-100 000 Hz	2.0
Distortion	0.1		
		Distortion	0.2
Frequency	0.05		
Accelerometer Effects, Transverse Sensitivity, Strain, Temperature, etc.	0.2	Accelerometer Effects, Transverse Sensitivity, Strain, etc.	0.2
		Amplifier Effects, Frequency Response, etc.	0.1
Amplifier Effects, Gain Stability Source Capacitance, etc.	0.3	Relative Motion, 900-10 000 Hz	0.5
		Voltage Ratio	0.2
Estimated Error, 100 Hz	0.5†	Estimated Error, 5-900 Hz	1.1†
		Estimated Error, 900-10 000 Hz	2.1†

*Assume 0° and 90° phase shifts for transfer admittance and voltage ratio measurements, respectively.

†Determined from the square root of the sum of the squares of the applicable individual errors.

Source: Ref. 29.
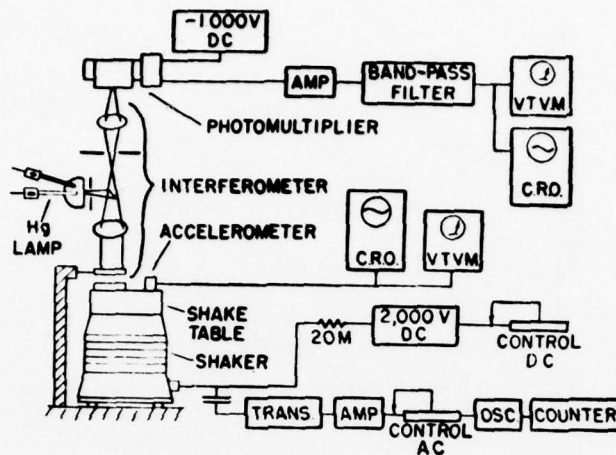
Fig. 5-12. Equipment formerly used for interferometric calibration
at the National Bureau of Standards

Figure 5-12 is a block diagram of an interferometer, shaker, and instruments
formerly used at the National Bureau of Standards. The interferometer is a
Fizeau type, which reflects light using a mercury source. The light is reflected
from a small, plain, unsilvered mirror attached immediately beside the acceler-
ometer base. The mirror and accelerometer experience the same vibration ampli-
tude. A small-curvature planoconvex lens is mounted on a stationary frame
above the plain mirror. An image of the Newton's ring pattern is brought to
focus on a circular aperture in such a way that only light from the center spot is
allowed to fall on the photomultiplier. The signal from the photomultiplier is
sent through a narrow-band filter tuned to the shaker driving frequency before
being measured by a vacuum-tube voltmeter.

A vibration isolation system is used to decouple the interferometer from
building vibrations.

As the vibration amplitude is gradually increased from zero, the fringe pattern
disappears and a null indicates zeros of a Bessel function of the vibration ampli-
tude and the interferometer light wavelength. The photomultiplier current
becomes zero at these nulls, as illustrated in Fig. 5-13. The light used is mercury
5461 Å. The first null corresponds to a vibration amplitude of 1045 Å. The
photoelectronic null detection used at the National Bureau of Standards per-
mitted determining this vibration amplitude with an uncertainty of 0.5%. The
calibration is completed by measuring the electrical output of the accelerometer
and the frequency from which the applied acceleration is computed. The total
calibration error would include errors present due to distortion in the sinusoidal
motion waveform and to measuring the voltage and frequency.
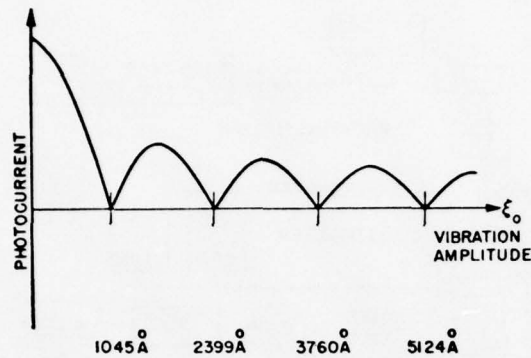
Fig. 5-13. Photomultiplier current versus vibration ampli-
tude sensed by an interferometer using 5461-A light, show-
ing characteristic nulls

Several interferometric calibration setups are used. Some laboratories use
lasers as a light source in the interferometer.

The instrumentation setup for interferometric calibrations is usually quite
elaborate, and the calibration errors are somewhat larger than those obtainable
by the reciprocity method, particularly at lower frequencies.

5.4 Zero-Frequency Calibrations

The earth's gravitational field provides a very accurate means for calibrating
accelerometers at zero frequency. This method is used with accelerometers
designed for measuring constant accelerations. Of course, vibration and shock
motion calibrations should also be performed on each accelerometer throughout
its operating frequency and amplitude range.

An indexing head used for zero-frequency calibrations is illustrated in Fig.
5-14. A good-quality level is used to adjust the head so that the sensitive axis
of the accelerometer attached to it is exactly parallel to the earth's gravitational
field. The output of the accelerometer is measured with a d.c. voltmeter with the
accelerometer in this position. The head is rotated exactly 180 degrees to change
the applied acceleration from exactly plus 1 g to exactly minus 1 g, and the out-
put of the accelerometer is again measured. The acceleration sensitivity is the
average of the two outputs. The estimated error in adjusting the tilting support
to 1 g is ±0.00 3 g. The total calibration error would also include the uncertainty
in measuring the voltage outputs of the accelerometer.

Fig. 5-14. Indexing head for performing zero-frequency calibrations [34]

Chapter 6
SINUSOIDAL COMPARISON CALIBRATIONS

The comparison method is used in most shock and vibration calibration laboratories. Absolute calibrations should be used only in establishing and maintaining primary standards; it is economical for the calibration laboratory to send its vibration and shock standards to a primary standards laboratory yearly for recalibration. These r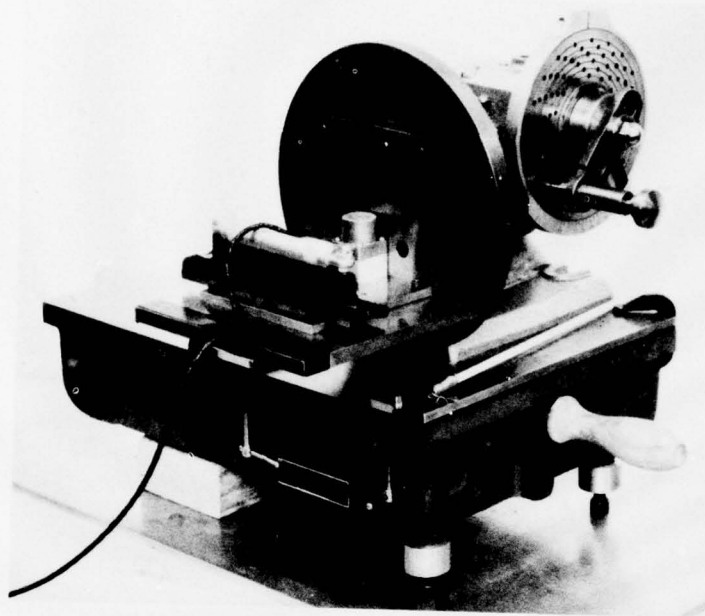ecalibrations can be used to establish a history of the accuracy and quality of the standards. Variations in calibration results from year to year should not exceed the calibration errors stated by the Primary Standards Laboratory. Significantly larger variations indicate that the standard is of poor quality or has been damaged.

6.1 Sensitivity and Frequency Response

Calibration Setup

The first step in performing accurate sensitivity and frequency response calibrations is to obtain good-quality instruments or at least evaluate the performance of those on hand. This precaution pertains particularly to accelerometer standard and shaker. The accelerometer standard should have good performance characterisitics, and the shaker should have good-quality motion throughout the operating frequency range. The shaker should not be used at frequencies at which excessive transverse motion or acceleration waveform distortion is present.

Generally, a simple setup makes it easy to perform accurate calibration. Attention to the following laboratory procedures is important for obtaining consistently accurate calibration results. Elaborate automatic systems, however, may be used to minimize human errors, shorten training periods for operators and aid in maintaining permanent records of calibrations.

A simple calibration setup is illustrated in Fig. 6-1. It includes a shaker and accelerometer standard to which the test accelerometer standard is attached. Charge amplifiers are used with both the standard and test accelerometers. The voltage divider is connected to the standard amplifier, since its output is made larger than the output of the test accelerometer by selecting the appropriate gain ranges on both amplifiers. The voltage divider is a precision resistance decade instrument that directly indicates the ratio of test to standard outputs with a precision of four significant figures. This ratio is obtained with the electronic voltmeter by alternating the switch to the up and down positions and adjusting the voltage divider until the two readings are identical. A dual-beam oscilloscope is used to monitor the waveforms from both accelerometers. This procedure is repeated at selected frequencies by manually adjusting the audio oscillator.

When a standard accelerometer-amplifier system with a sensitivity of 1000 mV/g, 100 mV/g, etc., is used, the decimal point of the test accelerometer

115
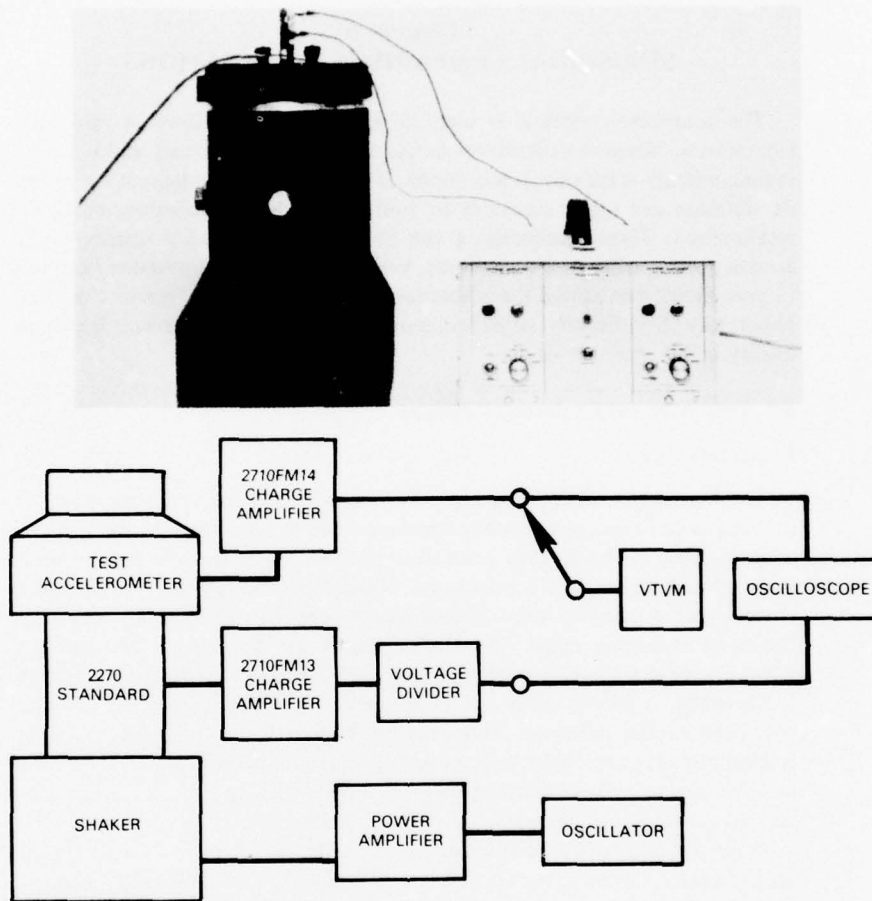
Fig. 6-1. Typical setup and block diagram for sinusoidal comparison calibration

sensitivity is determined by the ratio of gain ranges used on the amplifiers. This procedure is summarized in the following equation:

$$S_t = S_s R \frac{K_s}{K_t} \qquad (6\text{-}1)$$

where

S_t = sensitivity of test accelerometer, in millivolts per g
S_s = sensitivity of standard accelerometer, in millivolts per g
R = ratio of test accelerometer to standard accelerometer outputs

K_s = gain of standard amplifier

K_t = gain of test accelerometer amplifier.

The acceleration charge sensitivity of a piezoelectric accelerometer is determined by dividing the test accelerometer sensitivity by the gain of its charge amplifier, expressed in millivolts per picocoulomb.

An appropriate voltage amplifier is used in place of the test charge amplifier for calibrating piezoresistive or strain gage accelerometers.

Velocity pickups are usually calibrated without a test amplifier since the output may be measured directly with an electronic voltmeter. The sensitivity of the velocity pickup is given by

$$S_v = 0.6417\, S_s Rf, \text{ in millivolts per meter per second}$$

$$S_v = 0.0163\, S_s Rf, \text{ in millivolts per inch per second} \tag{6-2}$$

where

S_v = velocity sensitivity in millivolts per meter (or inch) per second

R = ratio of velocity pickup to accelerometer standard outputs

f = frequency, in hertz.

Typical Calibration Results

Calibration results for three representative piezoelectric accelerometers are illustrated in Fig. 6-2. The total mass of each accelerometer ranges from 2 to 78 g, and the sensitivity ranges from approximately 3 to 100 pC/g. The accelerometers using the P6 and P8* ceramic materials show a gradual decrease in acceleration sensitivity of somewhat less than 1% per octave increase in frequency. The accelerometer using the P10* ceramic material has virtually constant sensitivity throughout most of its operating frequency range. All the accelerometers increase in sensitivity at higher frequencies. This is due to the resonance frequency of the accelerometer.

The calibration errors applicable to these and similar piezoelectric accelerometers are given in Table 6-1. Each error listed is determined by careful consideration of the performance characteristics of the accelerometer standards, test accelerometers, charge amplifiers, shaker, and other instruments used. The estimated error of 1% is routine in laboratories using reasonably good laboratory practices. It is common for laboratory calibration to differ by less than 2% in the same accelerometer, even though the calibration instruments, procedures, and laboratory conditions vary somewhat. The calibration errors at frequencies up to 10 000 Hz increase to as much as 2.5%. It is necessary to state these larger

---

*P6, P8, and P10 identify proprietary ceramic materials made by Endevco, San Juan Capistrano, Calif.
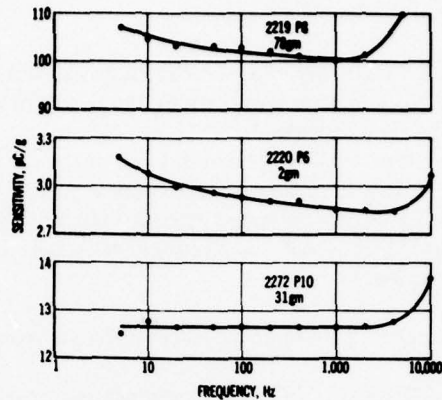
Fig. 6-2. Calibration results on three piezoelectric accelerometers [29]

errors, in order to demonstrate traceability with and to include the error in an accelerometer standard previously calibrated at the National Bureau of Standards. In practice, the larger calibration errors at higher frequencies are due mostly to environmental effects and to relative motion between test and standard accelerometers. The errors due to relative motion are substantially reduced by selecting accelerometer standards and shakers having very high resonance frequencies, preferably near or above 50 000 Hz.

Calibration results for a velocity pickup are illustrated in Fig. 6-3. The velocity sensitivity changes significantly over the operating frequency range. The calibration errors would be large compared to those obtainable with accelerometers.

Undesirable Calibration Results

Calibration are usually performed to accurately determine the sensitivities and operating frequency ranges of transducers. Other possible purposes include determining whether the transducer is adversely affected by certain environmental effects or whether undesirable resonances exist. For example, poor-quality piezoelectric accelerometers may experience sensitivity changes due to strain effects produced by different mounting torque requires some experimentation because the changes in sensitivity are constant over the entire frequency range. Errors due to strain and inertial forces produced by cable effects are present only at low frequencies, where visibly large displacement amplitudes are present.

A number of accelerometers may have responses similar to those shown in Fig. 6-4. The irregular response in Fig. 6-4a is due to the performance characteristics of the particular accelerometer. The minor resonance at 7300 Hz may be due to a resonance in the accelerometer case. Another accelerometer (Fig.

Table 6-1. Analysis of Errors in the Sensitivity of Test Accelerometers
Calibrated by the Comparison Method

Measurement	Sensitivity Error (%)
Reciprocity Calibration Error for Standard, 100 Hz	0.5
Stability of Standard	0.5
Comparison Frequency Response Calibration Error for Standard	
5 – 1000 Hz	1.1
1000–10 000 Hz	2.1
Relative Motion, 1000–10 000 Hz*	1.0
Distortion	0.2
Voltage Ratio	0.2
Amplitude Linearity, 0.2–100 g	0.2
Range Tracking, Standard Amplifier, 1, 10, and 100 g/V Ranges	0.2
Range Tracking, Test Amplifier	0.2
Amplifier Relative Frequency Response	0.1
Amplifier Gain Stability, Source Capacity, etc.	0.2
Environmental Effects on Accelerometers, Transverse Sensitivity, Strain, Temperature, etc.	0.5[†]
Environmental Effects on Amplifiers, Residual Noise, etc.	0.2[‡]
Estimated Error, 100 Hz	1.0[§]
Estimated Error, 5–1000 Hz	1.5[§]
Estimated Error, 1000–10 000 Hz	2.5[§]

*Highest frequency is 5000 Hz for test accelerometers, with a total mass exceeding 35 g.

[†] The error varies from 0–0.5% for most accelerometers operated under controlled laboratory conditions.

[‡] Applies for controlled laboratory conditions.

[§] Determined from the square root of the sum of the squares of the applicable individual errors.

Source: Ref. 35.

6-4b) has a minor resonance with unusually high sensitivity between 8000 and 94 000 Hz. Figure 6-4c shows an erratic frequency response that sometimes occurs in very small accelerometers. The frequency response of an accelerometer with damaged mounting threads is shown in Fig. 6-4d. These results are somewhat extreme and occur only in certain accelerometers.

It is important to know that the frequency response is normal throughout most, if not all, of the operating frequency range. The presence of large sensitivity changes in narrow frequency bands may be overlooked or mistakenly
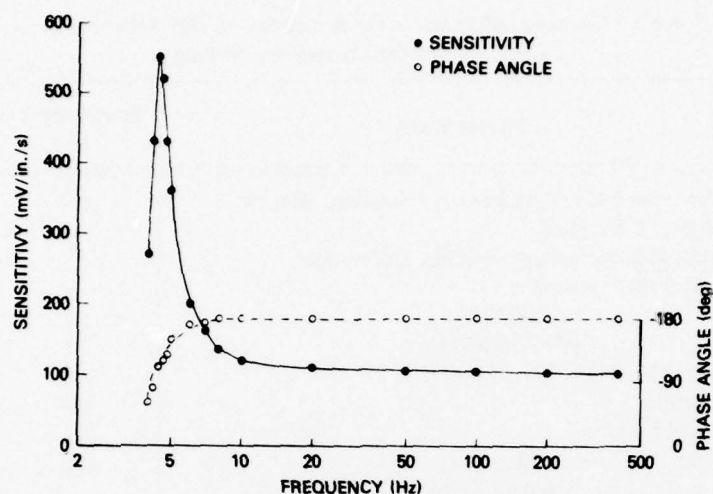
Fig. 6-3. Calibration of a velocity transducer

attributed to shaker characteristics if the calibration is performed on shakers having excessive transverse motion or acceleration distortion. In some test applications it is important to avoid accelerometers having poor frequency response, such as that illustrated in Fig. 6-4. It is easy to cull these accelerometers when routing frequency response calibrations are made. Abnormal frequency response in accelerometers may be due to internal damage, internal lead wire resonances, connector resonances, accelerometer case resonances, etc.

6.2 Resonance Frequency Calibrations

Although sensitivity and frequency response calibrations are required for the accurate use of accelerometers, the plot of resonance frequencies is a very important and definitive calibration. The resonance frequency calibration is the best method for evaluating the basic performance characteristics of any accelerometer and its operating conditions. It determines whether the accelerometer operates as a single-degree-of-freedom mechanical system. Perhaps even more important it can detect internal damage. Resonance frequency calibrations require the use of a high-frequency shaker (that is, one in which the resonance frequency of the moving element exceeds those of the accelerometers being calibrated). The resonance frequency of most accelerometers is less than 50 000 Hz. However, some accelerometers used for shock measurements have resonance frequencies above 100 000 Hz. Even with those accelerometers it is useful to perform resonance frequency calibrations up to 50 000 Hz to detect any unusual performance characteristics at lower frequencies.

Fig. 6-4. Calibrations of accelerometers with undesirable characteristics [35]

Ideal Accelerometers

Many accelerometers now used are similar in operation to the almost ideal accelerometer whose performance is shown in Fig. 6-5. It has a 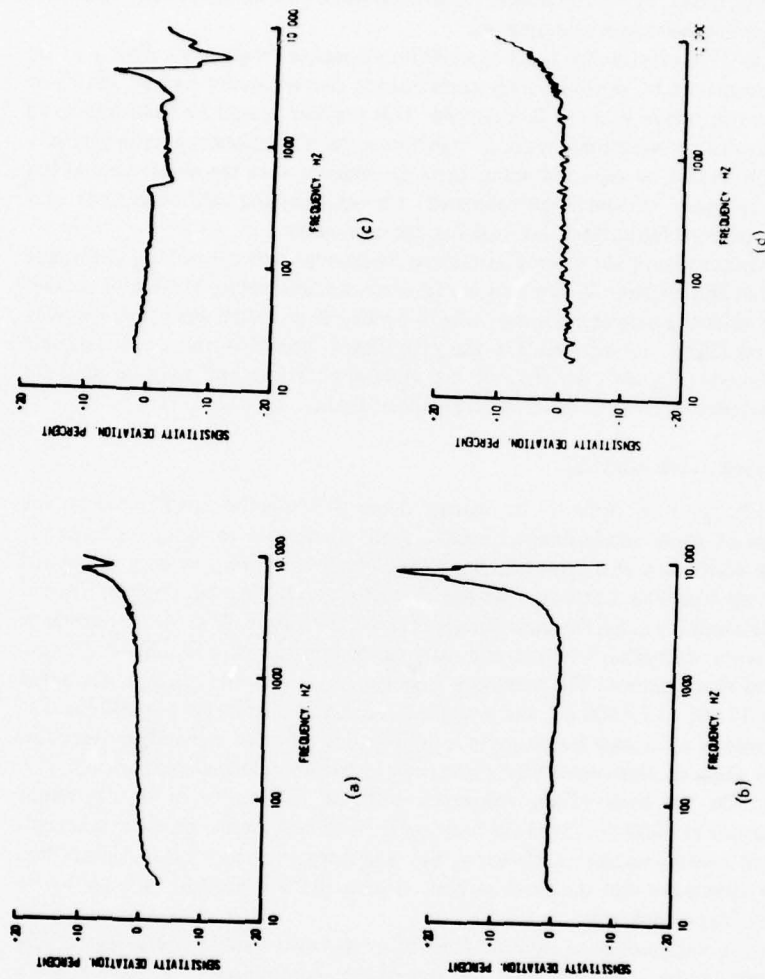single resonance and few, if any, minor resonances. This response is very similar to the theoretical response for seismic accelerometers.

It is good practice for users to perform resonance frequency calibrations on accelerometers to establish their performance characteristics and to allow any changes in future years to be detected. This practice should be followed on all accelerometers used for important measurements. The resonance frequency calibration should be repeated when there is evidence that the accelerometer has been subjected to severe environments or rough handling. Although there may be no external indications, internal damage may occur.

Another reason for making resonance frequency calibrations is to determine whether the response is like that of the ideal accelerometer. The use of accelerometers having a single resonance (Fig. 6-5) may be preferred when high accuracy and reliability are required. On the other hand, accelerometers with multiple resonances (Fig. 6-6) are suitable for most applications and may be used for other desirable characteristics, such as size or shape.

Damaged Accelerometers

Although it is difficult to damage many piezoelectric accelerometers, the design of some accelerometers makes them vulnerable to shock motions far above their rated environmental limits. Such high shock motions may be applied by rough handling. Resonance frequency calibration is the most accurate method for determining accelerometer damage. Figures 6-7a and 6-7b show the resonance frequency calibrations before and after an accelerometer was subjected to excessive shock motion. The resonance frequency of the accelerometer is decreased from 32 000 to 29 500 Hz, and a minor resonance is introduced at 9000 Hz. The decrease in resonance frequency is a definite indication of internal damage. This is the same accelerometer used during the frequency response calibration in Fig. 6-4b. On the basis of the frequency response calibration alone, the minor resonance at 9000 Hz may have been overlooked because the response is acceptable at lower frequencies. However, the resonance frequency calibration in Fig. 6-7b establishes that the accelerometer is damaged and probably should not be used in important tests.

It is good practice to perform resonance frequency calibrations to detect any changes in the operating characteristics of the accelerometers. In most accelerometers no malfunction is detected. An exception to this is the accelerometer shown in Fig. 6-8. The result of the shock motion calibration, illustrated in Fig. 6-8a, is perfectly normal. No unusual response is present in the oscillogram, and the shock motion sensitivity agrees precisely with the sinusoidal calibration. However, the routine resonance frequency calibration (Fig. 6-8b) shows multiple resonances and a resonance frequency of 28 500 Hz. The nominal resonance
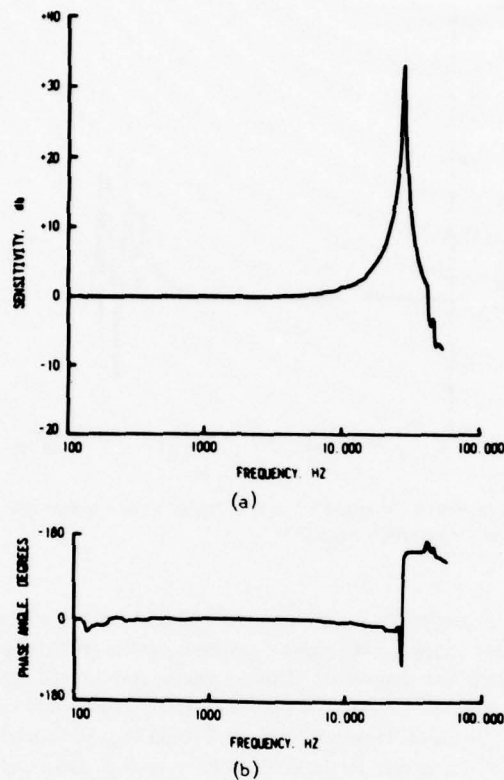
Fig. 6-5. Calibration of an accelerometer having almost
ideal characteristics [35]

frequency of this accelerometer is 35 000 Hz. The low resonance frequency
again indicates internal damage.

Failures in damaged accelerometers include such things as cracked piezoelectric
elements and epoxy joints, plastic deformation in screws, defaced accelerometer
mounting surfaces, deformed accelerometer cases, etc.

Minor Resonances

Minor resonances detected during frequency response calibrations are the
result of resonances in lead wires, accelerometer cases, etc. Minor resonances in
some accelerometers occur at frequencies above 10 000 Hz, which is the upper
limit of most frequency response calibrations. The accelerometer in Fig. 6-9a
has a minor resonance at 37 000 Hz. It is known that this is a minor resonance
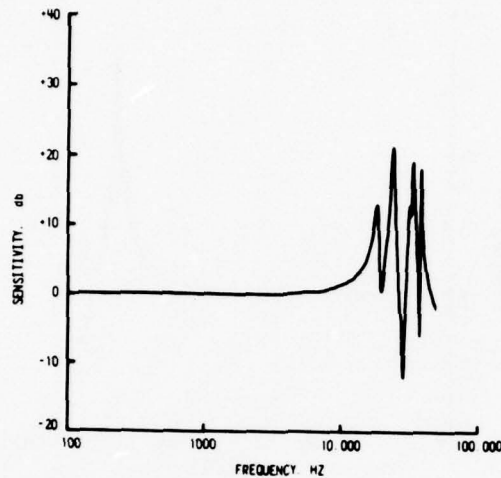
Fig. 6-6. Calibration of an accelerometer having multiple resonance frequencies [35]

because the phase angle changes abruptly to 100 degrees at the resonance and returns to 0 degrees above the resonance, and because the sensitivity increase is 20 dB, which is much less than usual. This accelerometer is used for shock motion measurements, and the presence of the minor resonance should have little effect in many test applications. However, it is good to be aware of such local resonance in selecting accelerometers, particularly when very high frequency components are to be measured. The calibration in Fig. 6-10 shows the response of a shock accelerometer having no minor resonances up to 50 000 Hz.

Accelerometer Effects on Structures

Resonance frequency data on an accelerometer are helpful in considering possible effects of the accelerometer on the motion of the structure. Neglecting the affects of rotary inertia, the motion of the structure with the accelerometer attached is given by

$$A = \frac{A_o M_s}{M_s + M_t} \tag{6-3}$$
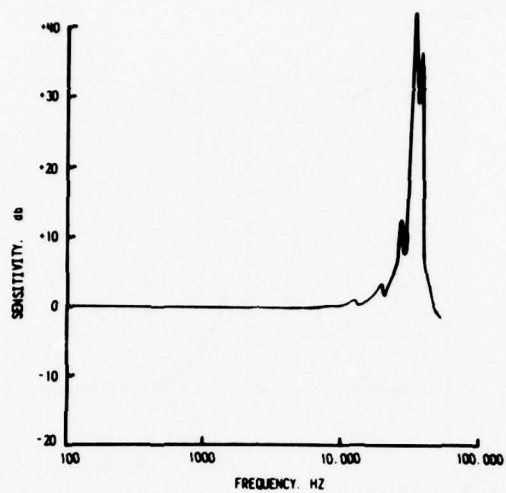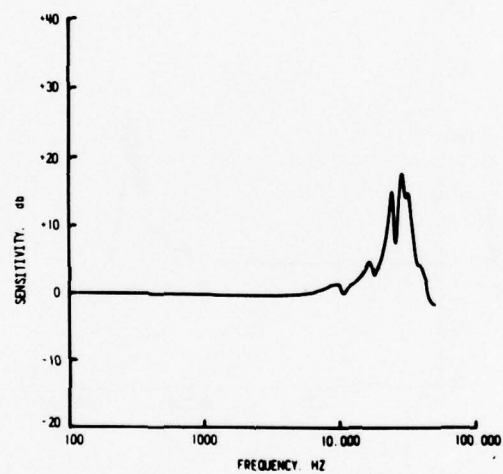
Fig. 6-7. Calibrations performed on an accelerometer, showing a resonance frequency of (a) 32000 Hz before damage and (b) 29500 Hz after damage [35]

2270
STANDARD

TEST
ACCELEROMETER

← 200 μs

(a)

(b)
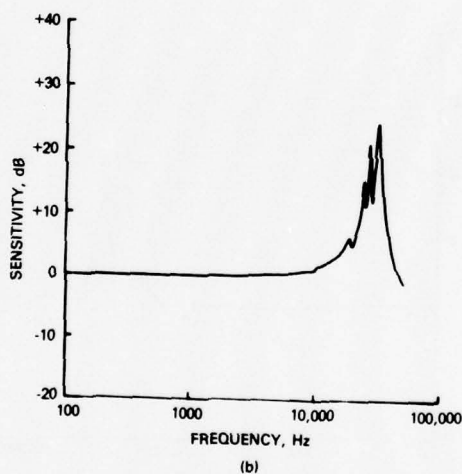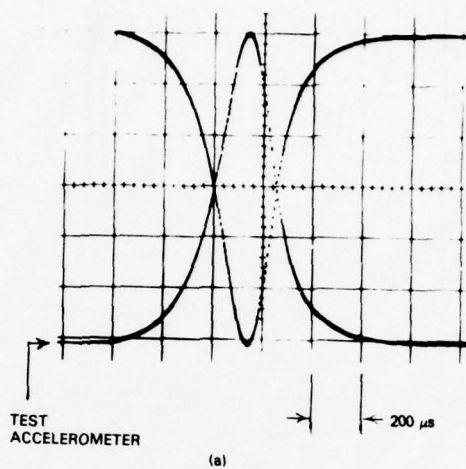
Fig. 6-8. Shock calibration of an accelerometer (a) appears normal, but (b) the resonance frequency calibration indicates internal damage [35]

where

A = amplitude of motion of the structure with accelerometer attached
A_o = amplitude of motion without accelerometer attached
M_s = point dynamic mass of the structure at the accelerometer mounting location in the sensitive direction of the accelerometer
M_t = dynamic mass of the accelerometer in its sensitive direction.

The dynamic mass of the accelerometer at frequencies below the lowest resonance is equal to the total mass of the accelerometer measured statically. However, it should be expected that the dynamic mass of the accelerometer changes significantly at minor resonances particularly if the response has a rather large sensitivity change at the resonance. The largest changes in dynamic
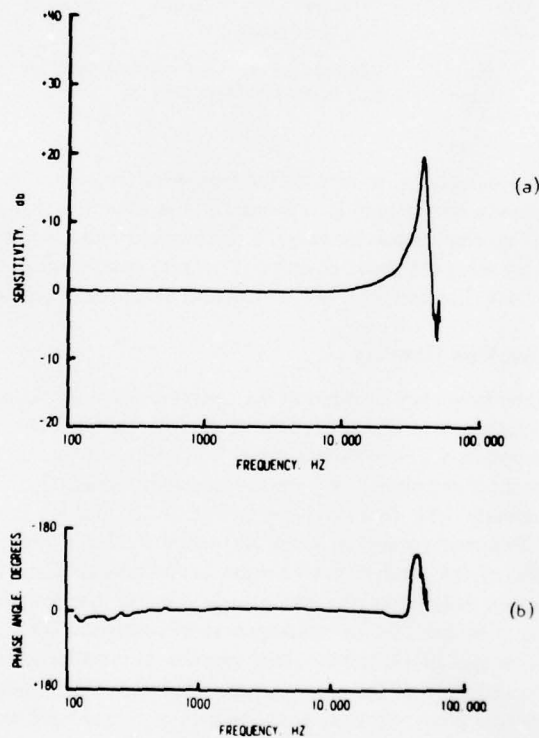
Fig. 6-9. Calibration of an accelerometer with a minor resonance [34]
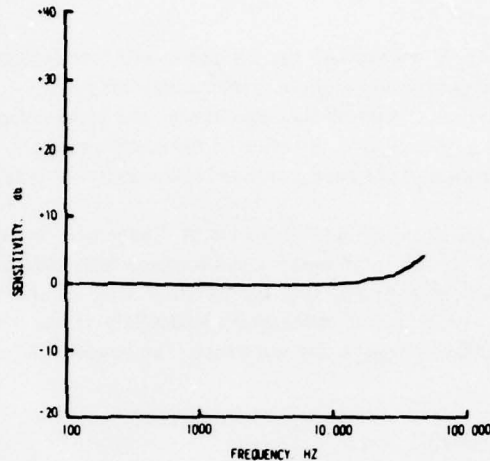
Fig. 6-10. Calibration of an accelerometer with no minor resonances below 50000 Hz [35]

mass should occur at the accelerometer resonance frequency. It is usually difficult to compute the change in response of the structure as a result of resonances in the accelerometer. However, a reasonable prediction of the effect can be obtained by using the above equation if the resonance frequency of the accelerometer and the characteristics of the structure being tested are known.

Accelerometers With Damping

A resonance frequency calibration on a piezoresistive accelerometer with oil damping is illustrated in Fig. 6-11. During manufacture the damping is adjusted at room temperature to approximately 0.7 of critical damping, to ensure that complex vibration and shock motions are measured accurately. The phase angle must vary linearly with frequency, as in Fig. 6-11b (taking into account the logarithmic frequency scale) to avoid distortion in the accelerometer output. The waveform of the accelerometer output is identical to that of the measured complex motion only when the phase angle response has this characteristic or is 0 degrees, as in the case of undamped accelerometers. The accelerometer is selected so that this proportionate phase response is maintained at all significant frequency components of the motion to be measured. This usually requires that the proportionate phase response is maintained at frequencies up to about two-thirds of the natural frequency for damped accelerometers.

Damped accelerometers are preferred when it is desirable to filter out frequencies near and above the natural frequency or resonance frequency of the accelerometer. However, if the damping changes significantly for any reason, the
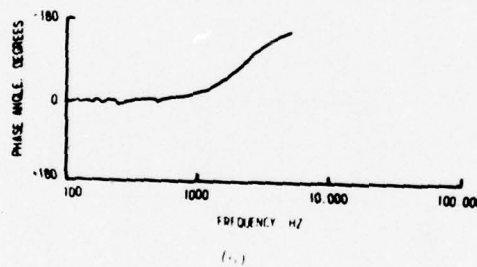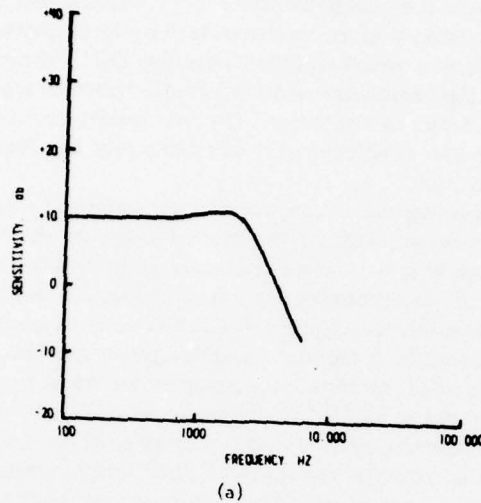
Fig. 6-11. Calibration of a damped piezoresistive accelerometer [35]

output will be distorted when damping exceeds about 0.5 to 0.85 of critical damping. Large changes in damping can occur in oil-damped accelerometers at temperature extremes, due to viscosity changes (see Fig. 3-15a). It is important that no large changes in damping occur due to damage or air leaks. Periodical resonance frequency calibrations should be useful for detecting changes in damping by comparing the response to that of an ideal accelerometer.

6.3 Transverse Sensitivity

Transverse calibration is done to determine the maximum value of the transverse sensitivity of a transducer, in a particular direction in a plane perpendicular

to the sensitive axis. It should be necessary for the manufacturer alone to measure the transverse sensitivity of an accelerometer or velocity pickup. Some have a very low maximum transverse sensitivity (less than 1%) by virtue of their design. Piezoelectric accelerometers have some variation in transverse sensitivity, depending on several factors in the design. The best quality accelerometers have a ·maximum transverse sensitivity value of significantly less than 3% of the accelerometer sensitivity.

Transverse sensitivity calibrations are routinely performed at a single frequency in the rated frequency range of the accelerometer. As the accelerometer is vibrated rectilinearly in a plane perpendicular to its sensitive axis, the output of the piezoelectric accelerometer depends on the angular position of the direction of vibration in this place (see Fig. 6-12). The variation in transverse sensitivity, as the accelerometer is rotated around its sensitive axis, describes a sinusoid. The maximum value of this curve is the maximum transverse sensitivity.

The accelerometer in Fig. 6-12 has a transverse sensitivity of less than 0.5%. It is useful, in evaluating electrodynamic shakers, to determine their suitability for measuring the transverse sensitivity of other accelerometers. Figure 6-13a shows the results of such an evaluation. The transverse motion of the shaker is less than 1% except at the shaker resonance frequencies, near 500 and 100 Hz. The shaker should not be used above 3000 Hz because of the significant resonance at 4500 Hz.
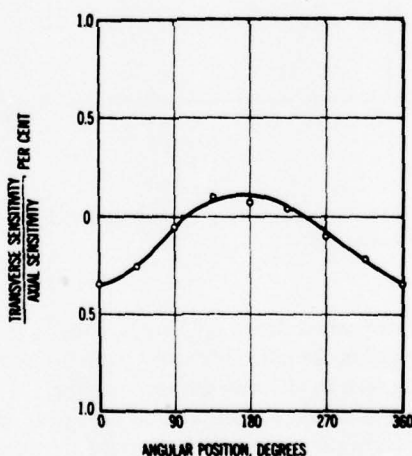
Fig. 6-12. Variation of transverse sensitivity with rotation of accelerometer
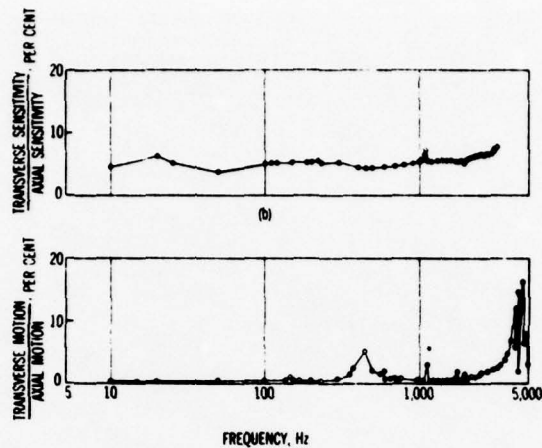
Fig. 6-13. Calibrations of the transverse motion of a shaker
with (a) an accelerometer with low transverse sensitivity and
(b) an accelerometer with high transverse sensitivity

Figure 6-13a also implies that the transverse sensitivity of the accelerometer,
which is less than 0.5%, as indicated in Fig. 6-12, is constant at various frequencies.
Results from another accelerometer, shown in Fig. 6-13b), indicate this more
clearly. This accelerometer, selected to have high transverse sensitivity as an ex-
ample, is useful for experimentally demonstrating the constant frequency char-
acteristic of transverse sensitivity. The transverse sensitivity of the accelerometer
is a constant value near 5% at all frequencies up to 3000 Hz, the useful range of
the shaker. The irregularities in the transverse sensitivity plot occur at the same
frequencies where the shaker exhibits resonance response (Fig. 6-13a).

6.4 Amplitude Linearity

Accelerometers are inherently linear, with little or no changes in the sensitivity
throughout their rated amplitude ranges. There is little need to perform
amplitude linearity calibrations on these accelerometers, particularly when
accurate information is available from the manufacturer. Amplitude linearity is
calibrated for accelerometers exhibiting measurable deviations from constant
sensitivity. However, the deviations are nearly the same for all accelerometers
having the same design and the same performance characteristics. This means it
is necessary to perform amplitude linearity calibrations on only a very few
accelerometers of each type.

The amplitude linearity calibrator is shown in Fig. 6-14a. High accelerations
are achieved with a resonant beam attached to a 50-N (10 lbf) force rated shaker.
The moving element of the shaker is small enough that the beam resonates at its
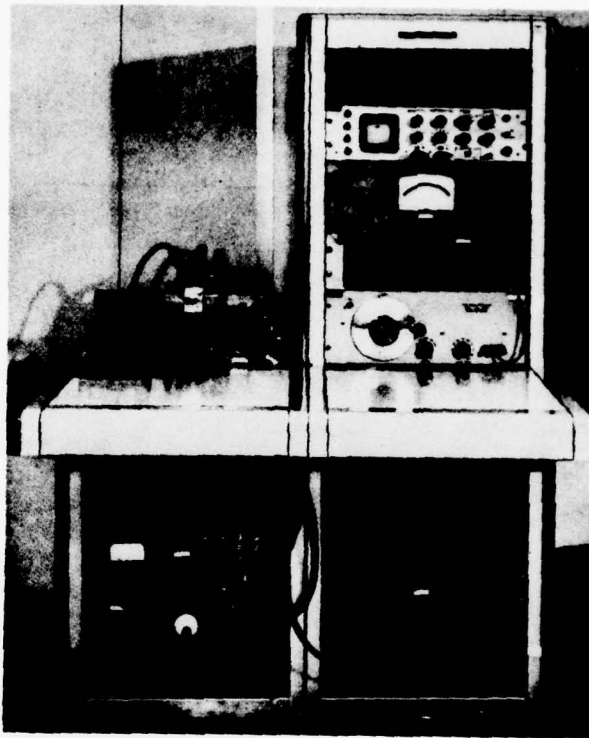
Fig. 6-14a. Amplitude linearity calibrator using a resonant beam [36]
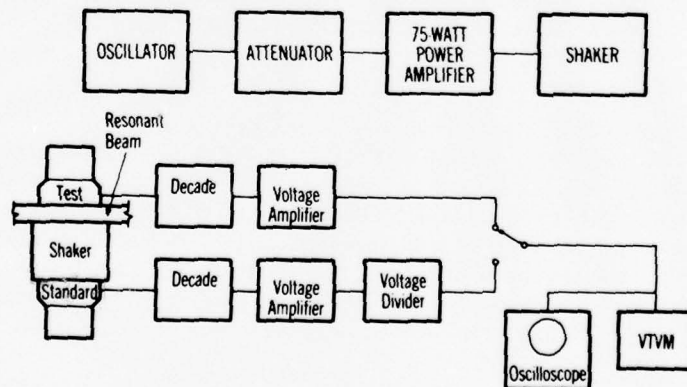
Fig. 6-14b. Block diagram of equipment used in measuring amplitude linearity [36]

fundamental free-free mode. The beam is designed with a clamping fixture to minimize stress concentrations on the beam and thus avoid excessive beam failures due to fatigue. The design of the beam with this particular shaker results in a resonance frequency of approximately 220 Hz. With this beam many hours of operation at 100 g can be obtained before fatigue failure of the beam occurs. Operation at up to 200 g can also be performed with somewhat lesser beam life. This design is particularly advantageous in that there is no relative motion between the test and standard accelerometers. The standard accelerometer is mounted at the opposite end of the shaker moving element from the beam. If desired, a back-to-back fixture may be used. Both test and standard accelerometers are then mounted on the fixture, and the fixture may be attached either on the beam or on the opposite end of the moving element.

Figure 6-14b shows a block diagram of the 100-g calibrator. The decade capacitors and the voltage divider are adjusted until the outputs from the test and standard accelerometers are equal at 10 g as indicated by the electronic voltmeter. The applied acceleration is then increased to the desired level while the frequency is adjusted to the beam resonance. Amplitude linearity deviations are determined from the change in voltage reading obtained by switching the voltmeter from the test accelerometer output.

The estimated error in measuring amplitude linearity deviations does not exceed 1%. The standard accelerometer is previously calibrated by one of the absolute calibration methods. The standard accelerometer may be verified by calibrating at higher accelerations on a shock calibrator.

6.5 Temperature Response Calibrations

The temperature response calibrator shown in Fig. 6-15a is used for calibrations from -184°C to +400°C (-300°F to +750°F). These calibrations are usually performed at a single frequency. A comparison method is used; the standard accelerometer is kept at room temperature outside the temperature chamber at the opposite end of the shaker moving element from the test accelerometer. The shaker is operated in the vertical direction. A ceramic rod is attached to the top of the moving element and passes through the wall of the chamber. A steel fixture with a thermocouple inserted is attached to the top of the ceramic rod, and the test accelerometer is mounted on the fixture. Chamber temperature is automatically controlled by the output of the thermocouple.

The block diagram of the calibrator is shown in Fig. 6-15b. The shaker is vibrated at approximately 3 g. In practice, as many as ten accelerometers may be calibrated simultaneously by using a larger mounting fixture and additional amplifier-voltmeters for each additional accelerometer. The standard accelerometer is monitored to ensure that the acceleration remains unchanged during calibration. Since the standard accelerometer is at the bottom of the shaker, it remains at room temperature. The sensitivity deviation at each temperature is indicated by the changes in voltmeter readings for each test accelerometer.
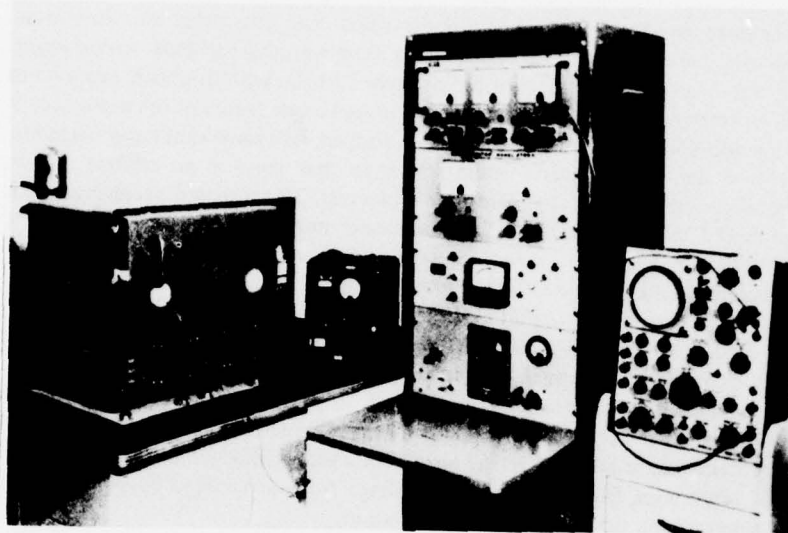
Fig. 6-15a. Temperature response calibrator [36]
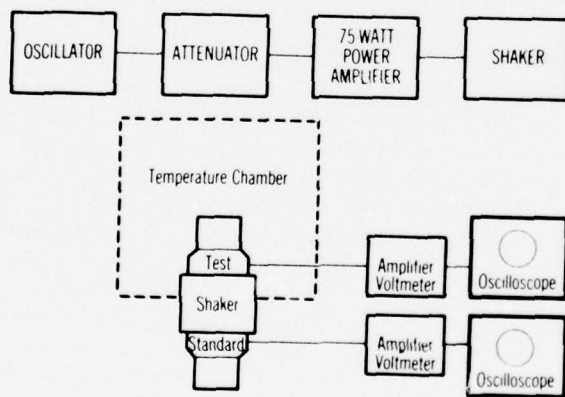
Fig. 6-15b. Temperature response calibrator [36]

Three sources of error are present in performing this calibration. First, the error in maintaining constant acceleration throughout the calibration is approximately 0.5%. Second, the scale reading of the voltmeter for the test accelerometer may be in error up to ± 2% if readings at all temperatures are made on the same

range. The third source of error is the combined effect of the temperature response of the particular accelerometer being calibrated and the accuracy of the temperature measurement. More specifically, it is determined by the rate of change of the test accelerometer output with respect to temperature. The temperature is measured by the thermocouple output on a potentiometer to within the accuracy of the thermocouple. For most accelerometers, the estimated total calibration error is significantly less than 5%.

6.6 Combined Environmental Calibrations

It is extremely difficult to combine calibrations of temperature response, amplitude linearity, and frequency response. Fortunately, accurate calibrations can be achieved by performing the amplitude linearity and temperature response calibrations at a single frequency, as described above, and then combining the results analytically with sensitivity and frequency response calibration data. This procedure is recommended for accelerometers with small internal damping that are not used near their resonance frequencies. It is particularly suitable for piezoelectric accelerometers that have almost zero damping and are normally used at frequencies below one-fifth of their resonance frequency. Although very small changes in internal damping and resonance frequency probably occur at temperature extremes, these changes have no effect on the response below one-fifth the accelerometer resonance frequency.

Other vibration pickups that are normally used near their resonance frequencies require combined amplitude linearity and temperature response calibrations. Fortunately, the transducer types that require combined environmental calibrations are normally used only at frequencies up to a few hundred hertz, and special back-to-back fixtures need not be used inside the temperature chamber.

The internal resistance of piezoelectric accelerometers decreases at elevated temperatures, and this may affect the response of the associated amplifier (particularly voltage amplifiers at frequencies below 50 Hz). For this reason, it is sometimes desirable to verify the response of the accelerometer-amplifier system at the lower frequencies while the accelerometer is subjected to high temperature. The combined high-temperature, low-frequency calibration may be omitted if the resistance of the accelerometer is measured at the maximum operating temperature and the low-frequency characteristics of the amplifier are known.

CHAPTER 7
SHOCK MOTION CALIBRATIONS

Shock motion calibrations are performed routinely at accelerations from 20 to 10 000 g. The most accurate calibrations are performed by the comparison method using an accelerometer standard. Absolute shock motion calibrations can be performed at the same accelerations, but the resulting calibration errors are somewhat larger than those achievable by the comparison method. Special test equipment is required for absolute shock motion calibrations at accelerations up to 100 000 g.

7.1 Comparison Calibrations

Comparison shock motion calibrations are made simply by subjecting the test and standard accelerometers to the same pulse and measuring the ratio of their peak acceleration outputs. The accelerometer standard is previously calibrated by the reciprocity method to determine its sensitivity and establish it as a primary standard. Frequency response calibrations are performed on the accelerometer standard up to 10 000 Hz, to demonstrate a constant sensitivity corresponding to the frequency components in the shock pulse. In addition, resonance frequency calibrations on the standard can identify resonances that may be excited during shock motion calibrations. Amplitude linearity calibrations are performed on the standard so that accurate correction factors may be applied for any changes in sensitivity occurring at the peak accelerations present during shock motion calibrations.

Calibration Procedure

Comparison shock calibrations are performed with the calibrator and other instruments shown in Fig. 7-1. The standard and test accelerometers are attached back-to-back on a cylindrical anvil, and the anvil is held in place with magnets. A steel ball is allowed to fall and strike the anvil.

The accelerometers are connected to amplifiers equipped with low-pass filters. The filter cut-off frequency should be between 15 and 20 kHz. Voltage dividers are used to produce approximately equal signals at the storage oscilloscope input and to make the pulse heights approximately 6 cm. A dual-trace oscilloscope is used to record both accelerometer outputs simultaneously. A common calibration voltage standard signal is afterwards applied simultaneously to both channels to calibrate the oscilloscope.
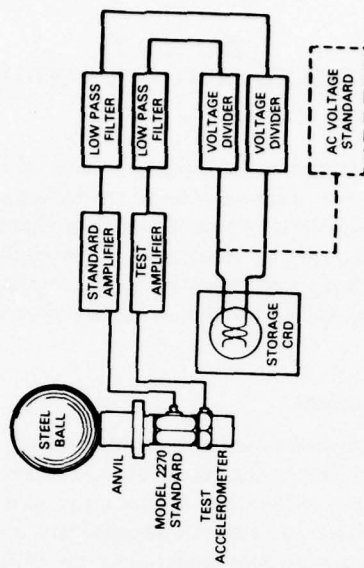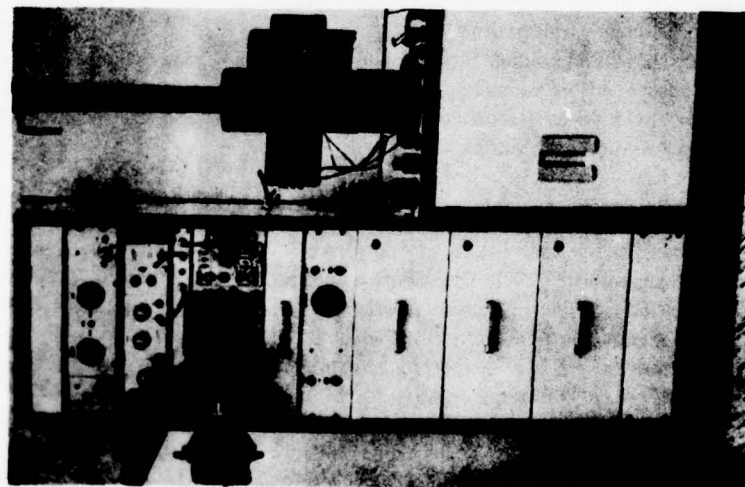
Fig. 7-1. Shock calibrator

The formula for calculating the sensitivity of the test accelerometer is

$$Q_t = \frac{H_t}{H_s} \frac{D_s}{D_t} \frac{C_t}{C_s} \frac{K_s}{K_t} A_s \qquad (7\text{-}1)$$

where

Q_s = sensitivity of test accelerometer, in picocoulombs per gram
H_t = pulse height of test accelerometer, in centimeters
H_s = pulse height of accelerometer standard, in centimeters
D_t = divider setting on test accelerometer
D_s = divider setting on accelerometer standard
C_t = calibration signal on test channel, in millivolts per centimeter (mV/in.)
C_s = calibration signal on standard channel, in millivolts per centimeter (mV/in.)
K_t = gain of test amplifier, in millivolts per picocoulomb
K_s = scale range of standard amplifier, in millivolts per gram
A_s = amplitude linearity correction for accelerometer standard.

Typical oscillograms obtained during a comparison shock calibration are illustrated in Fig. 7-2. The shock pulse outputs from the standard and test accelerometers are inverted with respect to each other for ease in separating the traces. The sinusoidal traces are for calibration purposes; the upper sine trace is for the standard channel, and the lower trace for the test channel. The gain and scale ranges used in the equation are noted from the test and standard amplifiers. Amplitude linearity correction A_s for the standard illustrated in Fig. 7-1 is 1% per 10 000 g or 0.1% per 1000 g.

The results of the calibrations illustrated in Fig. 7-2 are given in Table 7-1. The results show that the charge sensitivity of this accelerometer increases at high accelerations. A plot of the response indicates that the charge sensitivity increases linearly with applied acceleration to a value of 4.5% at 10 000 g.

Error Analysis

The error analysis must include estimated errors for the applicable performance characteristics of all the instruments used in comparison shock calibrations of test accelerometers. Such instruments include charge amplifiers for the test and standard accelerometers, low-pass filters, resistance decade dividers, and dual-trace oscilloscopes. The error analysis must include those characteristics of the test accelerometer that could produce error signals or change the sensitivity of the test accelerometer during calibration.

Customary procedures are used in performing the error analysis. The actual error used for certain performance characteristics is usually less than the maximum
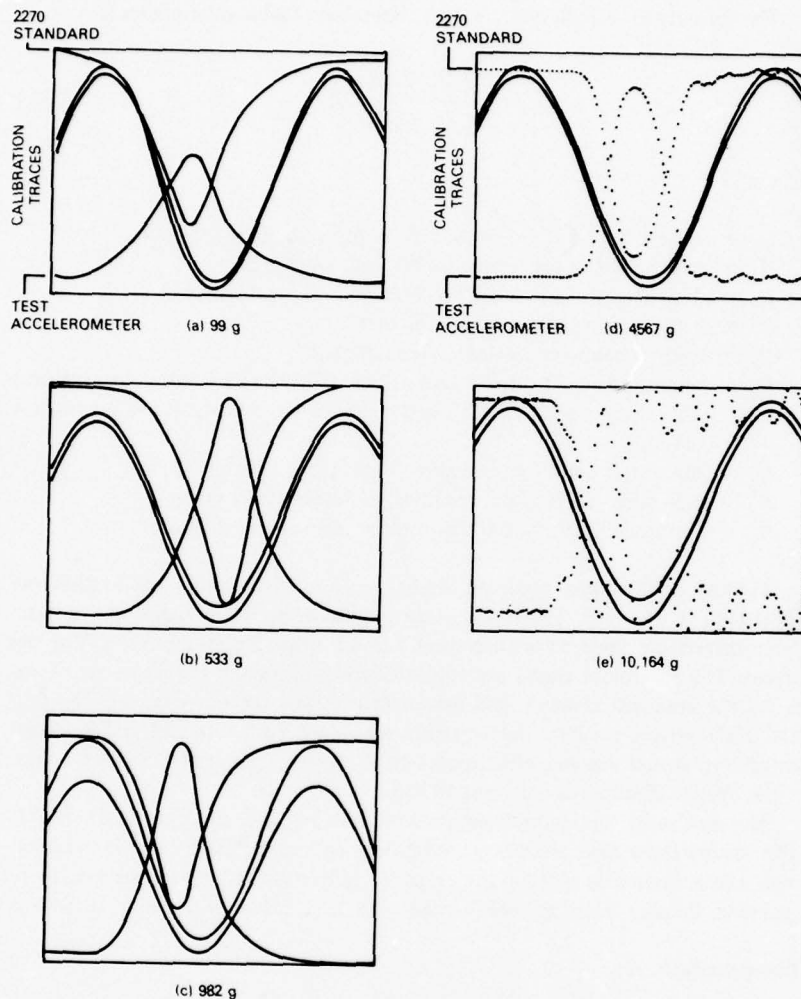
Fig. 7-2. Oscillograms obtained with a shock calibrator

limits stated for the instrument. This is acceptable because the nominal perform-
ance of the instruments is generally less than the limit established for acceptance
or rejection of instruments during manufacture. Furthermore, the specific errors
used in the analysis are sometimes less than nominal performance of the instru-
ment. This is to account for the fact that conditions during calibration are
generally not in the operating extremes of the instrument. Therefore, case is

Table 7-1. Calibration of Endevco Model 2225 Accelerometer, Serial Number JC62

Applied Acceleration (g)	Pulse Duration (ms)	D_t	D_s	C_t (mV/cm)	C_s (mV/cm)	K_t (mV/pC)	K_s (mV/g)	A_s	Q_t (pC/g)
99	2.6	1.0	1.0	202	203	10	10	1.000	0.732
533	85	.4	0.3	247	256	10	10	1.000	.729
982	.75	.2	1.0	236	201	10	1.0	1.001	.733
4567	.15	.8	0.6	510	507	1.0	1.0	1.005	.786
10 164	.10	.8	0.7	108	115	0.1	0.1	.010	.778

Source: Ref. 28.

taken in assigning errors so that the nominal error used in the analysis never exceeds two-thirds of the maximum possible error under extreme conditions.

The results of an error analysis are shown in Table 7-2. Experience shows that the errors of the reciprocity calibration of the accelerometer standard are usually less than the ±0.5% (See Table 5-3). Therefore, the estimated error in Table 7-2 is given as 0.35%. The accelerometer standard could be calibrated by the sinusoidal comparison method rather than the absolute reciprocity method if the standard is to be used only for shock motion calibrations. However, the reciprocity calibrations are accurate enough to demonstrate the stability of the standard with time.

Other possible errors in the accelerometer standard include 2.1% for the frequency response calibration of the standard. The errors for measurement 2 in Table 7-2 apply for good-quality charge amplifiers. The errors for the low-pass filters in the charge amplifiers are listed separately. Calibration of the low-pass filters is illustrated in Fig. 7-3. Identical filters are used in both amplifiers, and the errors due to gain and frequency response tend to cancel. Therefore, the errors of 1% in lines 3.1 and 3.2 in Table 7-2 should be more than adequate. The phase angle of the filters changes linearly with frequency (Fig. 7-3), which is the requirement for avoiding distortion in the shock pulse waveform. The proportional phase response extends to 10 000 Hz, which is adequate for the frequency components produced by the shock motion calibrator. Therefore, the errors due to phase angle characteristics of the filters, are estimated at less than 1%.

The comparison calibration is performed by simultaneously recording the outputs from the standard and test accelerometers on a dual-trace oscilloscope. Decade voltage dividers are used so that the height of the shock pulses and sinusoidal calibration signals on the oscilloscope can be adjusted in the range of 5 to 8 cm. If this procedure is followed, the pulse height can be measured with errors less than 2%. The oscilloscope is also calibrated to allow for differences between the voltage scales. An error of up to 2% is allowed for this calibration.

An error of 1% is allowed for environmental effects on the standard and test accelerometer and amplifiers. These include errors due to transverse sensitivity, strain effects, temperature, distortion, etc. To minimize distortion errors necessitates use of anvils that produce pulse durations of at least five times the natural period of the test accelerometer. This requirement is usually met because most accelerometers having a low resonance frequency are limited to use at low accelerations, and the low-acceleration anvils produce long pulse durations. Some distortion is also produced by exciting the resonance frequency of the outer case and base of the standard. These errors tend to cancel because they occur equally in both test and standard outputs.

The estimated error in the test accelerometer sensitivity is determined by calculating the square root of the sum of the squares of the individual errors listed in Table 7-2. This error in the shock motion comparison calibration of the test accelerometer sensitivity is 4.8%, but numerous shock motion calibrations, on accelerometers having known characteristics, indicate that the error is usually

Table 7-2. Analysis of Errors in the Sensitivity of Test Accelerometers
Calibrated on Endevco Shock Motion Calibrator Model 28701

Measurement	Error (±%)
1 Accelerometer Standard	
1.1 Reciprocity Calibration at 100 Hz	0.35
1.2 Stability of Sensitivity	0.35
1.3 Mass Effect on Sensitivity at 100 Hz	0.14
1.4 Comparison Frequency Response Calibration Error for Standard	2.1
1.5 Relative Motion up to 10 000 Hz	1.0
1.6 Amplitude Linearity Corrections up to 10 000 g	0.5
2 Charge Amplifiers	
2.1 Range Tracking of Standard Amplifier	0.7
2.2 Gain of Test Amplifier	0.35
2.3 Range Tracking of Test Amplifier	0.2
2.4 Relative Frequency Response	0.1
2.5 Gain Stability, Source Capacity, etc.	0.2
3 Low-Pass Filters	
3.1 Relative Gain	1.0
3.2 Relative Frequency Response to 10 000 Hz	1.0
3.3 Phase Angle Linearity	1.0
4 Voltage Ratio Measurement	
4.1 Decade Voltage Divider	0.05
4.2 Height of Standard Pulse	2.0
4.3 Height of Test Pulse	2.0
4.4 Calibration of Oscilloscope	2.0
5 Environmental Effects on Amplifiers and Accelerometers, including Transverse Sensitivity, Strain Effects, Temperature, Distortion, etc.	
6 Estimated Error in Test Accelerometer Sensitivity	4.8[*]

*Determined from the square root of the sum of the squares of individual errors.
  Source: Ref. 28.

significantly less. Errors of less than 3% are achievable if some skill is used to
measure accurately the pulse heights and sinusoidal calibration traces.
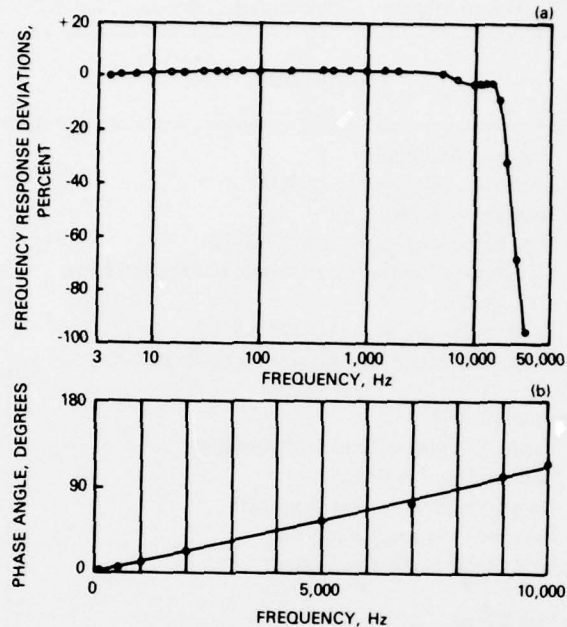
Fig. 7-3. Amplitude and phase angle response for a low-pass filter used in shock calibrations

7.2 Absolute Calibrations

An absolute shock motion calibration is made by subjecting the test accelerometer to a mechanical pulse and measuring the resulting velocity change. The pulse output from the accelerometer is integrated to determine the indicated velocity change. The acceleration sensitivity of the accelerometer is determined using the ratio of the indicated velocity to the actual velocity sensitivity measured by an absolute method.

Theory of Operation

An absolute calibration of the sensitivity of an accelerometer is performed by measuring the velocity of the anvil resulting from the shock motion and dividing it into the integral of the output from the accelerometer.

Velocity u_t of the anvil when its top is between the second and third photo-junction cells (Fig. 7-4) is given by

$$u_t = (u_2^2 + 2gs)^{1/2} \qquad (7\text{-}2)$$
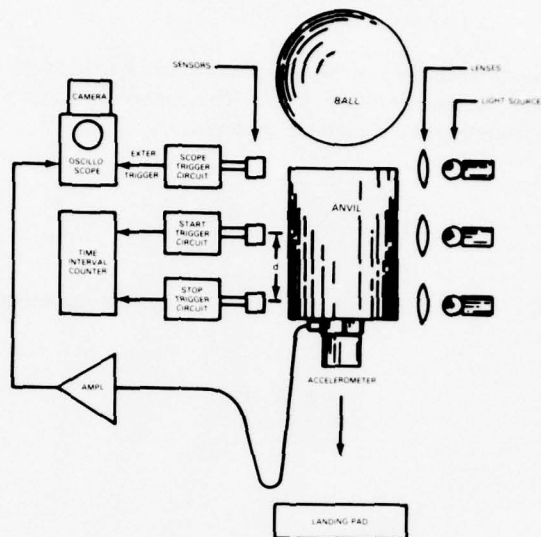
Fig. 7-4. Equipment for absolute shock motion calibration [37]

where

u_2 = anvil velocity at middle diode sensor, in meters per second (in./s)
g = acceleration of gravity, 9.81 m/s^2 (386 in./s^2)
s = distance, in meters (in.).

If $u_t = ds/dt$ is used, Eq. (7-2) can be integrated;

$$\int_0^\tau dt = \int_0^{S_2} \frac{ds}{(u_2^2 + 2gs)^{1/2}} . \tag{7-3}$$

Solving Eq. (7-3) yields

$$u_2 = \frac{S_2}{\tau} - \frac{\tau g}{2} \tag{7-4}$$

where

S_2 = distance between the second and third diode sensors
τ = time elaspsed while anvil travels distance S_2. Velocity u_1 of the anvil at the end of the shock motion pulse is

$$u_1 = (u_2^2 - 2gS_1)^{1/2} \tag{7-5}$$

where S_1 is the distance the anvil travels after the shock motion until the top of the anvil reaches the middle diode sensor. The change in velocity due to the shock pulse is determined by combining the equations:

$$u_1 = \left[\left(\frac{S_2}{\tau} - \frac{\tau g}{2} \right)^2 - 2gS_1 \right]^{1/2}. \tag{7-6}$$

The absolute calibration is completed by computing sensitivity S of the accelerometer:

$$S = \frac{K_1 K_2 A}{u_1} \tag{7-7}$$

where

K_1 = voltage scale factor
K_2 = time scale factor
A = area under the pulse of the accelerometer output vs. time.

The acceleration output is photographed from the oscilloscope. Numerical integration of the output is performed using transparent graph paper or a plainimeter; this accurately yields area A. Accelerometer voltage per division on the graph paper K_1, the time in seconds per division K_2, area A, and u_1 are substituted into Eq. (7-7). The result is the sensitivity of the accelerometer under shock motion conditions.

Description of Shock Calibrator

The shock calibrator for performing absolute calibrations is similar to that used for comparison calibrations. Additional circuitry is used for making an absolute measurement of the velocity resulting from the shock motion. Figure 7-4 illustrates the apparatus used for the sensitivity measurement. Light-activated diodes are used as sensors to trigger the oscilloscope and measure the velocity with a time interval counter. To complete the sensitivity measurement, necessitates an accurate measurement of the distance between the middle sensor and the bottom sensor, which produces signals for starting and stopping the counter. The best method for measuring this distance is to drop the ball from a known height while the anvil and accelerometer are removed from the calibrator. As the ball passes the middle and bottom sensors the distance between the sensors can be computed as follows:

$$S_2 = 4.43 \times 10^{-3} t \, h^{1/2} + 4.90 \times 10^{-6} t^2 \text{ m}$$

$$S_2 = 0.0278 \, t \, h^{1/2} + 0.193 \times 10^{-3} t^2 \text{ in.}$$

(7.8)

where

S_2 = distance between middle and bottom sensors, in meters (in.)
t = time for the ball to travel the distance S_2, in milliseconds
h = distance between the middle light beam and top of the ball just before release, in meters (in.).

The shock motion calibration is performed by inserting the anvil in the calibrator and dropping the ball onto the anvil to produce the desired shock pulse. Rubber padding is put on top of the anvil to control the desired pulse duration. The peak acceleration of the shock pulses is determined by the mass of the anvil, the mass of the ball, and the material of the padding.

Typical Results

Typical examples of absolute shock motion calibrations are illustrated in Fig. 7-5. The calibration of these three piezoelectric accelerometers of different design demonstrate the practicability of performing absolute calibrations. The Model 2221 accelerometer (Fig. 7-5a) shows some increase in acceleration sensitivity at 1250 g compared to the results at lower accelerations. This increase in sensitivity is typical for this accelerometer. The slight decrease in sensitivity at 7610 g for the Model 2225 accelerometer (Fig. 7-5b) is not typical. It is expected that the slight decrease in acceleration sensitivity at this high acceleration is due to calibration error, since the sensitivity should increase a few percent instead of decreasing. The nearly constant sensitivity of the Model 2242 accelerometer (Fig. 7-5c) is typical for this particular accelerometer.

Calibration Errors

The calibration errors present during the absolute shock motion calibration are listed in Table 7-3. The estimated calibration errors of ±4.3% are achieved consistently at accelerations up to at least 1000 g. At higher accelerations it is sometimes difficult to control the trajectory of the anvil to eliminate its rotation during the velocity measurement. When this rotation occurs the errors in the sensitivity measurement are somewhat larger than those given in Table 7-3. Considerable experience in performing absolute shock motion calibrations and familiarity with the amplitude linearity characteristics of the accelerometer being calibrated are necessary for culling poor calibration results. Accordingly, absolute shock motion calibrations in the range of 5000 to 10 000 g should be performed only in laboratories prepared to cope with this problem. Additional
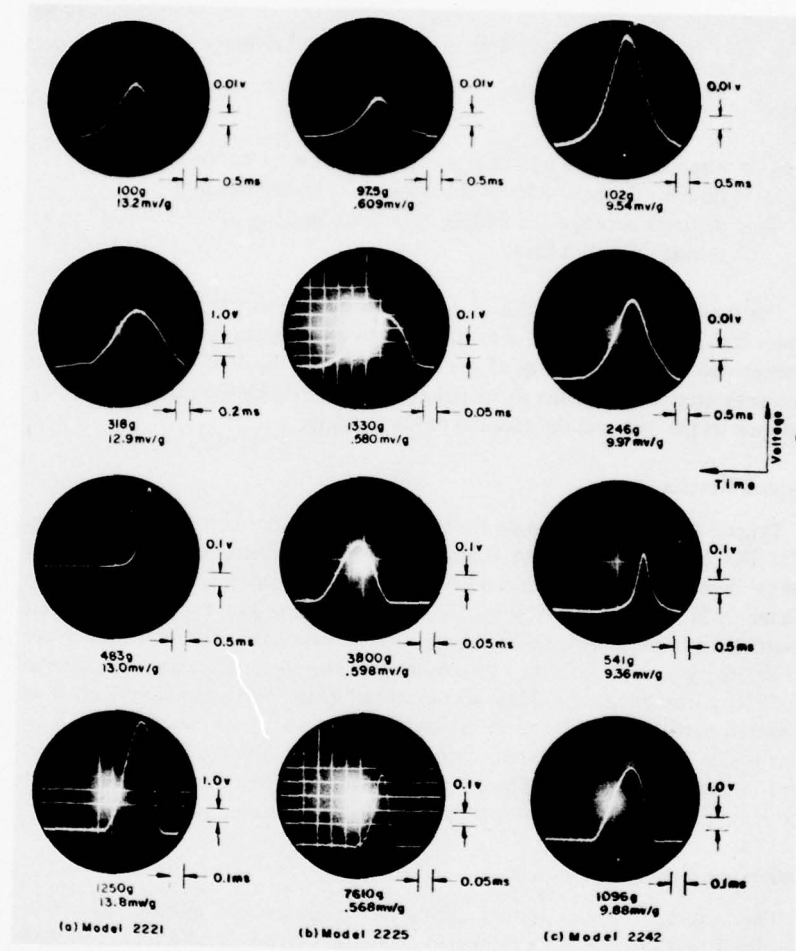
Fig. 7-5. Typical results of absolute shock calibration on three piezoelectric accelerometers [17]

development work on absolute calibration is needed, to lessen the errors in the comparison shock calibration method. Hopefully, this improvement will be accomplished by the use of lasers with specially designed shock calibrators.

Calibrations up to 100 000 g

Shock motion calibrations in the range of 10 000 to 100 000 g can be performed by applying pulses with an air gun making an absolute measurement of sensitivity. An air gun is illustrated in Fig. 7-6. Compressed air in the reservoir is applied to the ram projectile, which accelerates down the barrel and strikes the anvil to which the accelerometer is attached. The resulting shock pulse is recorded on an oscilloscope. The velocity sensitivity change resulting from the shock pulse is measured using photodiodes positioned above the slots in the barrel, as indicated in Fig. 7-7. The calibration is completed by following the absolute method of integrating the accelerometer pulse output and computing the sensitivity with the aid of the measured velocity change. Typical results, illustrated in Fig. 7-8, indicate that the sensitivity of this accelerometer increases 47% at an acceleration of 100 000 g. Since an accelerometer used for shock measurements should be limited to accelerations at which its sensitivity increase does not exceed 10%, this accelerometer should be restricted to 20 000 g. Accelerometers having with amplitude linearity deviations should be used for measurements above 20 000 g.

Table 7-3. Estimated Errors for Absolute Shock Motion Calibrations
Using Endevco Model 2965A Shock Calibrator

Measurement	Error ($\pm\%$)
1. Area under the Pulse	3
2. Velocity	2
3. Oscilloscope Voltage Scale	1.0
4. Oscilloscope Time Scale	.5
5. Scale Factors	2
6. Estimated Error in Accelerometer Sensitivity	4.3

*Determined from the square root of the sum of the square of the individual errors.
  Source: Endevco, San Juan Capistrano, Calif.
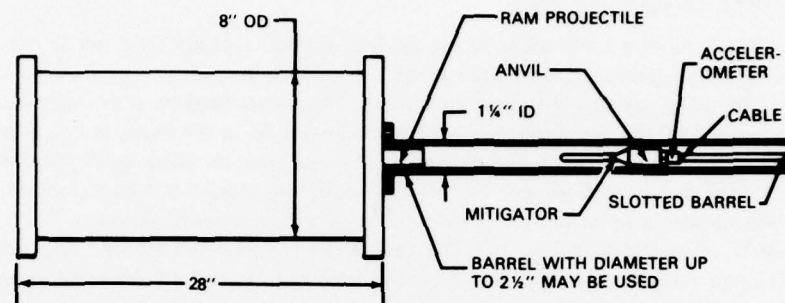
Fig. 7-6. Air gun used in shock motion calibration [38]
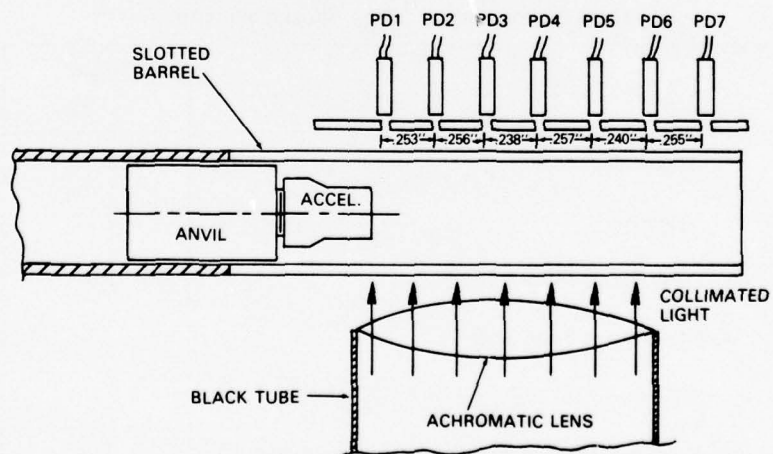
Fig. 7-7. Use of photodiodes to measure velocity of accelerometer in air gun [38]
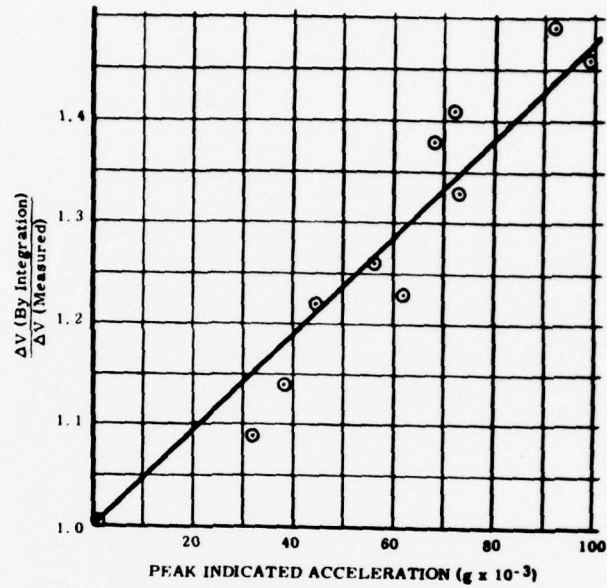
Fig. 7-8. Typical results of calibrations of a piezoelectric acceler-
ometer with an air gun, indicating that sensitivity increases with
applied acceleration [15]

CHAPTER 8
FORCE GAGES AND IMPEDANCE HEADS

Dynamic force gages (transducers) are built using piezoelectric ceramic, piezoresistive strain gage, or wire strain gage transducing elements. The basic construction of a force gage is similar to that of an accelerometer, except that force transducers have mechanical terminals. The top and bottom mounting surfaces of a force gage are the mechanical terminals; in an accelerometer only one end of the transducing element is attached to the case of the accelerometer. The force gage, having two mounting surfaces, is more susceptible to environmental effects such as externally applied strain.

Force and structural impedance play a very important role in shock and vibration and it is important to recognize any large errors in their measurement. In both calibration and testing, the errors in measurements made with force gages are several times greater than those made with accelerometers. However, with reasonable care very useful force measurements can be made and good accuracy maintained.

An impedance head (transducer) consists of a force gage with a built-in accelerometer. The impedance head has the internal accelerometer connected to one mounting end, and the force gage is connected to both ends. Impedance measurements may also be made with individual force gages and accelerometers. Care must be taken in the design of fixtures to avoid relative motion between the force gage and accelerometer. For this reason impedance heads are preferred for use at higher frequencies in making point impedance measurements. Transfer impedance measurements require the use of a force gage at one point on the structure and an accelerometer at another point, to measure the ratio of force to acceleration. A reasonable amount of skill in using these transducers is necessary if useful data are to be obtained with confidence. This should require only a small amount of experience, including some familiarity with the design and operating characteristics of force gages as well as experience in performing calibrations in the laboratory.

8.1 Description and Performance Characteristics

One type of impedance head is illustrated in Fig. 8-1. This head is 1 in. (25.4 mm) high and 2 in. (50.8 mm) in diameter. It contains three peizoelectric force gages and three piezoelectric accelerometers. The three accelerometers are attached to the bottom surface of the top plate on the head at the location of the three darkened circles in the figure. The force gages are attached to the top plate at locations between the three accelerometers. The other ends of the force

153

Fig. 8-1. Mechanical impedance trans-
ducer. (Endevco)

gages are attached to the bottom plate. The outputs of three accelerometers are
electrically connected internally in the head, as are those of the force gages.
Separate connectors are provided to transmit outputs from the accelerometer
and force gages. It is customary to connect the top plate of the head to the
structure being tested, particularly when high-frequency measurements are
made. The bottom plate of the head is attached to a shaker.

The impedance head in Fig. 8-1 is used with a bolt passing through the hole in
the center. This construction allows a most rigid connection of the head to a
structure, which is important for making measurements in the upper frequency
range, to about 5000 Hz. It is important to perform calibrations using the same
type of bolt to be used in making force or impedance measurements, because
the force is shared between the bolt and the head in proportion to their stiff-
nesses. For example, if the stiffness of the bolt is one-tenth that of the head, it
will carry one-tenth of the total load. Bolts made of materials having different
stiffnesses would carry a different share of the load. The force gage is calibrated
in terms of its output per unit of total applied force including that carried by
both the head and the bolt.

The impedance head and force gage illustrated in Figs. 8-2 and 8-3 are used
with two bolts, one attached to the top mounting surface and the other to the
bottom mounting surface. The total load applied is measured by the force gages,
and there is no load sharing with the mounting bolts. These force gages have
somewhat lower stiffness, which may limit their use at very high frequencies.
Calibrations should be performed over the frequency range in which force or
impedance measurements are to be made.

8.2 Calibration of Force Gages

Force gages and impedance heads are most accurately calibrated with sinusoidal
motion on a shaker at an amplitude in the range of about 5 to 50 N (1-10 lbf)
throughout the operating frequency range. Shock motion calibrations may also
be made, particularly for determining the amplitude linearity characteristics.
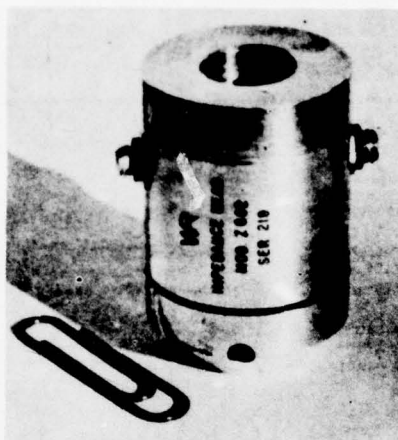
Fig. 8-2. Mechanical impedance transducer. (Wilcoxon Research)
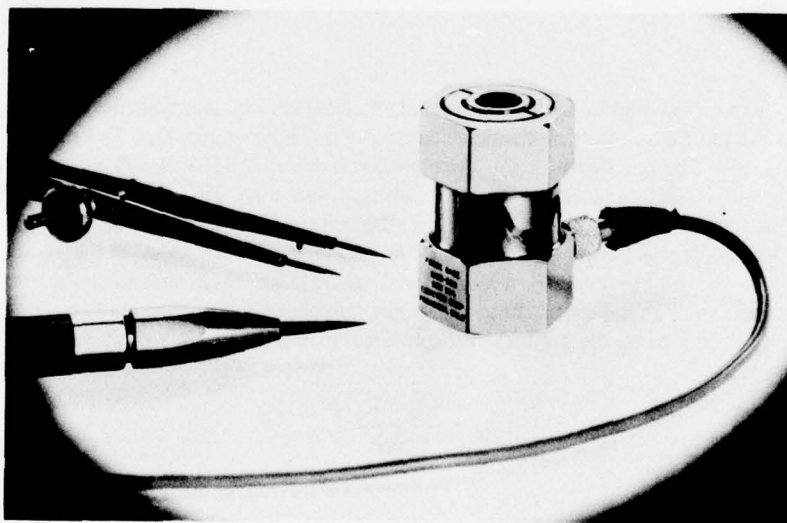
Fig. 8-3. Force transducer. (Endevco)
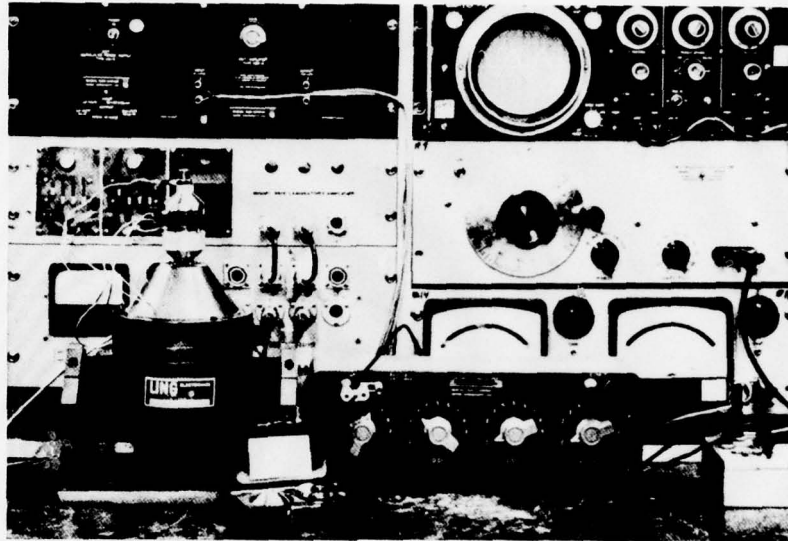
Fig. 8-4. Setup for calibrating the force transducer and accelerometer in an impedance head [39]

The sensitivities of the force gage and accelerometer in an impedance head are calibrated on an electrodynamic shaker using a test setup like that illustrated in Fig. 8-4. The sensitivity of the force pickup is determined by measuring its output at a selected acceleration, first without and then with an external mass attached to the impedance head. First, the output from the force gage, with a standard accelerometer mounted on top of the impedance head, is measured. Then the measurement is repeated with an external mass and accelerometer attached to the impedance head. The force sensitivity is the change in force gage output divided by the product of the external mass and the applied acceleration:

$$S_f = \frac{Q_m - Q_o}{Ma} \tag{8-1}$$

where

S_f = sensitivity, electrical output per unit force, in millivolts per newton (mV/lbf)

Q_m = electrical output with external mass attached, in millivolts

Q_o = electrical output without external mass, in millivolts

M = external mass, in kilograms (lbm)
a = applied acceleration, G $\times$ 9.81 m/s^2 (386 in./s^2).

The effective end mass of the impedance head and bolt is measured by repeating the above-described force calibration with several different attached masses. The output from the force gage corresponding to 1 g acceleration is measured for each weight applied externally to the impedance head. These data are plotted. The results for two impedance heads of the same type are shown in Fig. 8-5. The intercepts of the lines with the abscissa indicate that the effective end mass of the impedance head is about 0.3 16 (0.14 kg).

From this force sensitivity calibration performed at one frequency, the effective portion of the mounting bolt through the head (if a through bolt is used) and the effective end mass of the head are determined. If this total mass is known, the frequency response can be determined by measuring the ration of the force gage output to standard accelerometer outputs from 10 to 5000 Hz without the external mass attached. This part of the calibration is repeated to measure the ratio of the output of the accelerometer in the head to the standard accelerometer output throughout the operating frequency range. The external mass is not used at the high frequencies to avoid relative motion between the standard accelerometer and impedance head.

The results of a calibration are shown in Fig. 8-6. The sensitivity of the accelerometer in the impedance head is nearly constant throughout the frequency range, increasing slightly near 5000 Hz. The sensitivity of the force gage is also nearly constant in the same frequency range. The sensitivity for use with an aluminum 1/2-in.-diameter (12.7 mm) through bolt is 5.8 mV/lbf (1.3 mV/N). The sensitivity is reduced to 5.1 mV/lbf when a 1/2-in.-diameter (12.7 mm) steel through bolt is used. This change in sensitivity is due to the difference in stiffness of the bolts. A small portion of the total force is applied to the bolt while the rest of the force is applied to the head. The force sensitivity is the voltage output divided by the total force.

The phase angle between the force and acceleration outputs is 0 degrees throughout the frequency range. This indicates that the acceleration motion and force applied to a structure are faithfully reproduced in the output signals from the head, and no correction to the measured phase angle of the impedance need be made.

8.3 Environmental Characteristics

Considerable care is necessary in the design of a force gage to minimize errors in output due to mechanical strain on the mounting surface.

Static strain is applied to the force gage in the process of mounting and can effectively change its sensitivity. The amount of static strain depends on the torque applied to the mounting bolts. Accordingly, this may be evaluated by performing calibrations using different mounting torques. The amount of
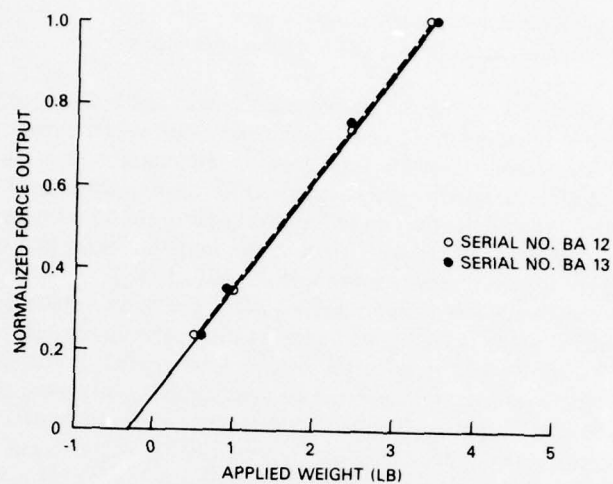
Fig. 8-5. Calibration of the effective and mass of a force transducer [39]
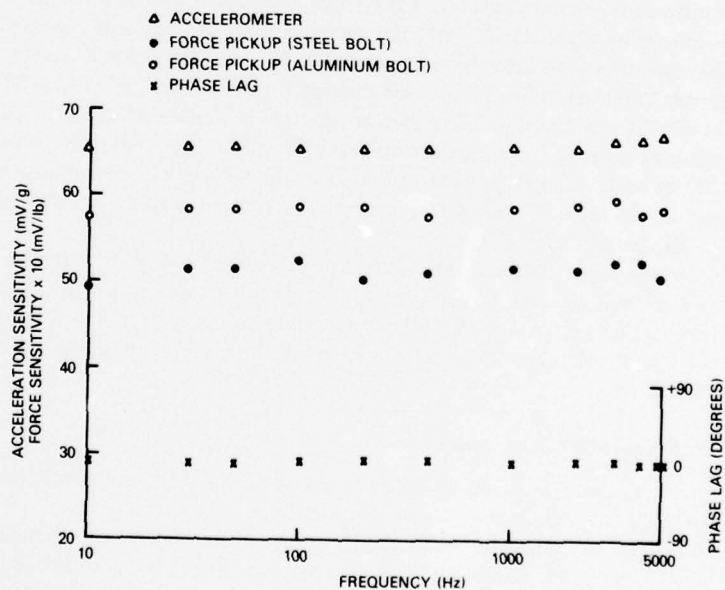
Fig. 8-6. Calibration of a mechanical impedance transducer [39]

variation in sensitivity with various torques is the measure of the gage's quality. It is good practice to perform final calibrations at the mounting torque of intended use.

Dynamic strains are present during shock and vibration excitation. Usually the error signal due to strain occurs at the same frequency as the force vibration. Therefore, the error signal from the strain adds or subtracts from the output due to the applied force, depending on the phase angle of the two signals. Since it is impractical to correct this error, evaluations to measure this environmental characteristic should be made.

The response of a force gage to strain at the mounting surface can be evaluated by using a beam. The amount of strain at the mounting surface of the force gage may be measured with strain gages or computed from beam theory. The results of data obtained on a beam are shown in Fig. 8-7. These results apply for an impedance head attached with a particular rotational orientation (0 degrees) relative to the direction of bending in the beam.

The results would be somewhat different if the impedance head were rotated around its sensitive axis to a different mounting position. For example, the results shown in Fig. 8-8 apply for a position at 30 degrees rotation, for which the force output due to strain is somewhat less. Compare Figs. 8-7 and 8-8. If the direction of bending strain is known in the testing application it is desirable to mount the impedance head in this position. At most mounting torques the error signal expressed as force increases with applied strain. Note in Fig. 8-8 that the inertial force in this test setup is less than the error signal produced due to bending strains. It was the intention of the test setup to produce large bending strains in the presence of low inertial force. The test results indicate that it is important to select mounting locations on the structure at which the dynamic bending strains are expected to be small.
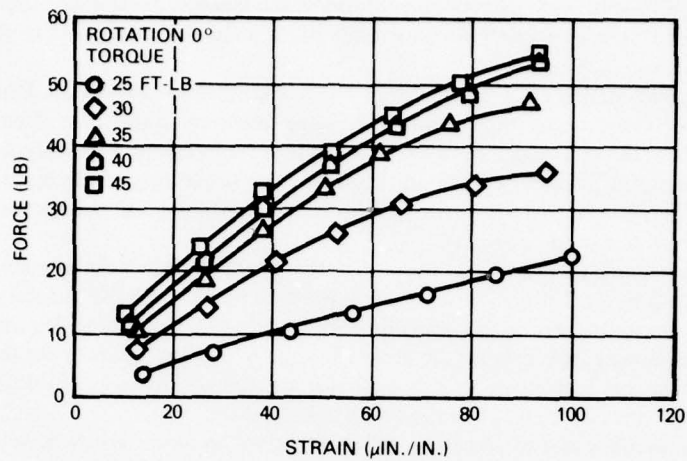
Fig. 8-7. Calibrations of strain sensitivity of a force transducer at rotation of 0 degrees [40]
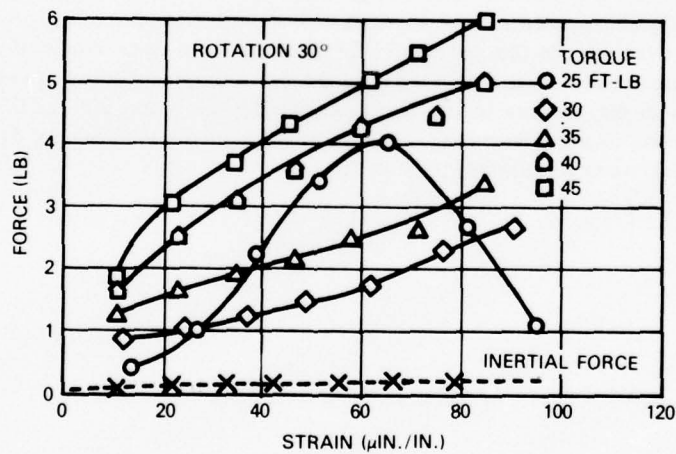
Fig. 8-8. Calibrations of strain sensitivity of a force transducer at rotation of 30 degrees [40]

REFERENCES

1. D. Pennington, "Basic Shock and Vibration Theory," *Environ. Quart.* (1965).
2. P. K. Stein, "Physical Quantities Which Characterize Vibration," *Meas. Eng.* **1**, 346-356 (1964).
3. F. Palmisano, "A Mechanical Shock Pulse Survey," *Shock Vib. Bull.* **35** (6), 209-227 (Apr. 1966).
4. A. F. Lawrence, "Crystal Accelerometer Response to Mechanical Shock Impulses," *Shock Vib. Bull.* **24**, 298-303 (Feb. 1957). Also Sandia Corp. Report 168-56-16.
5. J. W. Pendered, "The Shock Spectrum," *Environ. Eng.* **21**:13-19 (June 1966).
6. R. Lowe, "Correlation of Shock Spectra and Pulse Shape With Shock Environment," *Environ. Eng.* **1** (1) (Feb. 1959).
7. International Standards Organization, "International Standard on Vibration and Shock Terminology," ISO 2041, 1975.
8. American Standards Association, "American Standard on Acoustical Terminology (Including Mechanical Shock and Vibration)," SI.1-1960, May 1960.
9. R. I. Butler and R. C. Dove, "The Selection and Evaluation of Shock Test Instrumentation," IES Tutorial Lecture Series, *Dynamics*, p. 115-141 (1966).
10. American National Standards Institute, "American Standard Methods for the Calibration of Shock and Vibration Pickups," S2.2-1959, 1959.
11. S. Levy and W. D. Kroll, "Response of Accelerometers to Transient Accelerations," *J. Res. N.B.S.* **45** (4), 303-310 (Oct. 1950).
12. M. E. Gurtin, "The Effect of Accelerometer Low-Frequency Response on Transient Measurements," *Proc. Soc. Stress Anal.* **18** (1), 206-208 (June 1961).
13. B. Jaffe, "A Primer on Ferroelectricity and Piezoelectric Ceramics," Clevite Corp. TP217, Eng. Memo No. 60-14 (Dec. 1960).
14. R. L. Thomas, "Vibration Instrumentation for Nuclear Reactors," presented at International Symposium on Vibration Problems in Industry, Keswick, England, Apr. 1973.
15. R. R. Bouche, "Accelerometers for Shock and Vibration Measurements," Vibration Testing-Instrumentation and Data Analysis, American Society of Mechanical Engineers, AMD-Vol. 12, p. 25-59 (Sept. 1975).
16. R. W. Lally, "Application of Integrated-Circuits to Piezoelectric Transducers," Instrument Society of America Preprint No. P4-2-PHYMMID-67, Sept. 1967.
17. R. R. Bouche, "High Frequency Response and Transient Motion Performance Characteristics of Piezoelectric Accelerometers," Instrument Society of America Paper No. 50-LA-61, 8 p., 1961.
18. R. R. Bouche, "Ensuring the Accuracy of Shock and Vibration Measurements," *Proc. Inst. Environ. Sci.* 409-415 (1965).
19. R. R. Bouche, "Accelerometer Characteristics Used in Transient Motion and Nuclear Applications," presented at AFSWC Symposium on Instrumentation for Nuclear Weapons Effects Simulation, Kirtland Air Force Base, Albuquerque, N.M., Mar. 1970.
20. H. C. Merchant, "A Mechanical Shock Filter," Instrument Society of American Preprint No. 17.13-4-65, Oct. 1965.
21. E. Rule, F. J. Suellentrop, and T. A. Perls, "Capacitive Accelerometers with Optimum Frequency Response Characteristics," *J. Acoust. Soc. Amer.* **33** (1), 33-35 (Jan. 1961).
22. T. A. Perls, "Performance Tests on Consolidated Engineering Corporation Velocity Pickup Type 4-118," N.B.S. Report No. 4154, June 1955.

161

23. A. I. Dranetz, "Electromechanical Transducers," *Mach. Design* (Jan. 1958).
24. E. D. Jacobs, "New Developments in Servo Accelerometers," *Proc. Inst. Environ. Sci., 14th Ann. Tech. Meeting*, P. 517-523 (Apr.-May 1968).
25. A. Monahan and K. Bromley, "Vibration Analysis by Holographic Interferometry," *J. Acoust. Soc. Amer.* **44** (5), 1225-1231 (Nov. 1968).
26. R. R. Bouche, "High Frequency Shaker for Accurate Accelerometer Calibrations," *J. Environ. Sci.* (May/June 1970).
27. E. Jones, W. Yelon, and S. Edleman, "Extending Range of Piezoelectric Shakers," *N.B.S. Tech. News Bull.* 32-33 (Feb. 1970).
28. R. R. Bouche, "Comparison Shock Motion Calibrations," *Proc. Inst. Environ. Sci.* (1968).
29. R. R. Bouche, "Accelerometer Calibration with Reciprocity Vibration Standards," *Measurements and Data* (July-Aug. 1970).
30. R. R. Bouche, "Mechanical Vibration Standards of the Electrodynamic Type," *Proc. IX Int. Congr. Appl. Mech., Brussels, Belgium*, p. 395-406 (1956).
31. S. Levy and R. R. Bouche, "Calibration of Vibration Pickups by the Reciprocity Method," *J. Res. N.B.S.* **57** (4), 227-243 (Oct. 1956).
32. V. A. Schmidt, "Optical Calibration of Vibration Pickups at Small Amplitudes," *J. Acoust. Soc. Amer.* **34** (4), 455-458 (1962).
33. P. S. Lederer, "NBS Inter-Agency Transducer Project," N.B.S. Tech. Note 469, p. 11, Oct. 1968.
34. R. R. Bouche, "A Practical Application of Accelerometer Calibrations," *Shock Vib. Bull.* **41** (3), 1-9 (Dec. 1970).
35. R. R. Bouche, "Vibration Standards for Performing Comparison Calibrations," Instrument Society of America Preprint No. M18-3-MIS-MESTIND-67, Sept. 1967.
36. R. R. Bouche and L. C. Ensor, "Calibrators for Acceptance and Qualification Testing of Vibration Measuring Instruments," *Shock Vib. Ass. Environ. Bull.* **33** (3), 45-55 (Mar. 1964).
37. R. G. Burke, "Improved Velocity Measurement Techniques for the Shock Calibration of Accelerometers," *Proc. Inst. Environ. Sci.*, 247-250 (Apr. 1963).
38. R. Dove, R. I. Butler, and B. W. Duggin, "Calibration and Evaluation of Accelerometers in the 10 000 g to 100 000 g Range," Instrument Society of America Preprint No. 17.3-1-65, 13 p., Oct. 1965.
39. R. R. Bouche, "Instruments and Methods for Measuring Mechanical Impedance," presented at 30th SVIC Shock and Vibration Symposium, Detroit, Mich. Oct. 1961. (*Shock Vib. Bull.* **30** (II), 18-28 (Jan. 1962)).
40. E. F. Ludwig and N. D. Taylor, "Force Transducer Calibrations Related to Mechanical Impedance Measurements," *Shock. Vib. Bull.* **42** (1), 43-54 (Jan. 1972).

BIBLIOGRAPHY

FUNDAMENTALS FOR CALIBRATION

1-1. Anon., "Electrical Transducer Nomenclature and Terminology," Instrument Society of America, ISA-S 37.1 (July 1968).

1-2. Anon. "International System of Units Urged for Scientific Papers," *International EAR*, 8-11 (Apr. 1964).

1-3. R. A. Ackley, *Physical Measurements and the International (SI) System of Units* Technical Publications, San Diego, Calif., 1970.

1-4. P. H. Adams, "Motion and Its Derivatives," *Research/Development*, 30-32 (June 1970).

1-5. C. E. Crede, "Specification of Shock Tests," *Electro-Technology* (May 1963).

1-6. C. M. Harris and C. E. Crede, *Shock & Vibration Handbook*, Vol. 1, McGraw-Hill Book Co., New York, 1961.

1-7. G. M. Heiber, W. Tustin, and Engineering Staff of Spectral Dynamics Corp., "Understanding and Measuring the Shock Response Spectrum," *Sound Vib.* 42-49 (Mar. 1974).

1-8. International Organization for Standardization, "SI Units and Recommendations for the Use of Their Multiples and of Certain Other Units," ISO 1000-1973 (E).

1-9. R. T. McGoldrick, "A Vibration Manual for Engineers," David Taylor Model Basin Report R-189 NS712-100, U.S. Department of the Navy, Dec. 1957.

1-10. C. T. Morrow, "The Shock Spectrum," *Elec. Manufacturing,* (Aug. 1959).

1-11. J. C. Riedel, "The Accurate Measurement of Shock Phenomena," *Proc. Inst. Environ. Sci.* (Apr. 1962).

1-12. I. Ritlow, "Using Fourier Analysis In Designing," *Elec. Manufacturing,* 87-102 (Feb. 1959).

1-13. R. J. Roathaug, "Practical Aspects of Shock Spectrum Testing," *Proc. Inst. Environ. Sci.,* p. 303-308 (May 1972).

1-14. W. J. Sieger, "Waveform Effects In Shock Testing," Sandia Corp., Technical Memorandum SCTM 205-60 (12), 25 p. Aug. 1960.

1-15. R. Thomas, "Evaluation of the Distortion in Measurement of Half-Sine Shock Pulses Using PE and PR Accelerometers," Endevco Tech Paper 238 (not published).

1-16. H. M. Trent and B. Peterson, *Glossary of Terms Frequently Used in Acoustics,* American Institute of Physics, New York, Oct. 1960.

1-17. W. Tustin, "Measurement and Analysis of Machinery," *Chem. Eng. Progr.* 67 (6), 62-70 (June 1971).

1-18. K. Unholtz, "Mass and Force," *Vibration Top.* 1 (1) (aug. 1959).

1-19. I. Vigness," The Fundamental Nature of Shock and Vibration," *Elec. Manufacturing,* 89-108 (June 1959).

1-20. P. Vigoureux, "The International System of Units (SI)" National Bureau of Standards Special Publication 330, Apr. 1972.

1-21. G. E. White, "The Meaning of "Natural Frequency," *Statham Instrum. Notes* No. 12 (Nov.-Dec. 1949).

1-22. G. E. White, "A Relation Between Acceleration And Displacement Response," *Statham Instrum. Notes* No. 19 (Jan.-Feb.-Mar. 1951).

THEORY OF SEISMIC TRANSDUCERS

2-1. Anon., "Accelerometer Survey," *Instrum. Contr. Syst.* **41**, 81-94 (Nov. 1968).

2-2. Anon., "Which Accelerometer Resonance?" *Instrum. Tech.*, 57 (Mar. 1970).

2-3. D. Arlidge, "A Summary of Shock Test Instrumentation," *Proc. Inst. Environ. Sci.*, p. 24-28 (Apr. 1959).

2-4. R. R. Bouche, "Understanding Accelerometers," *Electron. Eng.* 90-94 (Apr. 1967).

2-5. R. O. Brooks, "Distortions of Controlled Transients by Shock Monitoring Systems," Instrument Society of America Preprint No. P13-5-PHYMMID-67 (Sept. 1967).

26. R. O. Brooks and F. H. Mathews, "Mechanical Shock Testing Techniques and Equipment," IES Tutorial Lecture Series, Dynamics, p. 69-113 (1966).

2-7. A. J. Buschman, "Omnidirectional Acceleration Sensor," *Shock Vib. Bull.* **35** (4), 55-60 (Apr. 1966).

2-8. R. I. Butler and M. McWhirter, "Transducers for Shock and Vibration Measurements," Instrument Society of America Preprint No. 16.6-1-66 (Oct. 1966).

2-9. L. E. Dunbar, "Development of an Omnidirectional Accelerometer," *Shock Vib. Bull.* **34** (4), 41-44 (Feb. 1965).

2-10. V. F. DeVost and P. S. Hughes, "Bidirectional Shock and High-Impact Effects on Shock Transducers," *Shock Vib. Bull.* **37** (2), 29-42 (Jan. 1968).

2-11. R. C. Dove, "Instrumentation for Shock Motion Measurement," *Proc. Inst. Environ. Sci.*, p. 277-284 (1963).

2-12. R. F. Gibson, "Optimum Damping for Accelerometers," *Instrum. Contr. Syst.* 87-88 (Sept. 1972).

2-13. E. V. Hardway, "Electrokinetic Transducers," *Instrum.* **26** (8), 1186-1188 (Aug. 1953).

2-14. D. R. Harting, "Digital Transient-Test Techniques," *Exp. Mech.*, 335-340 (July 1972).

2-15. J. S. Hernandez, *Introduction to Transducers for Instrumentation*, Statham Instruments, Inc., Los Angeles, 1959.

2-16. N. A. Leifer, "Random-Vibration-Induced Errors in a Missile Caused by Nonlinear Inertial Accelerometers," *Shock Vib. Bull.* **37** (2), 87-97 (Jan. 1968).

2-17. W. Mitchell, "Accelerometers—Displacement to Emission," *Shock Vib. Dig.* **5** (6), (June 1973).

2-18. J. T. Muller, "Transients in Mechanical Systems," *Bell Syst. Tech. J.* **27**, 657-683 (Oct. 1948).

2-19. Y. Muranaka and E. Furukawa, "Responses of Seismic Pickups to Displacement Pulses," *Science and Engineering,* Chuo University, Tokyo, 1966.

2-20. M. W. Oleson and R. F. Blake, "Studies of Random Vibration," *Shock Vib. Bull.* **24**, 133.

2-21. J. G. Parks, "An Acceleraometer Design Using Ferrofluid Ultrasonic Interferometry," *Shock Vib. Bull.* **41** (3), 17-24 (Dec. 1970).

2-22. T. A. Perls, "Frequency Response of Second-Order Systems with Combined Coulomb and Viscous Damping," *J. Res. N. B. S.* **57**, (1), Research Paper 2963 (July 1956).

2-23. M. A. Perry, "Flight Test Instrumentation," in *Proceedings of the First International Symposium,* Pergamon Press, New York, 1960.

2-24. G. N. Rosa, "Some Design Considerations for Liquid Rotor Angular Accelerometers." Statham Laboratories Instrument Notes No. 26 (Jan. 1954).

2-25. F. Schloss, "Inherent Limitations of Accelerometers for High-Frequency Vibration Measurements," *J. Acoust. Soc. Am.* **33** (4), 539 (Apr. 1961).

2-26. G. L. Schulz and W. E. Baker, "A Dynamic Data Compensation Technique for Seismic Transducers," *Shock Vib. Bull.* **40**, (7), 123-132 (Dec. 1969).

2-27. J. M. Slater, "Which Accelerometers for Spacecraft Guidance?," *Space/Aeronautics,* 227-240 (Oct. 1960).

2-28.   L. Stratham, "The Mass Effect in Fluid Damping," *Stratham Instrument Notes* No. 13 (Jan.-Feb. 1950).

2-29.   L. Stratham, "Design Parameters for Linear Accelerometers," *Stratham Instrument Notes* No. 9 (Jan. 1952).

2-30.   G. Von Vick, "Accelerometers," *Instrum, Contr. Syst.* **38**, 86-87 (Nov. 1965).

2-31.   l. Westin and A. Henningston, "Underwater Explosion Tests With the Swedish Full-Scale Submarine Test Section "Stalmyggan": Recording and Data Reduction System," *Shock Vib. Bull.* **43**, (1), 31-41 (June 1973).

PIEZOELECTRIC ACCELEROMETERS

3-1.   Anon., "Controls/Switches/Drivers Selection Checklist, Piezoelectric Accelerometers," *Electron. Prod. Mag.* (Apr. 1972).

3-2.   Anon., "Guide for Specifications and Tests for Piezoelectric Acceleration Transducers for Aero-Space Testing," Instrument Society of America ISA-RP 37.2 (1964).

3-3.   R. L. Allen and L. R. Flippin, "A Method of Embedding Accelerometers in Solid Propellant Rocket Motors," *Shock Vib. Ass. Environ. Bull.* **33**, (3), 27-43 (Mar. 1964).

3-4.   H. D. Arlowe, R. C. Dove, and B. W. Duggin, "Faithful Transmission of Piezoelectric Transducer Data," *ISA J.* 62-66 (Jan. 1966).

3-5.   S. A. Basri, "A Method for the Dynamic Determination of the Elastic, Dielectric, and Piezoelectric Constant of Quartz," National Bureau of Standards Monograph 9 (June 1960).

3-6.   D. Belincourt, "Domain Processes in Lead Titanate Zinconate and Barium Titanate Ceramics," *J. Appl. Phys.* **30** (11), 1803-1810 (1959).

3-7.   C. A. Bowes, "Engine Vibration Monitoring on the Boeing 747 Aircraft," ISA Symposium on Instrumentation in the Aerospace Industry, Vol. 16, p. 195-205 (May 1970).

3-8.   R. O. Brooks and J. A. Gusman, "Distortion of Controlled Transients by Shock Monitoring Systems," ISA Preprint P13-5-PHYMMID-67, 17 p. (1967).

3-9.   W. G. Cady, *Piezoelectricity*, Dover Publications.

3-10.   W. G. Cady, "Piezoelectricity and Ultrasonics," *Sound*, **2** (1), 46-52 (1963).

3-11.   M. Carteus and R. Gopal," Vibration Measurements in a PWR-Instrumentation," Westinghouse Nuclear Energy Systems, Pittsburgh, Pa.

3-12.   D. B. David, "Investigation of Zero Shift in Piezoelectric Ceramic Accelerometers," *Proc. Instrum. Soc. Amer.,* Paper No. 71-631, Oct. 1971.

3-13.   A. l. Dranetz, "Barium Titanate Applications," *Shock Vib. Bull.* **17**, 122.

3-14.   H. C. Epstein, "Development and Application of a 0.14 gm Piezoelectric Accelerometer," Instrument Society of America, *Test Measurement: Vibration,* Part 2C, Paper No. 72-619, Oct. 1972.

3-15.   J. R. Fowler and W. S. Tierney, "Accelerometer Sensitivity to Dynamic Pressure Pulses," *Shock Vib. Ass. Environ. Bull.* **31** (3), 183-194 (Apr. 1963).

3-16.   E. Furukawa, "An Investigation of Torsional Pickups of Low Natural Frequency," *Japan Soc. Prec. Eng. Bull.* **2** (6) (July 1968).

3-17.   R. E. Harper, "Transverse Sensitivity of Piezoelectric Accelerometers," Presented at 5th Transducer Workshop IRIG, Pratt and Whitney Aircraft, East Hartford Conn., Oct. 1967.

3-18.   R. A. Heising, "Quartz Crystal Theory, Fabrication and Performance Measurements," U. S. Army Tech. Manual TM 11-2540, U. S. Department of the Army, Dec. 1950.

3-19.   B. Jaffe, Clevite Corp. Electronic Research Div., "Transducer Properties of Lead Titanate Zirconate Ceramics," *IRE National Convention Record*, Part 6 (1959).

3-20.   C. Jako, "An Angular Accelerometer," ISA.

3-21.   E. Jones, S. Edelman, and E. R. Smith, "Small Vibration Pickups," *Shock Vib. Bull.* **23**, 234.

3-22.   D. R. Kemper, "Measurement of Piezoelectric Accelerometer Capacitance," *J. Eng. Sci.* **10** (2), 34-40 (Apr. 1967).

3-23.   R. J. Klingler, "A Method of Measuring Acoustic Sensitivity (of Accelerometers)," Sandia Corp. Tech Memo SC-TM 290-63(73) (Nov. 1973).

3-24.   H. H. A. Krueger, "Effects of High Static Stress on the Piezoelectric Properties of Transducer Materials," *J. Acoust. Soc. Amer.* **33** (10), 1139-1344 Oct. 1961).

3-25.   H. A. A. Krueger, "Stress Sensitivity of Piezoelectric Ceramics: Part 1, Sensitivity to Compressive Stress Parallel to the Polar Axis," *J. Acoust. Soc. Amer.* **42**, (3), 636-645 (1967).

3-26.   S. B. Lang and F. Steckel, "Method for the Measurement of the Pyroelectrical Coefficient, dc Dielectric Constant, and Volume Resistivity of a Polar Material," *Rev. Sci. Inst.* **36** (7), 929-932 (1965).

3-27.   R. A. Larder, "Use of Crystal Accelerometers at High Acceleration and Temperatures," Instrument Society of America Preprint P7-4 PHYMMID-67, 1967.

3-28.   R. C. Lewis, "The Design and Characteristics of a High Sensitivity Direct Current Operated Accelerometer," *J. Acoust. Soc. Amer.* **22** (3), 357-361 (May 1950).

3-29.   T. H. Lin, "The Effect of Spring Mass on Contact-Accelerometer Responses," ASME Paper No. 56-APM-3 (June 1956).

3-30.   B. Mangolds, "Effect of Mounting-Variables on Accelerometer Performance," *Shock Vib. Ass. Environ. Bull.* **33** (3) (Mar. 1964).

3-31.   S. T. Marks, "A Barium Titanate Velocity Gauge for Use on Short Coaxial Cables," Ballistic Research Laboratories, Memorandum Report No. 758, Jan. 1954.

3-32.   W. P. Mason *Physical Acoustics: Principles and Methods*, Academic Press, New York, 1964.

3-33.   A. J. Mullen, "Temperature Variation of the Piezoelectric Constant of Quartz," *J. Appl. Phys.* **40** (4), 1693-1696 (Mar. 1969).

3-34.   J. A. Nagy and C. E. Henley, Jr., "Influence of Fixture Stress Concentrations on Ring Accelerometers," *Shock Vib. Bull.* **37** (2), 43-50 (Jan. 1968).

3-35.   W. E. Nelson and G. W. Brown, "An Impulse Accelerometer," UCRL 7766, *Instruments*, Vol. C-37, TID-4500 (30th ed.), Lawrence Radiation Laboratory, Livermore, Calif., Mar. 1964.

3-36.   N. Newman, "Considerations in Computing the Useful Frequency Range of Piezoelectric Accelerometers," NBS Tech. Note 487, 20 p. (July 1969).

3-37.   M. W. Oleson, "Limitation of Instrumentation for Mechanical Shock Measurement," NRL Report 6342 U. S. Naval Research Laboratory, Washington, D.C., Dec. 1965.

3-38.   A. W. Orlacchio, "New Advances in Vibration Measurement to Meet More Stringent Environmental Conditions," *Proc. Inst. Environ. Sci.* p. 13-17 (Apr. 1959).

3-39.   R. D. Pennington, "Effects of Accelerometer Cross Axis Sensitivity on Measurement Accuracy," *Environ. Quart.* **10** (2) 34-35 (1964).

3-40.   D. Pennington, "Piezoelectric Accelerometer Manual," Endevco, 119 p. 1965.

3-41.   T. A. Perls, "A Simple, Objective, Test for Cable Noise Due to Shock, Vibration or Transient Pressures," N.B.S. Report No. 4094, May 1955.

3-42.   T. A. Perls, "Primary Pyroelectricity in Barium Titanate Ceramics," *J. Appl. Phys.* **29** (9), 1297-1302 (Sept. 1958).

3-43.   T. A. Perls, "Proceedings of Symposium on Barium Titanate Accelerometers," National Bureau of Standards Report No. 2654, Aug. 1963.

3-44.   R. B. Peters, "A New Method of Evaluating the Acoustic Response of Piezoelectric Accelerometers," *Proc. Inst. Environ. Sci.* (1965).

3-45.   F. P. Phelps, "Detuning Quartz Crystals." National Bureau of Standards Report No. 3326, May 1954.

3-46.   R. H. Plumee, "Zero-Shift in Piezoelectric Accelerometers," Sandia Laboratories, Report SC-RR-70-755, Mar. 1971.

3-47.   G. K. Rasanen, "Accelerometer Mounting and Data Integrity," *Shock Vib.* 8-15 (Nov. 1967).

3-48.   B. Reznek, "Design and Evaluation of a Small, Compressed Crystal Type, High-Internal-Capacitance Accelerometer," *Shock Vib. Bull.* **24**, 291.

3-49.   J. E. Rhodes, "Piezoelectric Transducer Calibration Simulation Method Using Series Voltage Insertion," *Environ. Quart.* 30-47 (Apr. 1962).

3-50.   D. W. Rockwell, "A Transverse Compensated Accelerometer," presented at Instrument Society of America. 19th National Instrumentation Symposium, May 1973.

3-51.   P. E. Scarborough, Jr., "Zero Shift in Piezoelectric Transducers," Sandia Corp., Report SC 1004-B, Oct. 1959.

3-52.   I. Smith, "Piezoelectric Accelerometer Instrumentation for Gas Guns," Harry Diamond Laboratories, Report TM-68-29, Oct. 1968.

3-53.   L. Walther and G. Beister, "Lead-Metaniobate Piezoelectric Vibration Pickup," *Hochfrequency-Technik Electroakustik* **74** (5-6), 204-205 (1965).

3-54.   J. Willis and B. D. Jimmerson, "A Piezoelectric Accelerometer," *Proc. IEEE* **52** (7), 971-872 (1964).

3-55.   D. B. Wright, "Sensitivity of Various Accelerometers to Structural Bending of the Mounting Surface," Westinghouse Research Laboratories, Research Memo 407-3000-M3, Apr. 1961.

WIRE RESISTIVE AND PIEZORESISTIVE ACCELEROMETERS

3-56.   B. Anzalone, "Understanding and Applying Strain Gages," *Instrum. Contr. Syst.* 55-56 (Dec. 1972).

3-57.   C. A. Bowes, "Variable Resistance Sensor Work Better With Constant Current Excitation," *Instrum. Technol.* (Oct. 1966).

3-58.   W. F. Caplan, "Miniature Biaxial Accelerometer-Damped," ISA-ASI 72239, p. 217-221 (1972).

3-59.   W. B. Dobie, *Electric Resistance Strain Gages,* The English Universities Press Limited. London, 1948.

3-60.   R. J. Fyffe and A. Arobone, "Strain Gage Transducers," *Electron. Instrum. Dig.* **5** (5), 31-32 (May 1969).

3-61.   M. Green, Semiconductro Strain-Gage Transducers," *Electron. Instrum. Dig.* **5** (5), 31-32 (May 1969).

3-62.   B. B. Helfand, "Calibration of Resistance Bridge Transducer Circuits Under Temperature Extremes," *Statham Laboratories Instrument Notes,* No. 14 (Mar.-Apr. 1950).

3-63.   E. Hollander and G. L. Vick, "The Piezoresistive Effect and its Application," *Rev. Sci. Instrum.* **31** (3), 323-327 (Mar. 1960).

3-64.   L. E. Hollander, Jr., "The Role of Solid State Materials in Transducers," *Solid/State/-Design* (Nov. 1962).

3-65.   W. P. Mason, "Use of Piezoresistive Materials in the Measurement of Displacement, Force, and Torque," *J. Acoust. Soc. Amer.* **29** (10), 1096-1101 (Oct. 1957).

3-66.   M. W. Oleson, "Calibration Study of (SFNSY) Floating Shock Platform," NRL Report 6069, U.S. Naval Research Laboratory, Washington, D.C., Mar. 1964.

3-67.   M. W. Oleson, "Components of a New Shock Measurement System," *NRL Progress,* U.S. Naval Research Laboratory, Washington, D.C., Dec. 1967.

3-68.   M. W. Oleson, "Shock Signal Integrator Description, Operation, and Schematics," NRL Memorandum Report 1903, U. S. Naval Research Laboratory, Washington, D.C., July 1968.

3-69.   M. W. Oleson, "Advances in Shock and Vibration Measurements for Naval Applications," Instrument Society of America, Paper No. 71-638, Oct. 1971.

3-70. P. R. Perino, "Standardization of Bridge Transducers," *Statham Instruments Notes* No. 34 (May 1959).

3-71. J. C. Sanchez, "The Micro-Sensor, a New Tool for the Experimental Stress Analyst," Micro Systems, Inc., Jackson, Miss., Oct. 1960.

3-72. J. C. Sanchez, "Recent Advances in Flexible Semiconductor Strain Gages," Instrument Society of America, No. 46-LA61, Sept. 1961.

3-73. J. C. Sanchez, "Recent Developments in Flexible Silicon Strain Gages," Instrument Society of America, No. 37-SL61, Jan. 1961.

3-74. I. G. Scott, "The Determination of Temperature Coefficient of Resistance Strain Gauges," Instrument Society of America, No. 25 LA61, Sept. 1961.

3-75. N. Sion, "Bridge Networks in Transducers," *Instrum. Contr. Syst.* **41**, 107-109 (Aug. 1968).

3-76. A. T. Snyder, "A New System for Monitoring the Over-All Transduction Ratio for Analog Recording Channels Employing Bridge Type Transducers," *Stratham Laboratories Instrument Notes* No. 28 (Oct. 1954).

3-77. P. K. Stein, "Some Properties of Input Conditioning Circuits for Wheatstone-Bridge-Based Transducers," Fifth Transducer Workshop Document 112-68, White Sands Missile Range, p. 243-256 (1967).

3-78. P. K. Stein, "How to Select a Strain Gage," *Strain Gage Readings*, **II**, (1) (Apr.-May 1959).

3-79. J. Tabata, "Study on the Minature Type High Sensitivity Accelerometer Using Semiconductor Strain Gages," NAL TR-146, National Aerospace Laboratory, Tokyo, Japan, 1967.

3-80. A. N. Waldman, "Piezoresistive Accelerometers," *Proc. Inst. Environ. Sci.,* p. 627-633 (Apr. 1961).

3-81. W. E. Wall, "Piezoresistive Strain Gage Accelerometers with Subcritical Damping and High Overload Capabilities," *12th instrum. Soc. Amer. Aerosp. Symp.* p. 11 (May 1966).

3-82. W. E. Wall, "Applications of Piezoresistance to Externally Excited Transducers," *22d Instrum. Soc. Amer. Conf.,* p. 12 (Sept. 1967).

3-83. W. E. Wall, "Piezoresistive Strain Gage Accelerometers Increase Spectrum of Shock and Vibration Measurement Capability," *Shock Vib. Bull.* **35**, (5) (1966).

CAPACITIVE ACCELEROMETERS

3-84. Y. T. Li and S. Y. Lee, "Air Damped High-*g* Accelerometer and Wide Band Veclcimeter for Shock Study in Free Mass Under Severe Air Blast," *Shock Vib. Bull.* (7), 133-139 (Dec. 1969).

INDUCTIVE TRANSDUCERS

3-85. A. C. Diechmiller, "How to Select Electromagnetic Vibration Pickups," *Elec. Manufacturing* **59** (1) (Jan. 1957).

3-86. M. L. Greenough, "Oil Fim Thickness Indicator for Journal Bearings," *AIEE Trans.* Paper 48-96, Jan. 1948.

3-87. D. Mori, "Measurement of Minute Acceleration by a Precision Accelerometer," Institute of Space and Aeronautical Science, University of Tokyo. (Paper presented at the Third CAS Symposium, Mar. 1970).

3-88. E. V. Sawyer, "Variable Permeance Transducers for Strain Measurement Applications," presented at Instrument Society of America Tenth Annual Instrument-Automation Conference, Sept. 1955.

3-89. F. E. Templeton, "Omnidirectional Electromagnetic Accelerometer," Air Force Cambridge Research Laboratories AFCRL-67-0470.

3-90. K. Unholtz, "MB Velocity Meters," *Shock Vib. Bull.* **8**, 28.

3-91.   M. J. Witt, "Development of a Velocity Transducer Evaluation System," Air Force Special Weapons Center, Technical Report No. AFSWC-TR-70-5, Vol. 4, p. 47-64 (Mar. 1970).

SELF-CONTAINED VIBRATION RECORDING INSTRUMENTS

3-92.   R. E. Blake, "Peak-Reading Accelerometers," *Shock Vib. Bull.* 8, 45.
3-93.   E. H. Schell, "Use of the Impact-O-Graph in the Determination of Field-Handling Conditions," *Shock Vib. Bull.* 25 (2), 103-109 (Dec. 1957).
3-94.   J. Upham and A. Dranetz, "A Tape Recording Accelerometer for Laboratory Playback, Analysis and Simulation," *Shock Vib. Bull.* 23, 223.
3-95.   I. Vigness, "Discussion of Some Peak Reading Instruments," *Shock Vib. Bull.* 16, 120.

AUXILIARY INSTRUMENTS

3-96.   H. D. Arlowe, "Electrical Noise in Instrumentation Systems," *Proc. Inst. Environ. Sci. 1963 Ann. Tech. Meeting,* p. 341-347 (Apr. 1963).
3-97.   H. D. Arlowe and R. C. Dove, "Circuitry for Conditioning the Transducer Output Signal," Instrument Society of America Preprint No. 16.6-3-66 (1966).
3-98.   H. D. Arlowe and G. W. Holmes, "On-Board Signal Conditioning for Peizoelectric Accelerometers," Instrument Society of America Preprint No. P4-4-PHYMMID-67, Sept. 1967.
3-99.   M. Bennett, "A Case for Low Impedance," *Proc. Inst. Environ. Sci. 14th Ann. Tech. Meeting,* p. 79-82 (Apr.-May 1968).
3-100. H. D. Cyphers and Frank J. Holley, "Automatic Calibration and Environmental Measurement System for Launch Phase Simulator," *Shock Vib. Bull.* 36 (6), 207-214 (Feb. 1967).
3-101. J. E. Jodd, "A New Differential Zero Drive*System for Direct Wideband Audio Data Transmission Over Standard Telephone Lines," Instrument Society of America Preprint No. P13-2-PHYMMID, 1967.
3-102. W. P. Kistler, "The Piezotron Concept as a Practical Approach to Vibration Measurement," *J. Inst. Environ. Sci.* 14 (2), 20-22 (Mar.-Apr. 1971).
3-103. R. Morrison, *Grounding and Shielding Techniques in Instrumentation* John Wiley and Sons, Inc., New York, 144 p., July 1967.
3-104. R. Morrision, "Modern Filter Theory," Instrument Society of America Preprint No. P13-4-PHYMMID-67, Sept. 1967.
3-105. D. Pennington, "Charge Amplifier Applications," *Instrum. Contr. Syst.* (Jan. 1965).
3-106. S. Rogero, "Miniaturized Piezoelectric Transducer Electronics Versus Charge Amplifiers-A Comparison of the Two Systems in Vibration and Pressure Applications," ISA-ASI 72240, p. 223-230, 1972.
3-107. J. J. Smithrick, "Effects of Cable and Circuit Parameters on the Precision Calibration of a Charge Amplifier," NASA Tech. Note NASA TN D-4300, Feb. 1968.
3-108. D. J. Torpy, "A Field-Effect Transistor Amplifier for Improving Piezoelectric Gage Measurements," Naval Ordnance Laboratory, NOLTR 67-104, Oct. 1967.
3-109. R. W. Towle and T. A. Perls, "Low-Impedance Vibration Coupler for Missile Use," *Shock Vib. Ass. Environ. Bull.* 27 (3), 211-214 (June 1959).
3-110. T. Usher, Jr., "Signal Conditioner Characteristics for Shock Applications," *J. Environ. Sci.,* 31-34 (Oct. 1967).

DISPLACEMENT MEASUREMENTS

3-111. R. Aprahamian and D. A. Evensen, "Applications of Holography to High-Frequency Vibrations and Transient Response," *Shock Vib. Bull.* 40 (7), 33-34 (Dec. 1969).

3-112. C. F. Bruce, "Interference Accelerometer," *Rev. Sci. Instrum.* **38**, (8), 1090-1093 (1967).

3-113. H. A. Deferrari and F. A. Andrews, "Laser-Interferometric Technique for Measuring Small-Order Vibration Displacements," *J. Acoust. Soc. Amer.* **39**, (5), 1, 979-980 (1966).

3-114. H. A. Deferrari, R. A. Darby, and F. A. Andrews, "Vibrational Displacement and Mode-Shape Measurement by a Laser Interferometer," *J. Acoust. Soc. Amer.* **42** (5), 982-990 (1967).

3-115. S. Edelman, "A Strosboscopic Vibration Analyzer," *N.B.S. J. Res.* **63**C (2), 97-104 (1959).

3-116. J. L. Goldberg, "Method of Measuring Vibratory Displacements in Terms of a Light Wavelength," *Shock Vib. Bull.* **37** (2), 13-16 (Jan. 1968).

3-117. G. A. Hotham, "Optical Displacement Follower Measures Vibration and Shock," *Test Eng.* 14-17 (Nov. 1959).

3-118. J. Johansson, "Accelerometer Calibration," *Instrum. Contr. Syst.* 79-81 (Dec. 1963).

3-119. C. D. Johnson and Gerald M. Mayer, "Hologram Interferometry as a Practical Vibration Measurement Technique," *Shock Vib. Bull.* **39** (2), 41-49 (Feb. 1969).

3-120. R. L. Johnson, R. Aprahamian and P. G. Bhuta, "Shock Loading and Holographic Interferometry in NDT," *Shock Vib. Bull.* **41** (3), 63-74 (Dec. 1970).

3-121. T. Kanazawa, "Trial Fabrication of a Displacement Vibrograph Suitable for Measurements of Horizontal Vibration of Ships," University of Tokyo, Faculty of Engineering.

3-122. J. W. Matthews, "Theory of Holography," California Institute of Technology Sci. Report No. 7, June 1967

3-123. J. Monahan and P. J. Nemergut, "Natural Frequencies and Mode Shapes of Plates with Interior Cut-Outs," *Shock Vib. Bull.* **41** (7), 37-49 (Dec. 1970).

3-124. W. J. Pastroius, "Vibration Analysis by Holography," *Mech. Eng.* 26-30 (June 1972).

CALIBRATION SHAKERS

4-1. A. J. Amico, "Determination of Frequency Response of Accelerometers at Low Frequencies," *Amer. Rocket Soc.* American Rocket Society, New York, Sept 1956.

4-2. Anon., "Characteristics of Electrodynamic Vibration Generators," ISO/TC108/WG4 (Secretariat-19) 42E, 20 pp.

4-3. Anon., "Dynamic Calibration of Accelerometers," *N.B.S. Tech. News Bull.* 226-227 (Oct. 1970).

4-4. Anon., "Extending Frequency Range of Calibration Vibrators," *Research/Development,* 30-31 (May 1967).

4-5. T. Dimoff, "Electrodynamic Vibration Standard with a Ceramic Moving Element," *J. Acoust. Soc. Amer.* **40** (3), 671-676 (Sept. 1966).

4-6. T. Dimoff and B. F. Payne, "Application of Air Bearings to an Electrodynamic Vibration Standard," *J. Res. N. B. S.* **67**C (4), 327-222 (Oct.-Dec. 1963).

4-7. S. Edleman, "Some Developments in Vibration Measurements," *J. Acoust. Soc. Amer.* **27** (4), 728-734 (July 1955).

4-8. S. Edleman, E. Jones, and E. R. Smith, "Barium Titanate Vibrators," *Shock Vib. Bull.* **23**, 175.

4-9. W. R. Elliott, "Measurement of Extraneous Motions in Commercial Linear Vibration Tables," Instrument Society of America Paper No. 55-21-1, Sept. 1955.

4-10. R. S. Jenkins, "Technique for Producing Low Level Quasi-static Accelerations," *Rev. Sci. Instrum.* **39** (8), 1212-1214 (1968).

4-11. E. Jones, W. Yelon, and S. Edlemen, "Extending Range of Piezoelectric Shakers," *N. B. S. Tech. News Bull.* 32-33 (Feb. 1970).

4-12.   A. B. Kaufman, "Measurement of Natural Frequency," *Instrum. Automation* **30**, 2266-2269 (Dec. 1957).

4-13.   L. Lemoine, "Table Vibrante A Bassee Frequence Pour L'E'talonnage Dynamic Des Accelerometers," *La Recherche Aeronautique* **69**, 27-37 (1959), Office National d'Etudes et Recherches Aeronautiques, Chatillon-sur-Bagneux (Seine), France.

4-14.   R. C. Lewis, "Electro-Dynamic Calibrators for Vibration Pickups," *Product Eng.* (Sept. 1951).

4-15.   H. Moore, "Vibration Generators, Ancillary Equipment and Applications," *J. Brit. Inst. Radio Eng.* 7 p. (Dec. 1953).

4-16.   N. Nezhni, "A Method for Minimizing Stray Magnetic Fields in the Electromagnetic Vibration Exciter," Jet Propulsion Laboratory, 32-709 (1965).

4-17.   A. W. Orlacchio, "Self Calibrating Accelerometer," Instrument Society of America, May 1960.

4-18.   L. A. Peterman, "Producing Motion with Magnetostrictive and Piezoelectric Transducers," *Elec. Manufacturing* (Dec. 1955).

4-19.   D. L. Schacher, "Vibration Calibrator," *Instrum. Automation* **30**, 470-471 (Mar. 1957).

4-20.   J. L. Sperrazza and Charles W. Bell, "A New Vibration Transducer Calibration System," *Proc. Inst. Environ. Sci.*, p. 480-485 (Apr. 1970).

4-21.   R. C. Tauscher, "Air Bearings for Vibration Exciters," *Sound Vib.* **1** (1), 23-25 (1967).

4-22.   K. Unholtz, *The Influence of Electrical and Motional Impedance on the Control and Performance of Some Vibration Machines,* MB Manufacturing Co., New Haven, Conn. p. 101-125, (1958).

4-23.   I. E. Walenta, "A Sinusoidal Vibrator for Generating High Acceleration at High Frequencies," Jet Propulsion Laboratory Tech. Report No. 32-13, Jan. 1960.

4-24.   W. A. Yates, "Wide-Range Calibrator for Vibration Pickups," *Electron.* (Sept. 1953).

PRIMARY SHOCK AND VIBRATION STANDARDS

5-1.   R. A. Ackley and S. H. Logue, "A Laser Interferometer and Its Application to Vibration Amplitude Measurement," *Proc. Inst. Environ. Sci.* **1**, 235-240 (Apr. 1967).

5-2.   Anon., "Photoelectronic Measurement of Vibration Displacements," *Test Eng.* 12-27 (July 1963).

5-3.   Anon., "Moire-Fringe Measures Low Frequency Vibration," *Design News* (May 1960).

5-4.   Anon., "Dynamic Calibration of Accelerometers," *N.B.S. Tech. News Bull.*, 226-227 (Oct. 1970).

5-5.   M. L. Aronow, "Steady-State Acceleration Test Equipment," *Proc. Inst. Environ. Sci.*, 206-208 (Apr. 1959).

5-6.   L. D. Ballard, W. S. Epstein, E. R. Smith, and S. Edelman, "Optical FM System for Measuring Mechanical Shock," *J. Res. N.B.S., C. Engineering and Instrumentation* 73C **3** (4), 75-78 (1969).

5-7.   Y. Beers, *Introduction to the Theory of Errors,* Addison-Wesley Publishing Co. Inc., Reading, Mass, 66 pp., 1957.

5-8.   R. J. Bobber, "General Reciprocity Parameter," *J. Acoust. Soc. Amer.* **39** (4), 680-687 (1966).

5-9.   C. F. Bruce, "Calibration of Sensitive Vibrometers by Interferometry," *Australian J. Appl. Sci.* **4** (1), 28-46 (1953).

5-10.   K. Cieplak, "Reciprocity Calibration of Vibration Pickups," *Environ. Test Equip.*, 15-18 (July 1968).

5-11. D. Cooke, "Moire Fringe Technique for Vibration Measurement," *J. Sci. Instrum.* **39**, 373-375 (1962).

5-12. H. A. Deferrari, "Laser Interferometric Technique for Measuring Small-Order Vibration Displacements," *J. Acoust. Soc. Amer.* **39** (5), Pt. 1, 979-980 (1966).

5-13. A. I. Dranetz and A. W. Orlacchio, "High-Frequency Calibration of Accelerometers," *Shock Vib. Bull.* **24** (Feb. 1957).

5-14. E. I. Feder and A. M. Gillen, "High-Frequency, High-G Calibration," *IRE Trans. Instrum.* **I-6**, (2) (June 1957).

5-15. P. W. Godt and H. S. Pyle, "The Application of a Laser Interferometer System for Calibrating Accelerometers and Dynamic Pressure Transducers," *J. Environ. Sci.,* 9-12 (Sept.-Oct. 1970).

5-16. J. L. Goldberg, "The Frequency Spectrum of the Photoelectric Signal From an Oscillating Interference Fringe Pattern," *Australian J. Appl. Sci.* **14**, (3), 231-242 (Sept. 1963).

5-17. J. L. Goldberg "A Non-Linear Control System for a Vibration Interferometer," *Mech. Chem. Eng. Trans. Inst. Eng. Australia* **MC3** (2), 195-206 (Nov. 1967).

5-18. J. L. Goldberg, "A Method of Measuring Vibratory Displacements in Terms of a Light Wavelength," *J. Sci. Instrum. (J. Phys. E)* Series 2, **1** (1968).

5-19. J. S. Hilten, "Accelerometer Calibration with the Earth's Field Dynamic Calibrator," N.B.S. Tech. Note 517, Mar. 1970.

5-20. P. M. Honnell, "The Absolute Calibration of a Brush Accelerometer and its Response to Square Waves of Displacement and Velocity," *Trans. Amer. Geophys. Union* **31** (5), 690-695 (Oct. 1950).

5-21. E. Jones, S. Edelman, and K. S. Sizemore, "Calibration of Vibration Pickups, at Large Amplitudes," *J. Acoust. Soc. Amer.* **33** (11), 1462-1466 (Nov. 1961).

5-22. W. Kissinger, "Determination of Sinusoidal Acceleration at Peak Levels Near that of Gravity by the "Chatter" Method" National Bureau of Standards Report No. 3339, Sept. 1954; Instrument Society of America Paper No. 54-40-1, Sept. 1954.

5-23. W. P. Kistler, "Precision Calibration of Accelerometers for Shock and Vibration," *Test Eng.* 16-22 *(May 1966).*

5-24. A. E. Kolesnikov, "Calibration of Vibration Pickups by the Reciprocity Method," *Measurement Tech.* (USSR) **11** 960-963 (1963).

5-25. P. S. Lederer and J. S. Hilten, "Easily Made Device Calibrates Accelerometers," *Test Eng.* **15** (3), 11-15 (Mar. 1966).

5-26. L. Lemoine, "Vibration Table for Use in Calibrating Accelerometers," *La Recherche Aeronautique-Bulletin Bimestriel,* No. 69, p. 27-38, Mar.-Apr. 1959, Office National d'Etudes et Recherches Aeronautiques (0NERA), Chatillon-sur-Bagneux (Seine), France.

5-27. S. H. Logue, "A Laser Interferometer and its Applicaton to Length, Displacement and Angle Measurement," *Proc. Inst. Environ. Sci.,* 465-467 (Apr.-May 1968).

5-28. E. M. McMillan, "Violation of the Reciprocity Theorem in Linear Passive Electromechanical Systems," *J. Acoust. Soc. Amer.* **18** (2), 344-347 (Oct. 1946).

5-29. G. A. Massey and R. R. Carter, "Portable Laser Instrument for Vibration Analysis and Transducer Calibration," *Shock Vib. Bull.* **37** (2), 1-6 (Jan. 1968).

5-30. A. F. Niemoeller, "Reciprocity Calibration of Electro-acoustic Transducers in the Time Domain," *J. Acoust. Soc. Amer.* **33** (12), 1712-1219 (Dec. 1961).

5-31. B. F. Payne, "An Automated Precision Calibration System for Accelerometers," presented at Instrument Society of America, 17th National Aerospace Instrumentation Symposium, Las Vegas, Nev., May 1971.

5-32. B. F. Payne, "Absolute Calibration of Vibration Generators with Time-Sharing Computer as Integral Part of System," *Shock Vib. Bull.* **36** (6), 183-194 (Feb. 1967).

5-33.   W. Ramberg, "Calibration of Shock and Vibration Pickups," *Noise Contr.* **3** (5), 23-33 (Sept. 1957).

5-34.   B. Reznek, "One "G" (Peak) Indicator for Use in Accelerometer System Calibration," *Proc. Inst. Enviorn. Sci.* 433-442. (Apr. 1964).

5-35.   E. Rule, F. J. Suellentrop, and T. A. Perls, "A Pick-Up to Read-Out Calibration for Vibration Channels," *Shock Vib. Ass. Environ. Bull.* **27** (3), 215-219 (June 1959).

5-36.   V. A. Schmidt, S. Edelman, E. R. Smith, and E. T. Pierce, "Modulated Photoelectric Measurement of Vibration, *J. Acoust. Soc. Amer.,* **34** (4), 455-458 (1962).

5-37.   O. P. Sheeks, "Methods for the Practical Reciprocity Calibration of Piezoelectric Accelerometers," Instrument Society of America Paper No. 68-581, 7 p., 1968.

5-38.   R. O. Smith, E. A. Willis, and J. S. Hilten, "A Dual Centrifuge for Generating Low-Frequency Sinusoidal Accelerations," *J. Res. N.B.S.,* **66D** (4), 357-362 (1962).

5-39.   S. R. Spron, "Use of a Centrifuge for the Precision Measurement of Accelerometer Characteristics," *Trans Amer. Soc. Mech. Eng.,* Paper No. 60-WA-195 (Aug. 1960).

5-40.   P. Stein, "Traceability–The Golden Calif," Arizona State University, College of Engineering Sciences, Publ. No. 7, (Apr. 1967).

5-41.   E. J. Stowe, "A Comparison of the Reciprocity and Interferometer Methods of Calibrating Piezoelectric Accelerometers," David Taylor Model Basin Report No. 786, U.S. Department of the Navy, May 1954.

5-42.   A. A. Zuehlke, "Instrument Error Band Concepts," *6th Nat. Flight Test Instrum. Sym.,* 5 p., May 1960.

SINUSOIDAL COMPARISON CALIBRATIONS

6-1.   American National Standards Institute, "American National Standard for the Selection of Calibrations and Tests for Electrical Transducers Used for Measuring Shock and Vibration," S2.11-1969, 19 p., 1969.

6-2.   J. M. Blair, "Estimating Errors in Experimental Data," *Instrum. Contr. Syst.* 95-97 (May 1972).

6-3.   R. S. Chernoff, "Comparison Calibration," *Measurement and Data,* 112-115 (Mar.-Apr. 1968).

6-4.   E. W. Clements and M. G. Stone, "Techniques for the Rapid Estimation of Accelerometer Natural Frequencies, NRL Report 5681, U.S. Naval Research Laboratory, Washington, D.C., Oct. 1961.

6-5.   R. B. Lewis, "Piezo Accelerometer Calibration by Comparison Methods," *Environ. Eng.* **31**, 9-10 (Mar. 1968).

6-6.   T. D. Finley, "A Comparison Method to Measure Accelerometer Transverse Sensitivity," Instrument Society of America Paper No. 69-666, Oct. 1969.

6-7.   B. R. Glen, "PROTECT–A Method of Optimizing Available Calibration Time in a Test Equipment Recall System," U.S. Naval Avionics Facility, AD 635 899, May 1966.

6-8.   G. M. Hieber and B. Mangolds, "Automatic Accelerometer Check-Out Equipment," *Shock Vib. Ass. Environ. Bull.* **33** (3), 69-72 (Mar. 1964).

6-9.   J. R. Houghton, "Voltage Ratio Detector for Millivolt Signals," N.B.S. Technical Note 266, 1965.

6-10.   B. W. Jameson, "Error Considerations in an Accelerometer Calibration System," *Test Eng.* 22-39 (Sept. 1963).

6-11.   E. Jones, D. Lee, and S. Edelman, "Improved Transfer Standard for Vibration Pickups," *J. Acoust. Soc. Amer.* **41**, (2), 354-357 (1967).

6-12.   J. E. Judd, "Lateral Motion Measurement in Vibration Testing," *Instrument-Automation Conference fof the Instrument Society of America:* Pt. 1, p. 4-7, Pt. 2, p. 4-5 (1960).

6-13.   R. W. Kelly, "Evaluation and Error Analysis of Vibration Calibration System," Sandia Laboratory Tech. Memorandum SC-TM-65-634, 32 p. Dec. 1965.

6-14.   R. E. Kemp, "Accuracy for Engineers," *Instrum. Tech.* 41-46 (May 1967).

6-15.   D. R. Kemper, "Measurement of Piezoelectric Accelerometer Capacitance," *J. Environ. Sci.,* 34-39 (Apr. 1967).

6-16.   P. S. Lederer, "Resonant Frequencies of Piezoelectric Accelerometers and the Evaluation of an Electrical Technique for Their Determination," N.B.S. Report No. 7566, 13 p., July 1962.

6-17.   W. B. Murfin, "Phase Measurement in Vibration Testing," *Shock Vib. Ass. Environ. Bull.* **31** (3), 127-133 (Apr. 1963).

6-18.   W. C. Nieberding, "Modified Vibration Transducer Calibration System Which Directly Yields a Plot of Sensitivity Versus Frequency," NASA Tech. Note NASA TN D-4760, Aug. 1968.

6-19.   K. M. O'Toole, "An Accelerometer Calibrator for the Low-Frequency Large-Displacement Range," *J. Sci. Instrum.,* **1** (Series 2), 672-673 (Feb. 1968).

6-20.   B. F. Payne, "An Automated Precision Calibration System for Accelerometers," presented at Instrument Society of America, 17th National Aerospace Instrumentation Symposium Las Vegas, Nev., May 1971.

6-21.   E. T. Pierce, O. W. Price, S. Edelman, and E. Jones, "Accelerometer Resonances Affect Vibration Measurement," *J. Environ. Sci.,* 17-21 (Dec. 1967).

6-22.   J. D. Ramboz, "A Treatise Concerning the Measurement of Accelerometer Transverse Sensitivity Ratio," *Proc. Inst. Environ. Sci.* **1**, 297-305 (Apr. 1967).

6-23.   J. D. Ramboz, "A Proposed Method for the Measurement of Vibration Transducer Transverse Sensitivity Ratio," Instrument Society of America Preprint No. M18-6-MESTIND-67, Sept. 1967.

6-24.   G. K. Rasanen, "Determining the Resonant Frequency of an Accelerometer's Installation," *Proc. Inst. Environ. Sci.,* 401-406 (Apr. 1970).

6-25.   J. R. Reed, "System to Calibrate Vibration Transducers at Low Displacements," *Shock Vib. Bull.* **34** (4), 13-19 (Feb. 1965).

6-26.   R. J. Ricci, "Vibration Test Instrumentation Calibration," I. E. S. Tutorial Lecture Series, p. 171-173 (Apr. 1967).

6-27.   D. W. Rockwell and J. D. Ramboz, "Measurement of Accelerometer Transverse Sensitivity," *Shock Vib. Bull.* **35** (4), 73-97 (Feb. 1966).

6-28.   W. R. Taylor and C. D. Robbins, "Calibration of Water Cooled High Temperature Accelerometers," *Shock Vib. Ass. Environ. Bull.* **33** (3), 19-25 (Mar. 1964).

6-29.   P. L. Walter, "A Technique for the Evaluation of Seismic Velocity Gages Through Generation of Large Amplitude Sinusoidal Velocities," *Proc. Inst. Environ. Sci.,* 21-24 (Apr. 1969).

6-30.   M. H. Woodward, "Evaluation Report of Endevco Model 2958A Calibration Fixture," ER No. 4, SC-DC-65-1719, Mar. 1965, Sandia Corp., Albuquerque, N. Mex.

6-31.   M. H. Woodward, "Automated Vibration Calibration Data Acquisition System," Instrument Society of America, *Test Measurement: Vibration,* Preprint 72-620, Oct. 1972.

6-32.   D. R. Workman, "New Instrument For Accelerometer Calibration," *Shock Vib. Bull.* **34** (4), 31-39 (Feb. 1965).

6-33.   D. R. Workman, "Calibration of Piezoelectric Accelerometer Reference Systems by Function Separation," *Proc. Inst. Environ. Sci.,* 386-395 (Apr. 1970).

6-34.   W. J. Youden, "Uncertainties in Calibration," *IRE Trans. Instrum.,* Paper No. 3.1, p. 133-138, Dec. 1962.

SHOCK MOTION CALIBRATIONS

7-1.   Anon., "Mechanical Shock Measured Optoelectrically," *N.B.S. Tech. News Bull.*, 124-126.

7-2.   Anon., "Sandia Corp. Standard Environmental Test Methods," Sandia Corp. Report SC-4452 D(M), June 1966.

7-3.   Anon., "Transducer Evaluation," Sandia Corp. Progress Report RS 7342/15, Apr. 1966.

7-4.   W. E. Baker and R. C. Dove, "Transient Calibration of Piezoelectric Accelerometers," *J. Environ. Sci.* 5 20-21, 24 (Oct. 1962).

7-5.   R. L. Bell, "Development of 100 000 g Test Facility," *Shock Vib. Bull.* 40 (2), 205-214 (Dec. 1969).

7-6.   R. R. Bouche, "The Absolute Calibration of Pickups on a Drop-Ball Machine of the Ballistic Type," *Proc. Inst. Environ. Sci.*, 115-121 (1961).

7-7.   R. M. Brengelman and J. W. Grubbs, "Shock Calibration of Piezoelectric Accelerometers," Report ABL/B-24, Allegany Ballistics Laboratory, Cumberland, Md., Dec. 1962.

7-8.   R. O. Brooks, "Generating Specified Shock Pulses," *J. Environ. Sci.* 10 (2), 28-33 (Apr. 1967).

7-9.   J. E. Cannon, "Transient Method of Calibrating a Piezoelectric Accelerometer for the High g-Level Range," American Society of Mechanical Engineers Paper No. 71-Vibr-43 (May 1971).

7-10.   A. J. Ciaponi, "Short Duration Shock Machine," *Proc. Inst. Environ. Sci.* 2, 335-340 (Apr. 1967).

7-11.   G. W. Cohrs and J. D. Favour, "Use of a Linear Air Bearing Sled for Dynamic Calibration of Velocity Transducers," ISA-ASI 72229, p. 149-156, 1972.

7-12.   R. W. Conrad and I. Vigness, "Calibration of Accelerometers by Impact Techniques," Instrument Society of America Paper No. 53-11-3, Sept. 1953.

7-13.   V. F. DeVost, "Hand-Held Shock Tester WOX-6A," *Shock Vib. Bull.* 34 (3), 329-334 (Dec. 1964).

7-14.   J. D. Favour, "Accelerometer Calibration by Impulse Excitation Techniques," Instrument Society of America Preprint No. P13-1-PHYMMID-67, Sept. 1967.

7-15.   J. D. Favour, "Calibration of Accelerometers by Impulse Excitation and Fourier Integral Transform Techniques," *Shock Vib. Bull.* 37 (2), 17-27 (Jan. 1968).

7-16.   M. Gertel, "A Peak Shock Velocity Recorder for Studying Transportation Hazards," *Shock Vib. Ass. Environ. Bull.* 33, 57-62 (Mar. 1964).

7-17.   W. D. Godshall, "The FPL Linear Deadweight Accelerometer Calibrator," University of Wis., Forest Products Laboratory, Report No. 2239, Feb. 1962.

7-18.   A. Goldberg, "Use of the JAN-S-44 Shock Test Machine as a Means of Transient Calibration for Barium-Titanate Accelerometers for an Acceleration Range up to 1000 G's," Frankford Arsenal Report No. S-4336, Mar. 1955.

7-19.   P. M. Honnell, "Instrumentation for the Transient Testing of Accelerometers," Instrument Society of America Paper No. 52-16-2, Sept. 1952.

7-20.   A. B. Kaufman, "Accelerometer Calibration by Ballistic Pendulum," *Instrum. Automation* 29 (7) (July 1956).

7-21.   R. W. Kelley, "Calibration of Shock Accelerometers," Instrument Society of America Preprint M18-2-MESTIND-67, 1967.

7-22.   R. W. Kelley, "Instrumentation for Accelerometer Shock Calibration," *Proc. Inst. Environ. Sci.* 2, 341-352 (Apr. 1967).

7-23.   R. L. Lyon, "Impact-Force Source and Impact-Force Calibrator," *Exp. Mech.*, 257-264 (June 1973).

7-24.   W. W. Mebane, "Some Practical Considerations in Measurement and Analysis of Shock Records," *Shock Vib. Dig.* 2 (7), 3-5 (July 1970).

7-25.   K. Oishi, "Evaluation of the Endevco Drop-Ball Shock Calibrator," Sandia Laboratory Report SC-TM-65-1, 49 p., Jan. 1965.

7-26.   D. F. Palmer, "An Accurate Shock Calibrator for Accelerometers," Sandia Corporation Tech. Memorandum SCTM 96-61 (73), 15 p., Apr. 1961.

7-27.   D. F. Palmer, "Accelerometer Shock Calibration," Sandia Corporation Tech. Memorandum 99-63 (73), May 1963.

7-28.   D. F. Palmer, "Accelerometer Shock Calibration," *J. Environ. Sci.*, 18-21 (Oct. 1963).

7-29.   T. A. Perls and C. W. Kissinger, "High-Range Accelerometer Calibrations," N.B.S. Report 3299, 12 p. June 1954. Also Instrument Society of America Paper No. 54-40-2, Sept. 1954.

7-30.   T. A. Perls, "High-*g* Accelerometer Calibrations by Impact Methods with Ballistic Pendulum, Air Gun and Inclined Trough," Instrument Society of America Paper No. 54-40-2, Sept. 1954.

7-31.   T. A. Perls, "A Method for Steady-State Accelerometer Calibrations up to ± 4000 *g* and Test Results on Two Accelerometers, Model A314-T," N.B.S. Report 3924, Mar. 1955.

7-32.   J. D. Ramboz, "Equipment Evaluation Report on Endevco 2965 Shock Calibrator," Metrology Engineering Center Report No. ESEE08, Nov. 1966.

7-33.   M. H. Woodward, "Ballistic Pendulum Shock Calibrator," Sandia Laboratories Tech. Memorandum SC-TM-66-567 (N67-31473), Nov. 1966.

7-34.   M. H. Woodward, "The Use of a Force Transducer as an Acceleration Standard for High Level Shock Calibration," Sandia Laboratories Tech. Memorandum SC-TM-67-493, July 1967.

FORCE GAGES AND IMPEDANCE HEADS

8-1.   R. O. Belsheim, "The Need for Precision in Measuring Mechanical Impedance," Instrument Society of America Preprint No. 51-LA-61, Sept. 1961.

8-2.   R. R. Bouche, "Instrumentation for Shock and Vibration Measurements," presented at American Society of Mechanical Engineers Colloquium Experimental Techniques in Shock and Vibration, New York, Nov. 1962.

8-3.   T. Dimoff and R. Koyanagi, "Performance of a Mechanical Impedance Head," N.B.S. Report 9526, June 1967.

8-4.   D. J. Ewins and M. G. Sainsbury, "Mobility Measurements for the Vibration Analysis of Connected Structures," *Shock Vib. Bull.* **42** (1), 105-122 (Jan. 1972).

8-5.   S. Levy, "Mechanical Impedance, The Language of Shock and Vibration," *Mag. Stand.* **35** (7), 1980201 (July 1964).

8-6.   C. T. Morrow, "Instrumentation for Measurement of Vibratory Motion and Mechanical Impedance Within Assembled Aerospace Equipment," *Shock Vib. Bull.* **40** (7), 29-32 (Dec. 1969).

8-7.   G. J. O'Hara, "Mechanical Impedance and Mobility Concepts," NRL Report 6406, 16 p., U.S. Naval Research Laboratory, Washington, D.C., July 1966.

8-8.   G. W. Painter, "Use of Miniature Force Transducers in the Measurement of Shock and Vibration Environments," *Shock Vib. Bull.* **34** (4), 45-53 (Feb. 1965).

8-9.   R. Plunkett, "Effect of Contact Area on Mechanical Impedance Measurements," University of Minn. Report on Contract No. Nobs-86783, Sept. 1963.

8-10.   G. M. Remmers and R. O. Belsheim, "Effects of Technique on Reliability of Mechanical Impedance Measurement," *Shock Vib. Bull.* **34** (3), 37-58 (Dec. 1964).

8-11.   J. P. Salter, "Impact and Mobility," *J. Environ. Sci.* **XIV** (3), 17-20 (May-June 1971).

8-12.   F. Schloss, "Recent Advances in the Measurement of Structural Impedance," David Taylor Model Basin Report 1584, 40 p. U.S. Department of the Navy, Jan. 1963.

8-13.   F. Schloss, "Recent Advances in Mechanical Impedance Instrumentation and Applications," *Shock Vib. Bull.* **34** (3), 3-14 (Dec. 1964).

8-14.   F. Schloss, "Measurements of the Effect of Geometric Scale on Structural Impedance and Radiated Sound," *J. Acoust. Soc. Amer.* **41**, 1193-1195 (May 1967).